Title

Acclimation and evolution in a changing climate: Integrating physiology, transcriptomics, and genomics of a thermal specialist

Author

Tonione, Maria

Publication Date

2018

Peer reviewed|Thesis/dissertation

Acclimation and evolution in a changing climate: Integrating physiology, transcriptomics, and genomics of a thermal specialist

By

Maria Tonione

A dissertation submitted in partial satisfaction of the

requirements for the degree of

Doctor of Philosophy

in

Environmental Science, Policy, and Management

in the

Graduate Division

of the

University of California, Berkeley

Committee in charge:

Professor Neil D. Tsutsui, Chair
Professor Caroline M. Williams
Professor Ian J. Wang

Spring 2018

Acclimation and evolution in a changing climate:
Integrating physiology, transcriptomics, and genomics of a thermal specialist

By Maria Tonione

ABSTRACT

Acclimation and evolution in a changing climate:
Integrating physiology, transcriptomics, and genomics of a thermal specialist

By

Maria Tonione

Doctor of Philosophy in Environmental Science, Policy, and Management

University of California, Berkeley

Professor Neil D. Tsutsui, Chair

Climate change is one of the top causes of biodiversity loss. Organisms will experience many pressures associated with climate change, one of the most obvious being increased temperature. It is therefore important to understand how animals will react to this stress. Ectotherms, such as ants, are especially sensitive to the climate as they rely on environmental temperature for everything from optimal foraging to development time. In this dissertation, I explore the individual and population level reactions to thermal stress of a cold-specialist, the winter ant, *Prenolepis imparis*. I also identify the role past climatic fluctuations have had in shaping this species' current distribution.

In my first dissertation chapter, I conducted a RNA-seq analysis to identify stress-induced genes in *P. imparis* individuals at the transcriptome level. To identify candidate genes involved in the stress response, I induced stress by placing the ants at a low or high temperature. Then, I sequenced the transcriptome of these stressed individuals. The genes that show an increase during transcription are candidates for allowing individuals to recover from the stress. I identified a total of 709 differentially expressed genes. In the cold-stressed ants, I did not identify a strong response, indicating that the temperature we chose for trials was not cold enough. Conversely, I found a strong response to the heat. Those transcripts we found highly induced include protein folding genes, heat shock proteins, proteins associated with heat shock proteins, Ca^{2+} ion transport, and a few unknown genes. I also found functional categories relating to protein folding, muscles, and temperature stimulus increased in the heat-stress response.

In my second dissertation chapter, I measured the short-term acclimation ability of high- and low-elevation populations of *P. imparis* across California. In addition, I also characterized the thermal environment both above and below ground. I found that the high-elevation sites showed increased tolerance and reduced capacity in acclimation ability relative to the low-elevation counterparts at their lower limits, suggesting an evolutionary trade-off between tolerance and acclimation ability. In addition, I found less acclimation capacity across all populations in their upper limits. I also found that the high-elevation sites experience cooler temperatures both above and below ground. The greater acclimation response at lower limits in high-elevation populations could suggest that they are better physiologically prepared to survive cooler temperatures.

In my final dissertation chapter, I used phylogenetic and population genetic analyses to identify population genetic structure and historical demographic patterns across the range of *P. imparis*. I relate the genomic patterns to those expected as seen with *in situ* diversification, or maintained connectivity. I recovered five well-supported genetically isolated clades across the distribution. I also investigated gene flow between these major genetic clades and did not find evidence of gene flow between clades. High support for five major geographic lineages and lack of evidence of contemporary gene flow indicate *in situ* diversification across the species' range, probably influenced by glacial cycles of the late Quaternary.

Overall, the results from this dissertation give insight into plasticity as well as the evolutionary processes that have shaped this species. My results suggest molecular pathways by which phenotypic plasticity will allow individuals to overcome heat-stress: the candidate genes provided here are a valuable resource in understanding pathways and proteins necessary for survival at unfavorable temperatures. I also report that individuals from different populations show different levels of thermal tolerance and plasticity. All the populations show less tolerance and reduced plasticity to the heat. This is troubling in the face of climate change, this limited acclimation response at the upper thermal limits suggests evolutionary constraints in heat tolerance, so major changes at the molecular level will be needed for these populations to persist in warmer environments. Finally, the entire range of this species has been profoundly affected by climatic fluctuations during the Quaternary. These fluctuations led those individuals to have separate evolutionary histories and raises the possibility that there are several unique species of *P. imparis*.

Table of Contents

Table of Contents i
List of Figures iii
List of Tables iv
Acknowledgements v
Chapter 1 RNA-seq reveals expression signatures of genes involved in temperature stress in a thermally sensitive ant, the winter ant (*Prenolepis imparis*) 1
1.1 Introduction 1
1.2 Methods 2
1.3 Results 4
1.4 Discussion 5
1.5 Acknowledgements 9
1.6 Figures 10
1.7 Tables 13
Chapter 2 Thermal acclimation ability varies at lower limits between high- and low-elevation populations of *Prenolepis imparis* 20
2.1 Introduction 20
2.2 Methods 22
2.3 Results 24
2.4 Discussion 25
2.5 Acknowledgements 27
2.6 Figures 28
2.7 Tables 30
Chapter 3 Phylogeography and population genetics of a widespread North American ant, *Prenolepis imparis* 36
3.1 Introduction 36
3.2 Methods 37
3.3 Results 41
3.4 Discussion 43
3.5 Acknowledgements 45
3.6 Figures 47

3.7 Tables 51
Literature Cited 53
Appendix A. Supplementary Information for Chapter 1 67
A.1 Supplemental Table 67
Appendix B. Supplementary Information for Chapter 2 93
B.1 Supplemental Table 93
Appendix C. Supplementary Information for Chapter 3 95
C.1 Supplemental Figures 95
C.2 Supplemental Table 97

List of Figures

Figure 1.1. Principal component analysis (PCA) of all annotated transcripts used in differential expression analysis for *P. imparis*. 10

Figure 1.2. Hierarchical clustering and heatmap of all transcripts tested for differentially expressed genes based on transcript counts. 11

Figure 1.3. Hierarchical clustering and heatmap of differentially expressed genes (fold-change ≥ 2, FDR < 0.01) during heat-treated individuals. 12

Figure 2.1. Survivorship curves for low-and high-elevation populations of *P. imparis*..... 28

Figure 2.2. Mean chill-coma recovery times (CCRT) and knockdown times for populations of *P. imparis*. 29

Figure 3.1. Map of United States and Mexico with samples used..... 47

Figure 3.2. Phylogenetic and population clustering of *P. imparis* individuals. 48

Figure 3.3. Map of California with individuals sequenced indicated 49

Figure 3.4. Nonparametric *k*-means clustering of total genetic diversity across all samples of *P. imparis*. 50

Supplemental Figure C.1. Phylogenetic clusters of *P. imparis*. 95

Supplemental Figure C.2. STRUCTURE results for K = 3 and K = 4 for individuals within the CA clade of *P. imparis.* 96

List of Tables

Table 1.1. Reads obtained for each *P. imparis* transcriptome sequenced, before and after trimming. 13

Table 1.2. Proteins that have been upregulated based on transcript counts found at a ≥ 10 fold-change (FC) in individuals of *P. imparis* after heat-stress relative to control. 14

Table 1.3. Proteins that have been differentially expressed based on transcript levels (TPM) in individuals of *P. imparis* after cold-stress relative to control. 15

Table 1.4. GO enrichment for the 706 DETs during heat-stress. 16

Table 1.5. Biological categories found to have significantly changed expression patterns during cold-stress of *P. imparis*. 19

Table 2.1. A listing of the 19 climatic variables found in the WorldClim dataset. 30

Table 2.2. Locality name, altitude (m), GPS coordinates (longitude and latitude), and mean weight. 31

Table 2.3. Populations in which above ground temperature was collected during 2015 and 2016. 32

Table 2.4. Populations in which underground temperature was collected during 2015 and 2016. 33

Table 2.5. For each locality, chill-coma recovery times (CCRT) and knockdown times after a 10°C and 27°C acclimation are reported. 34

Table 2.6. Paired samples t-tests comparing high- and low-elevation climatic variables. 35

Table 3.1. Demographic statistics for UCEs of *P. imparis*. 51

Table 3.2. Mean values (maximum) of corrected sequence divergence between populations. 52

Supplemental Table A.1. Differentially expressed genes after a two-hour recovery to heat stress and the fold-change (FC) of their expression relative to the control. 67

Supplemental Table B.1. Bioclimatic variables for populations of *P. imparis* that were used for tolerance assays. 93

Supplemental Table C.1. Samples of *P. imparis* included in this study 97

Acknowledgements

This work could not have been completed without the support of my adviser: Neil Tsutsui. I am thankful for getting the opportunity to be mentored by an adviser that has shown unwavering enthusiasm for my projects and science in general.

Of course, a dissertation cannot be completed alone; there have been many that have helped me throughout my time. The support from the entire Tsutsui Lab has been essential: Kate Mathis, Rebecca Sandidge, Kelsey Scheckel, Virginia Emery, Kaustubh Gokhale, Brian Whyte, Nina Pak, Jan Buellesbach, Elizabeth Cash, and Josh Gibson, have all been supportive throughout my dissertation. In this lab, I was also lucky enough to have worked with several extremely helpful and enthusiastic undergraduates such as So Mi Cho, Christian Irian, and Gary Richmond on many aspects of this project. Sometimes the only thing that kept me going was the encouragement from them.

Both my dissertation and my qualifying committee members have pushed me to learn more than I thought possible and have encouraged my growth as a scientist. I would sincerely like to thank my qualifying exam committee for giving me so much of their time and wisdom: Michael Nachman, Rosie Gillespie, Patrick O'Grady, and Brian Fisher. Also, I would like to thank my dissertation committee for holding many fruitful discussions and providing much needed feedback on all aspects of my work: Caroline Williams and Ian Wang.

My passion for science would have stalled had it not been for one person – Craig Mortiz. I was lucky enough to be mentored starting as an undergraduate by quite possibly the world's best mentor. He took me under his wing and into his lab without much experience and taught me everything I know. There is no way I could repay his kindness and patience with me. Within his lab, I found many friends that have helped me become the scientist I am today: Sonal Singhal, Roberta Damasceno, Tamí Mott, and Ricardo Pereira unknowingly gave me the courage and inspiration to do a PhD. Within the MVZ, I met many other great scientists that have inspired me through their amazing science, life lessons, and interesting conversations: David Buckley, Iñigo Martinez-Solano, Jason MacKenzie, Julia Gardner, Ana Carnaval, Matt Fujita, Adam Léache, Matt MacManes, Kevin Rowe, Karen Rowe, Sean Rovito, Mark Phuong, Marisa Lim, Shobi Lawalata, Lydia Smith, and Ke Bi.

I would like to thank my Master's adviser, Eric Routman, for cultivating seeds of scientific thought and passion with a bit of humor. For this I am ever grateful.

A special acknowledgment needs to be given to two of the hardest working people I know: Ke Bi and Lydia Smith. Ke has been instrumental in getting this work finished and polished. He pushed me to create something better than I would have done alone. Lydia has not only been a fantastic lab manager, but she has also been a great friend that was willing to teach me and support me throughout every frustrating mistake or setback.

This work could not be completed without the full support of all of my family: Philip, Sebastian, and Ophelia have given their unending support and love throughout my entire dissertation and for that I am extremely grateful. Sebastian and Ophelia have provided a huge inspiration for this work. I hope they indulge their passion for learning and exploring to enjoy the many wonders of this world.

My love of the outdoors has been cultivated at an early age by my parents and siblings. Mom and dad, I am so thankful to have such amazing parents eager to get me outside exploring. Everything I contribute to this world can be traced back to these early days and unwavering support from my wonderful parents. My siblings have helped shape the person I am by inspiring

me, pushing me, and teaching me throughout my life. In every way, they are my role models and best friends. Dominic, Vincent, and Christine, if I never said it before, thank you.

Finally, throughout my PhD, I had the tremendous support of my good friends, Janet Fang, Rachel Graziani, Kim Tsao, and Kristina Yamamoto. These friends have been responsible for getting me through many difficult times, and I simply can't express how important their continued emotional support has been throughout this whole process.

Chapter 1 RNA-seq reveals expression signatures of genes involved in temperature stress in a thermally sensitive ant, the winter ant (*Prenolepis imparis*)

1.1 Introduction

Humans have had a profound impact on the natural world; we are altering the environment in ways that are devastating for global biodiversity. Climate change is among the top drivers of biodiversity loss (Sala et al., 2000), and extinctions will likely increase with continued climatic changes. Stressed species will need to either adapt, migrate, or face extinction once subjected to these conditions. If unable to migrate, populations must manifest evolutionary adaptations to the thermal conditions they experience or respond to these new conditions via phenotypic plasticity (Chevin, Lande, & Mace, 2010; M. B. Davis, Shaw, & Etterson, 2005). Evolution and phenotypic plasticity can work in concert to enable persistence during environmental change (Chevin et al., 2010; DeBiasse & Kelly, 2016). Transcriptomics (RNA-seq) has emerged as a powerful tool in discovering the plastic responses of pathways and genes associated with survival under stressful conditions (C. D. Kenkel, Meyer, & Matz, 2013; Carly D. Kenkel & Matz, 2016). With these gene expression analyses, we can understand, at a molecular level, the influence of both abiotic and biotic stressors on individuals and populations (Colinet, Lee, & Hoffmann, 2010b; DeBiasse & Kelly, 2016; Koo, Son, Kim, & Lee, 2015).

Environmental stress causes proteins to misfold, denature, or form aggregates, and this can result in impaired organismal function. In a diverse array of organisms, we see a similar heat shock response (HSR) to combat environmental stress, which typically includes physiological adjustments in gene expression (DeBiasse & Kelly, 2016; Gleason & Burton, 2015; Lockwood, Sanders, & Somero, 2010). The HSR involves upregulation of genes that encode for "heat shock proteins" (Hsps), chaperones or co-chaperones of Hsps, or other genes associated with maintaining proteostasis (i.e. Feder & Hofman, 1999; King & MacRae, 2015; Kurzik-Dumke & Lohmann, 1995; Lancaster et al., 2016). Most organisms are capable of producing Hsps in response to heat or other stressors. *Heat-shock protein 70* and *Hsp90* are among the most conserved proteins (Lindquist & Craig, 1988), while proteins from the *Hsp40*, *Hsp60*, and *Hsp70* families make up the most prolific proteins in the HSR (Fink, 1999). Some studies suggest that upregulation of genes expressed during physiologically stressful times helps those individuals overcome those scenarios (Barreto, Schoville, & Burton, 2015; M E Feder, Cartaño, Milos, Krebs, & Lindquist, 1996; Gong & Golic, 2006; Kalosaka, Soumaka, Politis, & Mintzas, 2009; Schoville, Barreto, Moy, Wolff, & Burton, 2012). Alternatively, this response could be a panic or "emergency response," and researchers have associated higher levels of Hsps with reduced knockdown resistance (Jesper G Sørensen, Dahlgaard, & Loeschcke, 2001). Other studies have noted no upregulation of Hsps with temperature stress (Barshis et al., 2013; Bradley A. Buckley & Somero, 2009; Franssen et al., 2014), suggesting an organismal response to heat stress can be

more nuanced than simply overall upregulation of Hsps, and other genes can play an important role. Testing expression levels of specific Hsps suggests that ants from a warmer environment (*Cataglyphis*) induce Hsps at a higher temperature than ants from a cooler environment (*Formica*) (Gehring & Wehner, 1995). Identification of genes in a diverse array of organisms is of importance to understand the response to environmental stress; however, we are unaware of any studies that characterize the transcriptomic response to thermal stress in ants.

In general, ants have proven to be extremely useful model systems for monitoring environmental impacts: they are abundant, widespread, important to ecosystems, sensitive to environmental stress, and relatively easy to collect (Ribas, Campos, Schmidt, & Solar, 2012). For ants, the environmental conditions constitute a primary force in determining seasonal activities (Dunn, Parker, & Sanders, 2007) and so, are typically constrained by temperature (Netherer & Schopf, 2010). In this study, we use RNA-seq to identify the stress response at the level of gene expression in a thermally sensitive ant, the winter ant (*Prenolepis imparis*). Activity of *P. imparis* is often reduced during the warmer months and instead is increased in the cooler months when most other ant species have reduced foraging (early spring and late fall) (Dunn et al., 2007). They are found from sea level up to high-elevation (www.antwiki.com), are associated with cooler microhabitats in mesic forests (Cuautle, Vergara, & Badano, 2016; Frye & Frye, 2012; Wheeler, 1930) and respond negatively to warming (Stuble et al., 2013). Understanding the underlying mechanisms for survival to temperature stress is particularly relevant for populations of the winter ant given that studies have found that ants which have lower warming tolerances and which occupy warmer, mesic forests are physiologically susceptible to warming temperatures (Diamond et al., 2012).

The overarching goal of this research was to reveal candidate genes or biological functions necessary for recovery from temperature stress. To do this, we examined the transcriptomic response to short-term temperature stress in *P. imparis*. We hypothesized that at a cold or hot temperature, *P. imparis* will experience physiological stress and, accordingly, will modulate the expression of genes necessary to survive these stressful conditions. The analyzed data provide an overview of the genes and processes involved in response to stress in *P. imparis*.

1.2 Methods

Sample collection and stress exposure

Ants were collected from a population in Berkeley, California in June 2014. After the ants were collected, they were immediately placed at one of three separate thermal conditions: (1) a walk-in cold room at approximately 5°C (cold-stress), (2) on a room-temperature bench-top approximately 21°C (a mid-temperature control), and (3) in an incubator (Fisher Scientific Isotemp Model 650D Large 600 Series Incubator CAT# 11-690-650D) at 35°C (heat-stress).The heat- and cold-stress temperatures were chosen after initial trials at higher or lower temperature, respectively, produced mortality. During initial heat-stress trials, ten ants were placed at 37°C in the incubator for three hours and allowed to recover for two hours. After the two hour recovery, four had died. We reduced the temperature by 2°C and placed ten more individuals in the incubator for three hours and allowed them to recover for two. After the recovery, all survived, so we choose this as the temperature to induce heat-stress without incurring mortality. For the initial cold-stress trials, we placed ten ants in 1.5mL Eppendorf tubes in ice for three hours. After a two hour recovery, five had died. We then placed ten different ants at 5°C and allowed them to

recover for two hours. After this recovery, none had died, so we chose this as the temperature to induce cold-stress without incurring mortality. During these initial trials, ants were collected on separate days. We collected all ants sequenced in this study at the same time and placed them in their separate temperature treatments immediately after collection. All three groups remained in those conditions for a total of three hours and given only water to ensure expression was not confounded by dietary changes. During a two-hour recovery phase, they were given a 30% sugar water solution. A two-hour recovery was used because previous studies have found that genes implicated in stress recovery have a maximum peak response two hours after the stress (Colinet et al., 2010b).

RNA isolation and mRNA sequencing

After the two-hour recovery phase, ten whole ants from each temperature condition were ground in TRIzol (Invitrogen) using a disposable pellet mixer and cordless motor (VWR #47747-370) until homogenized (approx. 15 seconds). RNA extraction was performed according to Rio et al. (2010), with the following changes: 1) we used 0.1mL of BCP Phase separation reagent (Molecular Research Center) for every mL of TRIzol and 2) each sample was re-suspended in 28μL RNAse-free water. All materials and surfaces used were treated with RNase AWAY (Thermo Scientific). Based on Nanodrop concentration estimates, we chose three samples that had roughly the same RNA concentration from each condition to continue library production, all samples used in library preparation were ~35ng/μL in concentration. The integrity and yield of the RNA extractions were checked by a Bioanalyzer 2100 (Agilent Technologies, Cedar Creek, Texas). All samples had an RNA integrity number (RIN) > 7.0, which indicated quality sufficient for poly(A) selection and cDNA library preparation. 0.5-2ug of the mRNA isolated was used as the template for cDNA library construction according to manufacturer's recommendations in the TruSeq RNA Sample Preparation Kit v2 (Illumina: RS-122-2001). The RNA was sheared for eight minutes during the poly(A) selection. To increase the heterogeneity of the cDNA libraries, we split the reaction in half and combined them after enriching the samples for ten cycles. Library quality was assessed using qPCR, the Qubit dsDNA High Sensitivity Assay Kit on a Qubit fluorometer, and Bioanalyzer 2100. All nine samples were pooled to 13pM equal molar and sequenced using one lane of a 150-bp paired-end Illumina HiSeq2500 run (Vincent J. Coates Genomics Sequencing Laboratory, UC Berkeley).

***P. imparis de novo* transcript assembly and annotation**

A total of nine individuals were sequenced and aligned to create a *de novo* transcriptome. Raw fastq reads were filtered using Cutadapt (Martin, 2011) and Trimmomatic (Bolger, Lohse, & Usadel, 2014) to remove low quality reads and adapter sequences. Exact duplicates were eliminated using Super Deduper (https://github.com/dstreett/Super-Deduper). After quality trimming and adapter trimming, reads from all individuals were merged and assembled together using Trinity r2014-07-17 (Grabherr et al., 2011) on XSEDE (Couger et al., 2014). The resulting *de novo* assembly served as a reference with only the longest isoform per gene retained. This reference assembly was annotated against 8 different reference protein databases: *Camponotus floridanus*, *Cardiocondyla obscurior*, *Harpegnathos saltator*, *Linepithema humile*, *Pogonomyrmex barbatus*, *Solenopsis invicta*, *Atta cephalotes*, and *Acromyrmex echinatior* (Bonasio et al., 2010; Elsik et al., 2016; C. D. Smith et al., 2011; C. R. Smith et al., 2011; Suen

et al., 2011; Wurm et al., 2011). The initial round of annotation was done by using BLASTX (Stephen F Altschul et al., 1997) with an e-value of 1e-10 and a minimal percent mismatches of 50. The reading frame of each of the matched blast hits were then defined by Exonerate (Slater & Birney, 2005). For each reference-specific annotation, when more than one transcript fragment matched against a reference protein, these transcripts were joined together with Ns based on their relative BLAST hit positions to the reference. The resulting annotation from each species was then merged together to purge redundancies. Namely, when the same transcript was annotated with a protein ID from a different reference, only one of the protein IDs was kept. This annotation was used for the Gene Ontology (GO) analysis (see below).

Read mapping and quantification

We also used the quasi-mapping approach implemented in the program Salmon (Patro, Duggal, Love, Irizarry, & Kingsford, 2017). In this case, the cleaned and trimmed individual reads were quasi-mapped to our *de novo* assembly produced in this study. To filter out nonexpressed genes or genes with low expression, only genes harboring a TPM value of ≥ 1 in all the samples were considered.

Gene expression analysis

Count data were normalized using DESeq2 1.18.1 (Love, Huber, & Anders, 2014). We ran two tests: (1) cold-stressed ants (5°C) versus control ants (21°C) and (2) heat-stressed ants (35°C) versus control ants (21°C). Transcripts were considered to be differentially expressed transcripts (DETs) if they had an adjusted *p*-value < 0.01 and the absolute $\log_2$FoldChange > 1.0 (Benjamini and Hochberg adjusted false discovery rate [FDR]<0.001). From the $\log_2$FoldChange value, we were then able to calculate the relative fold-change (FC). The software package ErmineJ 3.0.2 (Lee, Braynen, Keshav, & Pavlidis, 2005) was applied to evaluate the biological pathways associated with each differentially expressed GO term. The analysis was run with the following options: gene score resampling (GSR), a maximum gene set of 100, a minimum set of 20, a maximum iteration of 200,000, and full resampling. GO terms with GO adjusted *p*-values < 0.05 were semantically summarized and visualized with REViGO with an allowed similarity of 50, in order to substantially reduce our categories (Supek, Bošnjak, Škunca, & Šmuc, 2011).

1.3 Results

In this study, we generated nine *P. imparis* transcriptome libraries to identify differentially expressed genes during temperature stress. From the 9 libraries, the Hi-Seq 2500 run produced a total of 296 million reads of 150bp in length. Libraries ranged from 29,924,670 to 37,698,086 sequences, with means of 32,082,531, 33,846,271, and 32,745,831 sequences for the 5°C, 21°C, and 35°C treated ants, respectively. The data showed no significant differences in the number of sequences between the three datasets (AMOVA, p=0.83). After trimming, we obtained a total of 31.25 Gb of cleaned sequences for further downstream analyses (Table 1.1). We then assembled a *de novo* transcriptome to which we aligned the sequences from the nine *P. imparis* libraries.

Gene identification and annotation

We performed BLASTX to annotate the winter ant transcriptome assembly and inform downstream differential gene expression analysis. After BLASTX annotation, a total of 13,324 contigs had a significant BLAST hit to a gene from one of the previously annotated eight unique ant genomes with an e-value cutoff of 1E-5. To obtain a complete annotation, we carried out the same BLASTX with the SwissProt database and NR database. Altogether, 11,219 (84%) were annotated in the NR and SwissProt databases. Of these, 7,011 (62%) contigs matched the GO annotations, and 4,600 (41%) contigs aligned to the KEGG database. Because of the lack of genome information for *P. imparis*, only a fraction of contigs with hits from the ant genomes were annotated for genes, GO terms, and KEGG numbers (4,580; 38%). An additional 2,113 (16%) were not functionally informative because they did not match any known genes from the NR or UniProt databases. They were assumed to be unique hits for further analyses and treated as individually expressed transcripts.

Identification of differentially expressed transcripts

A total of 8,934 transcripts were tested for differential expression after filtering for low TPM values. To summarize our treatments and control we performed hierarchical clustering across all transcripts. The resulting tree clustered the cold-stressed and control ants together, while the heat-stressed ants were in their own cluster (Fig. 1.1 & 1.2). Our PCA analysis revealed that most of the variation (60%) was between the heat-stressed individuals and the other two treatments together, the cold-stressed and control individuals. For the two tests performed (cold-stressed versus the control ants and hot-stressed versus the control ants), there was a total of 709 unique transcripts that showed significant differential expression (Fig. 1.3, Supplemental Table A.1). Nearly all of these transcripts (706 of 709) showed differential expression in response to the heat treatment. Of these, 14 had an expression response ≥10 fold-difference, 457 were upregulated, and 249 were downregulated. In contrast, only three transcripts were differentially expressed between cold-stressed and control ants, and none of these had an altered expression ≥10-fold difference (Table 1.2). Of the three transcripts that had different expression during the cold-treatment, two were upregulated and one was downregulated (Table 1.3).

Gene set enrichment and pathway analysis

We explored the enriched gene categories by performing a gene ontology (GO) analysis. Using the transcripts obtained through our DESeq analysis with a FC ≥ 2, and FDR < 0.01, we filtered GO terms for *p*-value to determine significantly overrepresented gene categories using ErmineJ. In the heat-stressed ants, we found increased expression in eight biological functions, which can be summarized in five GO categories after removing redundant GO terms in REViGO (Table 1.4). We found decreased expression in 44 biological function categories, which can be summarized in 13 categories (Table 1.4). In the cold-stressed ants, we found increased expression in two biological functions that can be summarized as coenzyme biosynthetic process, and one category with decreased expression: DNA integration (Table 1.5).

1.4 Discussion

The maintenance of thermal homeostasis is of fundamental importance for all organisms, and the mechanisms for tolerating both high and low temperatures are obvious targets for natural

selection. Adaptations to the thermal environment define some of the most important features of an organism's biology including activity patterns (e.g. circadian and seasonal), range limits, niche, competitive outcomes, and many others. In addition, the growing threat of climate change has placed additional emphasis on understanding how species will respond to increasing temperature.

In this study, we examined the genes, biological processes, and genetic pathways used by the winter ant (*Prenolepis imparis*) to tolerate both heat- and cold-stress. We found that cold-stress produced virtually no changes compared to room-temperature controls, indicating that this temperature was not extreme enough to produce a strong physiological response. In contrast, heat-stress treatment resulted in altered expression of >700 transcripts, and some of these transcripts displayed enormous changes in the magnitude of expression. Many of these genes have been implicated in thermal stress response in other species (see below), and are thus likely involved in the physiological response of winter ants to heat. These data provide a useful model for how invertebrates in general may respond to thermal stress under future climate regimes.

Response to heat stress

Because of the stress that heat puts on proteins, it is not surprising we see the enrichment of gene functional categories for response to temperature and protein folding. The relative amounts of Hsps vary between organisms (Martin E Feder & Hofman, 1999). In this study, we found the highest levels of expression changes in a gene from the protein *lethal(2)essential for life* (*l2(efl)*). The product of this gene has been associated with upregulation in a HSR (Lancaster et al., 2016) and crowding response (King & MacRae, 2015) and downregulation during pathogen stress (Guo et al., 2015). In our study, expression levels of this gene were increased 165-fold for the temperature treated ants relative to the control. Based on the high levels of *l2(elf)* we detected during heat-stress, it appears to be one of the most important genes in recovering from this stress. Transcripts in this protein were also found in high abundance during the HSR in a damselfly (Lancaster et al., 2016).

In this study, we detected an increase in *Hsp70* expression almost 23-fold higher during heat-stress. No other Hsps were detected in the *de novo* transcriptome (data not shown), presumably they were not transcribed by any of the individuals, and so accordingly, we were unable to test for differential expression at any of the other Hsps. It is also a possibility that these genes were not conserved enough between the annotated ant genomes available and this species, and so remain unknown. *Hsp70* has been implicated in other studies as a HSR (Gleason & Burton, 2015; Lancaster et al., 2016; Nguyen et al., 2017; Rinehart et al., 2007; Jesper G Sørensen et al., 2001) as well as cold-stress response (Rinehart et al., 2007; J. G. Sørensen & Loeschcke, 2001). In addition, it has been shown to protect organisms during other stresses such as crowding, viral infections, and energy depletion (Martin E Feder & Hofman, 1999; Kregel, 2002; J. G. Sørensen & Loeschcke, 2001). Though we did not detect upregulation of other Hsp genes, we did detect a 10-fold increase in aryl hydrocarbon receptor nuclear translocator (ARNT) protein, a protein that forms a complex with *Hsp90* (Peng et al., 2017; Perdew & Bradfield, 1996).

Bcl-2-associated athanogene (BAG)-family proteins are a multifunctional group that perform in a range of physiological processes that include cell cycle, apoptosis, and stress response (Doong, Vrailas, & Kohn, 2002; Kabbage & Dickman, 2008). In this study, we found differentially expressed transcripts (DETs) with substantially elevated levels of a gene in the

BAG domain-containing protein *Samui* in individuals under heat-stress. This is not surprising given that *Samui* has been shown to interact with *Hsp70* to regulate their activity (Doong et al., 2002; King & MacRae, 2015). Other studies have found a homologous gene, *Starvin* (*Stv*) associated with both heat-stress and cold-stress, muscle maintenance, and food uptake (Arndt et al., 2010; Colinet & Hoffmann, 2010; Coulson, Robert, & Saint, 2005; Lancaster et al., 2016; Sima, Yao, Hou, Wang, & Zhao, 2011; Telonis-Scott, Clemson, Johnson, & Sgrò, 2014). *Samui* was the only BAG family protein found to be upregulated in this study.

In addition to reduced fitness and impaired function caused by damaged protein structure or protein aggregates, heat-stress can also cause oxidative stress on the cellular level, creating transcription errors (Finkel & Holbrook, 2000; Nover & Scharf, 1997). Histones are crucial in overcoming this DNA damage (Bungard et al., 2010; Debec, Courgeon, Maingourd, & Masonhaute, 1990; Foster & Downs, 2005). In our study we saw greater than a 10-fold increase of expression levels of Histone H2B and Histone H2A indicating that these proteins are integral to the stress response in *P. imparis*.

During the heat-stress, we also found that expression of ubiquitin-associated-like domain-containing protein 2-A (UBA2A) increased greater than 10-fold. This protein has been implicated in targeting proteins for degradation and shuttling them to the proteasome for degradation (Heinen, Acs, Hoogstraten, & Dantuma, 2011; Schwartz & Hochstrasser, 2003). Upregulation of such pathways is one expected physiological response to heat stress, as misfolded or otherwise damaged proteins may begin to accumulate.

In response to heat, we also noted a large expression difference in a gene relating to calcium ion transport, *calcium-transporting ATPase type 2C member 1* (*ATPC21*). Calcium signaling has been suggested as a rapid response to low temperatures: calcium signals begin the temperature-hardening pathways, inducing a number of physiological changes implicated in stress response including energy metabolism and apoptosis (Teets & Denlinger, 2013). Genes relating to maintenance of calcium ion homeostasis have been found upregulated in response to heat-stress (Barshis et al., 2013) and Truebano et al. (2010) found that genes involved in Ca^{2+} signaling were increased in the Antarctic bivalve (*Laternula elliptica*) during cold stress, indicating the calcium ions could be biomarkers of the physiological state of the individuals during heat-stress as well as cold-stress. The high levels of *ATPC21* that we observed in heat-stressed winter ants suggest that it might play a key role in initiating the physiological response to heat and inducing a heat-hardening pathway.

We also observed the induction of gene functional categories relating to muscular components, including actomyosin structure organization, cellular component assembly involved in morphogenesis, and striated muscle cell development. Because heat stress can cause osmotic shock, the heightened expression of these genes may indicate attempts to restore osmotic balance (B. A. Buckley, Gracey, & Somero, 2006; Di Ciano et al., 2002). As the ants' cells work to overcome stress-related issues, we can expect other biological processes to be put on hold. Indeed, we see gene functional categories relating to metabolism (isoprenoid metabolic process, pigment biosynthesis process, DNA integration, and dicarboxylic metabolic process), the immune response (lymph gland development), and aggression (inter-male aggressive behavior) downregulated during recovery from this stress. Surprisingly, we also see downregulation of gene functional categories we might expect would be necessary to escape a thermal stimulus (detection of stimulus, and visual perception). In addition, we see less expression for gene functional categories in apoptotic related proteins (apoptotic process involved in development), which is surprising because damage to DNA, as happens with heat-stress, will often induce an

apoptosis response. Though Barshis et al. (2013) also found downregulation of genes involved in apoptosis and apoptosis regulation in addition to others that were upregulated during heat-stress.

Finally among the top upregulated genes, we found five transcripts that were either uncharacterized or hypothetical and an additional transcript linked to a protein with unknown function: mantle protein-like. To our knowledge, mantle protein-like does not have any hypothesized functions and, has not been implicated in stress. Additional work is needed to understand the function of the mantle protein-like and other unknown proteins found here and, in particular, why they are recovered with such large expression differences in the heat-stressed individuals.

Response to cold stress

Similarly to heat-stress, cold-stress can also cause denatured or misfolded proteins, leading to harmful aggregates and impaired function. We can also expect cold-stress to cause ion imbalance, impairment of cellular metabolism, depletion of cellular ATP, and buildup of toxic metabolic end products (Teets & Denlinger, 2013). Therefore, we expected transcripts relating to these processes to be over-expressed in cold-stressed individuals. Our results, however, show the cold-stressed individuals and control individuals exhibited very few differences as depicted by the PCA, heatmap, and DETs. This could indicate our experimental temperature was not low enough to elicit a strong physiological response. Both the PCA and heatmap show the cold-stressed individuals and control clustering together or within the same group. Additionally, we only found three DETs with minor expression changes. Transcripts from the two genes that were upregulated were *laccase-3* and *peritrophin-1*. Previous studies have linked *peritrophin-1* and other members of the peritrophin class of proteins as integral to the peritrophic matrix (PM) lining the midgut of insects. This lining forms a protective barrier that prevents invasion by pathogens as well as maintaining gut homeostasis and gut integrity (Du et al., 2006; Narasimhan et al., 2014). Within the midgut PM, Lang et al. (2012) also found laccases and linked them to oxidation of toxic materials in preparation for excretion. Interestingly, proteins necessary for gut osmoregulation have been implicated in other stress responses including cold-stress (*mucin* gene in damselfly) (Lancaster et al., 2016) and heat-stress and cold-stress (*Frost* gene in Drosophila) (Colinet, Lee, & Hoffmann, 2010a) indicating that gut homeostasis could be integral to cold-stress survival.

The one gene that was downregulated during cold-stress was *transcription termination factor 2* (*MTERF2*). The *MTERF2* protein plays a role in the regulation of transcription including termination of transcription and initiating transcription and in mtDNA replication (Bonasio et al., 2010). At present, it is unclear if these DETs found in the cold-stressed individuals are related to temperature-stress, and more work is necessary to understand the role these proteins may play in cold-stress.

Conclusions

Our annotations provide a valuable resource for investigating the role of biological pathways and proteins necessary for surviving unfavorable temperatures. However, because these individuals are all from the same population, the geographic variability of the plastic response to temperature stress is unknown. Other studies have found differences in expression levels in geographically

distinct locations (Gleason & Burton, 2015; C. D. Kenkel et al., 2013; Telonis-Scott et al., 2014), associated with the leading edge of an expansion (Lancaster et al., 2016), and in populations originating from high- and low- temperature environments (Jesper G Sørensen et al., 2001). The ant species in our study*, P. imparis,* occurs across the United States and into Mexico, from sea-level to high-elevation (5 – 2,286m; www.antwiki.com) and so would be an excellent candidate for looking at expression differences across elevations and temperatures.

The molecular mechanisms behind recovery from temperature stress are complex. In this study, we looked at gene expression levels over the entire ant body at one time-point. Other studies have noted that different organs have different expression patterns (Liu et al., 2013; Yu et al., 2014), which can even vary over different time-points (Bradley A. Buckley & Somero, 2009; Colinet et al., 2010b) and development stages (Yu et al., 2014). Therefore, a productive next step would be to investigate the responses of these genes and others at multiple time points, either by RNA-seq or a quantification method such as qPCR (quantitative PCR). In addition, testing the different life stages and castes of the winter ant to determine which life stage or caste is the most vulnerable to temperature stress will be crucial to predict the species' responses to climate change.

Although our analysis has revealed a clear pattern of transcriptome change in response to heat stress, it would be interesting to follow up with physiology tests and correlate that with expression. Previous studies have used RNA interference (RNAi) to suppress the expression of a candidate gene and then compare the resulting phenotype with the unmanipulated phenotype (Barreto et al., 2015; Clements et al., 2017). By doing this, we can examine the role of genes putatively involved in local adaptation. It is unclear from our study if these expression changes are an adaptive response or a large transcriptomic response is actually signal of more stress (Auld, Agrawal, & Relyea, 2010; DeBiasse & Kelly, 2016; Fraser, 2013). Future studies should focus on a functional link between the candidate genes proposed here and thermal tolerance.

Hymenopteran genomes are characterized by gene fragments scattered throughout the genome and multiple episodes of gene family expansions resulting in multiple putatively functional genes and also pseudogenes (Simola et al., 2013). Our analyses uncovered multiple copies of genes (see Supp. Table A.1) from different transcripts and so are assumed to be functional and from unique gene copies. The levels of gene or gene family duplication events were not accessed, and so we can only relate our results to transcript levels.

Our transcriptomic analysis provides an investigation of the gene expression profiles in heat-treated *P. imparis* compared with a control. The transcriptomic analysis has identified many heat-regulated genes that are key components of necessary biological functions and pathways. The DETs and pathways identified here could further facilitate investigations into the detailed molecular mechanisms and provide a foundation for future studies of response to heat-stress in *P. imparis*.

1.5 Acknowledgements

Funding for this chapter was provided in part by the Margaret C. Walker Fund for Systematics as well as the Bob Lane Endowed Graduate Support provided by the ESPM Department at UC Berkeley. We would like to thank Lydia Smith for troubleshooting in the lab and helpful suggestions. We would also like to thank Pierre De Wit for troubleshooting scripts. This work used the Vincent J. Coates Genomics Sequencing Laboratory at UC Berkeley, supported by NIH S10 Instrumentation Grants S10RR029668 and S10RR027303.

1.6 Figures

Figure 1.1. Principal Component Analysis (PCA) of all annotated transcripts used in differential expression analysis for *P. imparis*. Circles represent individuals and are color coded according to treatment.

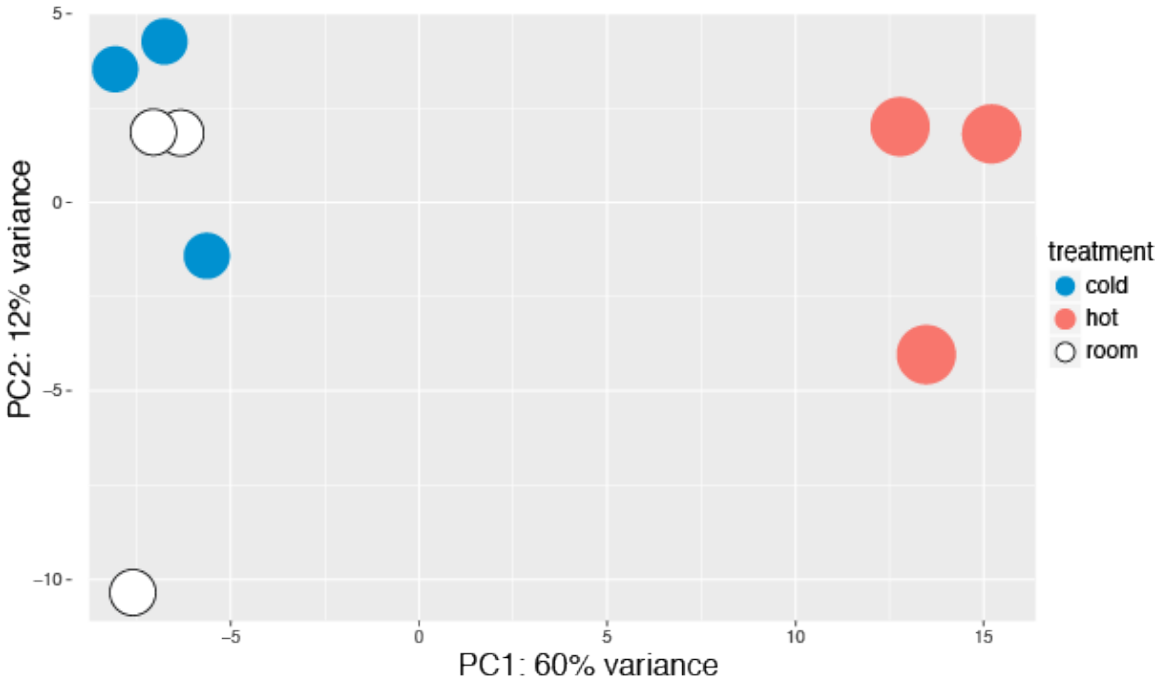

Figure 1.2. Hierarchical clustering and heatmap of all transcripts tested for differentially expressed genes based on transcript levels. Individual clustering is based on the distance matrix of the similarities between samples. Colors indicate magnitude of change of expression indicated by the z-score calculated from individual transcript levels per gene. Downregulation of a gene is indicated in green, and upregulation is indicated in orange. Individuals are listed at the bottom of the heat map and color coded to indicate their treatment: red = heat-stressed, blue = cold-stressed, black = control.

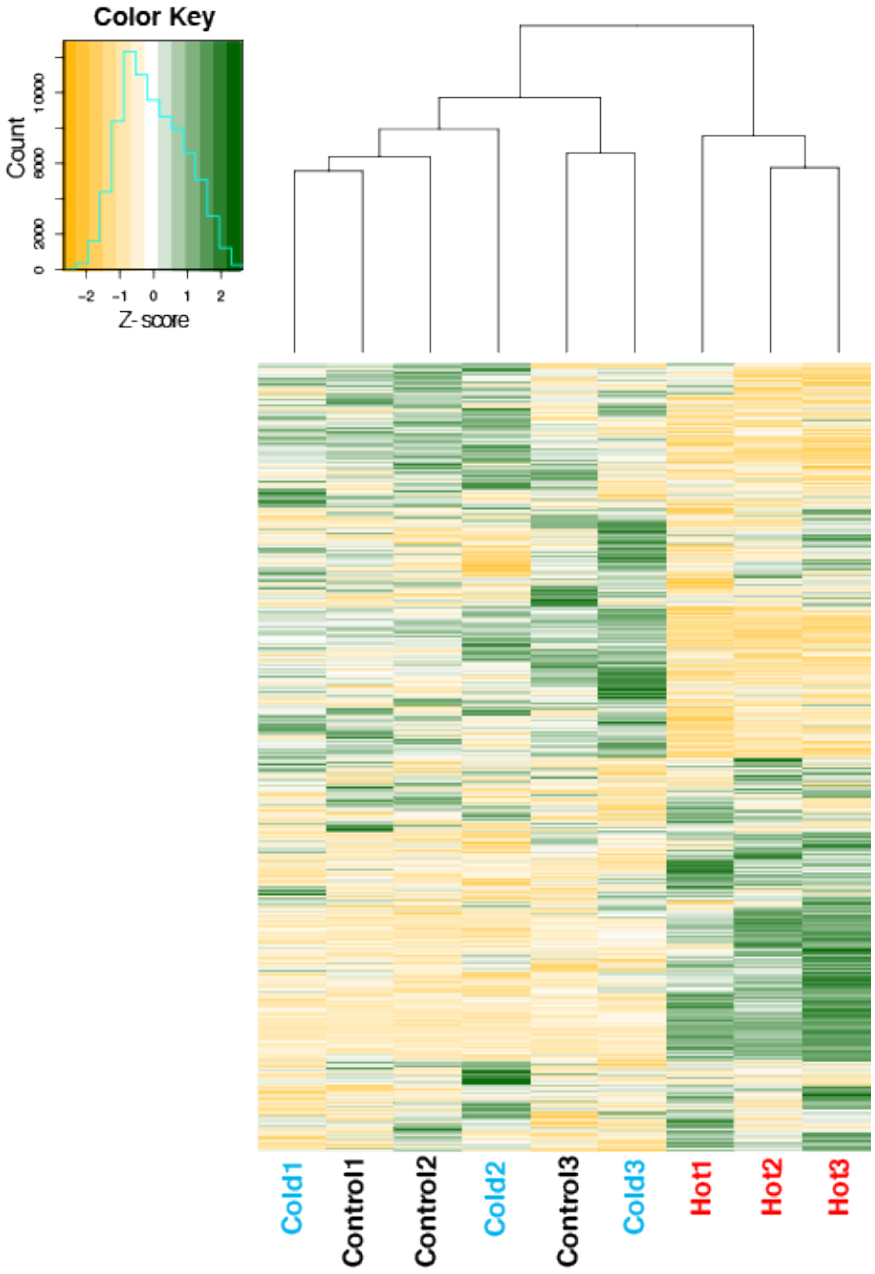

Figure 1.3. Hierarchical clustering and heatmap of differentially expressed genes (fold-change ≥ 2, FDR < 0.01) during heat-treated individuals. Individual clustering is based on the distance matrix of the similarities between samples. Colors indicate magnitude of change of expression indicated by the z-score calculated from individual transcript counts per gene. Downregulation of a gene is indicated in blue, and upregulation is indicated in red. Individuals are listed at the bottom of the heat map and color coded to indicate their treatment: red = heat-stressed, black = control.

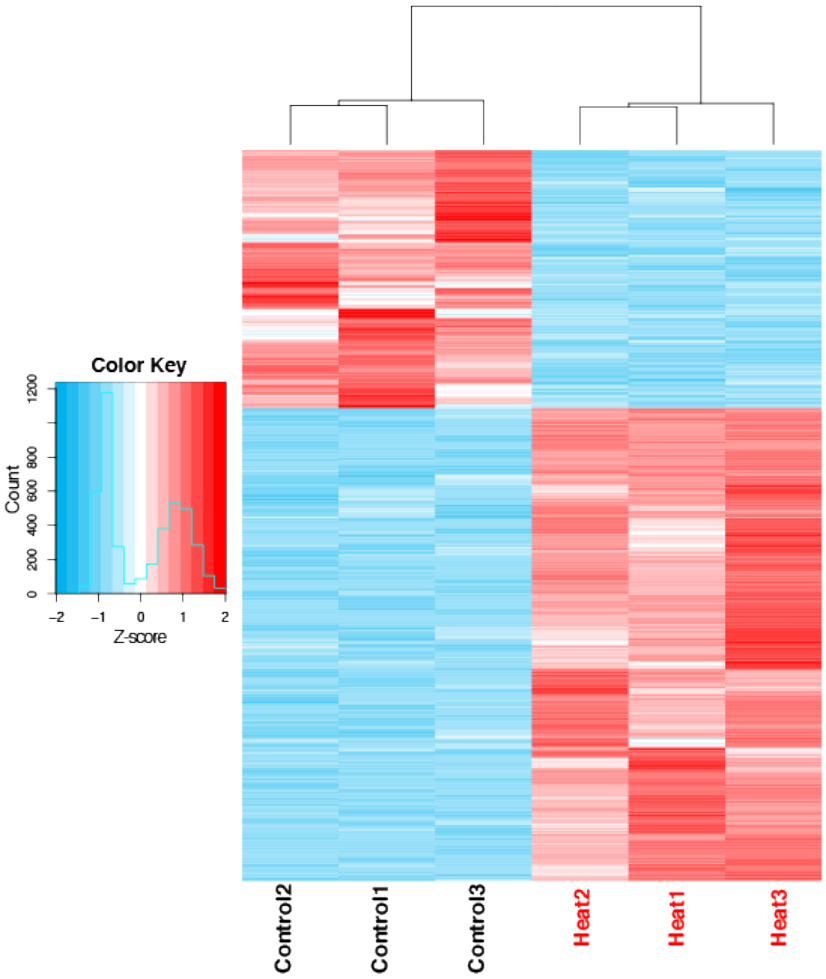

1.7 Tables

Table 1.1. Reads obtained for each *P. imparis* transcriptome sequenced, before and after trimming.

sample ID	treatment	Number of raw reads, million	Read length, bp	Number of reads after trim, million	Average length after trim, bp	Total bases after trim, Gb
Toni036	21°C	30.51	150	24.28	136.3	3.31
Toni038	21°C	30.40	150	24.14	118.3	2.86
Toni039	21°C	35.34	150	27.83	132.3	3.68
Toni046	5°C	36.36	150	29.31	143.8	4.21
Toni047	5°C	30.23	150	24.53	125.2	3.07
Toni048	5°C	34.95	150	28.12	142.9	4.02
Toni057	35°C	30.61	150	23.38	132.6	3.10
Toni060	35°C	37.70	150	29.90	127.0	3.80
Toni061	35°C	29.92	150	24.03	133.3	3.20

Table 1.2. Proteins that have been upregulated based on transcript counts found at a ≥ 10 fold-change (FC) in individuals of *P. imparis* after heat-stress relative to control.

Best matched gene ID[1]	FC	Protein Name	GO Term[2]
ENSCFLO19236	165.53	protein lethal(2)essential for life	unfolded protein binding (GO:0051082)
ENSPB20669	67.28	mantle protein-like	No GO term
ENSCFLO23110	22.96	heat shock 70 kDa protein cognate 4	ATP binding (GO:0005524)
ENSCFLO19899	18.16	bag domain-containing protein samui	DNA binding (GO:0003677);metal ion binding (GO:0046872)
ENSSI2.2.0_03007	13.99	hypothetical protein	No GO term
ENSCFLO19771	13.24	histone H2B	DNA binding (GO:0003677);protein heterodimerization activity (GO:0046982)
ENSACEP19315	12.92	UBA-like domain-containing protein 2-A	No GO term
ENSLH26041	12.39	hypothetical protein	No GO term
ENSSI2.2.0_07291	12.29	hypothetical protein	No GO term
ENSPB23714	11.01	calcium-transporting ATPase type 2C member 1	ATP binding (GO:0005524);calcium ion binding (GO:0005509);calcium-transporting ATPase activity (GO:0005388);manganese ion binding (GO:0030145);manganese-transporting ATPase activity (GO:0015410);signal transducer activity (GO:0004871)
ENSCobs_00196	10.86	aryl hydrocarbon receptor nuclear translocator homolog	No GO term
ENSCFLO11886	10.60	uncharacterized protein	No GO term
ENSLH21966	10.52	histone H2A	DNA binding (GO:0003677);protein heterodimerization activity (GO:0046982)
ENSCFLO11320	10.13	hypothetical protein	No GO term

[1]Contig name based on BLASTx annotation
[2]Based on the biological process

Table 1.3. Proteins that have been differentially expressed based on transcript counts in individuals of *P. imparis* after cold-stress relative to control.

Best matched gene ID[1]	FC	Direction	Protein Name	GO Term[2]
ENSCFLO19140	3.70	Upregulated	Laccase-3	copper ion binding (GO:0005507);hydroquinone (GO:0052716)
ENSCFLO15808	5.47	Upregulated	Peritrophin-1	chitin binding (GO:0008061)
ENSCFLO16203	4.30	Downregulated	Transcription termination factor 2	ATP binding (GO:0005524);DNA binding (GO:0003677);DNA-dependent ATPase activity (GO:0008094);helicase activity (GO:0004386)

[1]Contig name based on BLASTx annotation
[2]Based on the biological process

Table 1.4. GO enrichment for the 706 DETs during heat-stress.

Summary	Biological function	GO term	Direction
actomyosin structure organization	actomyosin structure organization	GO:0031032	Upregulated
cellular component assembly involved in morphogenesis	cellular component assembly involved in morphogenesis	GO:0010927	Upregulated
protein folding	protein folding	GO:0006457	Upregulated
response to temperature stimulus	response to temperature stimulus	GO:0009266	Upregulated
striated muscle cell development	myofibril assembly	GO:0030239	Upregulated
	muscle cell development	GO:0055001	Upregulated
	striated muscle cell development	GO:0055002	Upregulated
	striated muscle cell differentiation	GO:0051146	Upregulated
apoptotic process involved in development	programmed cell death involved in cell development	GO:0010623	Downregulated
	nurse cell apoptotic process	GO:0045476	Downregulated
	apoptotic process involved in development	GO:1902742	Downregulated
	gonad development	GO:0008406	Downregulated
	development of primary sexual characteristics	GO:0045137	Downregulated
axon midline choice point recognition	axon midline choice point recognition	GO:0016199	Downregulated
	axon choice point recognition	GO:0016198	Downregulated
detection of stimulus	detection of stimulus	GO:0051606	Downregulated
dicarboxylic acid metabolic process	dicarboxylic acid metabolic process	GO:0043648	Downregulated
DNA integration	DNA integration	GO:0015074	Downregulated
establishment of tissue polarity	establishment of tissue polarity	GO:0007164	Downregulated
inter-male aggressive behavior	aggressive behavior	GO:0002118	Downregulated

	inter-male aggressive behavior	GO:0002121	Downregulated
	multi-organism behavior	GO:0051705	Downregulated
isoprenoid metabolic process	isoprenoid metabolic process	GO:0006720	Downregulated
	terpenoid metabolic process	GO:0006721	Downregulated
lymph gland development	antimicrobial humoral response	GO:0019730	Downregulated
	lymph gland development	GO:0048542	Downregulated
	humoral immune response	GO:0006959	Downregulated
pigment biosynthetic process	pigment biosynthetic process	GO:0046148	Downregulated
regulation of imaginal disc-derived wing size	R3/R4 cell fate commitment	GO:0007464	Downregulated
	larval somatic muscle development	GO:0007526	Downregulated
	post-embryonic hemopoiesis	GO:0035166	Downregulated
	larval lymph gland hemopoiesis	GO:0035167	Downregulated
	regulation of imaginal disc-derived wing size	GO:0044719	Downregulated
	R3/R4 cell differentiation	GO:0048056	Downregulated
	R7 cell development	GO:0045467	Downregulated
	eye photoreceptor cell fate commitment	GO:0042706	Downregulated
	compound eye photoreceptor fate commitment	GO:0001752	Downregulated
	photoreceptor cell fate commitment	GO:0046552	Downregulated
	establishment of ommatidial planar polarity	GO:0042067	Downregulated
	R7 cell differentiation	GO:0045466	Downregulated
	neuron fate commitment	GO:0048663	Downregulated
	establishment of planar polarity	GO:0001736	Downregulated
	compound eye photoreceptor development	GO:0042051	Downregulated
	larval development	GO:0002164	Downregulated
	eye photoreceptor cell development	GO:0042462	Downregulated
	morphogenesis of a polarized epithelium	GO:0001738	Downregulated
	photoreceptor cell development	GO:0042461	Downregulated
somatic muscle development	somatic muscle development	GO:0007525	Downregulated

	visual perception	GO:0007601	Downregulated
	sensory perception of light stimulus	GO:0050953	Downregulated
visual perception	sensory perception of chemical stimulus	GO:0007606	Downregulated
	detection of stimulus involved in sensory perception	GO:0050906	Downregulated

Table 1.5. Biological categories found to have significantly changed expression patterns during cold-stress of *P. imparis*.

Summary	Biological category	GO term	Direction
coenzyme biosynthetic process	coenzyme biosynthetic process	GO:0009108	Upregulated
	pyridine nucleotide metabolic process	GO:0019362	Upregulated
DNA integration	DNA integration	GO:0015074	Downregulated

Chapter 2 Thermal acclimation ability varies at lower limits between high- and low-elevation populations of *Prenolepis imparis*

2.1 Introduction

One of the top drivers of biodiversity loss is climate change (Sala et al., 2000). When these novel climatic conditions are physiologically stressful, species will need to either adapt via genetic change, migrate, face extinction, or persist via plasticity (Fuller et al., 2010). Migration to a new suitable habitat will prove to be difficult for most species, though it is possible (Parmesan & Yohe, 2003). Of the potential outcomes stressed species will face, adaptation and plasticity are the only options which do not involve local extinction. Though there are examples of rapid heritable genetic changes in populations from climate change (Bradshaw & Holzapfel, 2008), most organisms' life-spans are too long and climate change is happening too fast for the evolution of adaptive heritable traits. In this case, an organisms' susceptibility to these new environmental conditions can be buffered by plasticity in fitness-related traits (Huey et al., 2012; Seebacher, White, & Franklin, 2015; Somero, 2010). In order to understand how species will respond to these changing conditions, we need a better understanding of how plastic fitness-related traits, such as thermal tolerance, are in natural populations (Bozinovic, Calosi, & Spicer, 2011; Fuller et al., 2010; Seebacher et al., 2015).

Populations of a species are likely to be occupying a heterogeneous environment, thus they are expected to have evolved novel physiological adaptations, tolerances, and acclimatization capacities, especially those occupying ecological gradients such as those found along latitudinal and altitudinal transects (Bozinovic et al., 2011). Though patterns of plasticity in populations of organisms will be important in understanding responses to climate change, the drivers behind the evolution of phenotypic plasticity are unclear. One hypothesis is that climate variability is expected to increase thermal tolerance (climate variability hypothesis; CVH) (Addo-Bediako, Chown, & Gaston, 2000; Bishop, Robertson, Van Rensburg, & Parr, 2017; Bozinovic et al., 2011; Pither, 2003; Shah, Gill, et al., 2017; Shah, Funk, & Ghalambor, 2017; Sunday, Bates, & Dulvy, 2011) and thermal plasticity (Vázquez, Gianoli, Morris, & Bozinovic, 2017). Sites along latitudinal and elevation transects are typically temperature gradients (Körner, 2007) with populations at high elevation and high latitude experiencing more daily and seasonal variability (A. A. Hoffmann, Chown, & Clusella-Trullas, 2013). An analysis of previous studies done by Gunderson and Stillman (2015) found plasticity in cold thermal tolerance can be associated with seasonality. This pattern is not the same for both upper and lower limits. This

same study was unable to relate plasticity in heat tolerance with latitude or seasonality. In addition to being influenced by climate, plasticity might be an evolutionary trade-off, that is, the evolution of thermal tolerance has been done at the expense of plasticity of this tolerance, especially for those organisms already close to their thermal limits (Calosi, Bilton, Spicer, Votier, & Atfield, 2010; A. A. Hoffmann et al., 2013; Stillman, 2003; Sunday et al., 2011).

Ectotherms, such as ants, will be especially affected by climate change as many basic biological functions rely on temperature such as growth, reproduction, and foraging. Ants are also ecologically dominant and useful as models to study effects of climate change because they are typically constrained by temperature and are sensitive to the climate (Netherer & Schopf, 2010). Models based on physiological thermal tolerances in ants predict that tropical ants have lower warming tolerances and hence are at the most risk from climate change (Diamond et al., 2012). Hoffmann et al. (2013) noted that insects from mid-latitudes (20° to 40°) are particularly susceptible to stress from warmer temperatures. Gunderson and Stillman (2015) found that plasticity in thermal tolerance should be able to mitigate effects of climate change. Though in terrestrial ectotherms, upper limits have less variation (Bishop et al., 2017; Sunday et al., 2011) and lower plasticity (A. A. Hoffmann et al., 2013). There have been a few studies on the acclimation capacity of thermal tolerances in ants (Angilletta et al., 2007; Chown, Jumbam, Sørensen, & Terblanche, 2009; Clusella‐Trullas, Terblanche, & Chown, 2010; Diamond, Chick, Perez, Strickler, & Martin, 2017; Jumbam, Jackson, Terblanche, McGeoch, & Chown, 2008; Oms, Cerdá, & Boulay, 2017). However, none of these studies look at an ant that is sensitive to high temperatures and thus expected to be at risk from climate change.

The winter ant (*Prenolepis imparis*) is particularly well suited for studying the response to temperature changes. It is found across a large elevational gradient in California and thus provides an opportunity to study adaptations in a variety of different natural populations. Worker ants are usually found in high abundance when colonies are actively foraging (Fellers, 1989; Lynch, Balinsky, & Vail, 1980). *Prenolepis imparis* is sensitive to high temperatures – workers are rarely seen at temperatures exceeding 26°C. At the same time, *P. imparis* is adapted to cold temperatures – workers are able to forage during the cooler months, when other ants decrease activity (Tschinkel, 1987). The workers can even be seen foraging at near-freezing temperatures (Talbot, 1943). They are typically seen above ground in high numbers between the months of October and April. All other times of the year, they are rarely found above ground (Tschinkel 1987). These unique physiological requirements and broad geographic range make the winter ant a good candidate to study plastic responses to thermal stress.

In this study, we examine populations of *P. imparis* for evidence of localized patterns of thermal tolerance and plasticity. We used slower knockdown time and faster chill-coma recovery in individuals of *P. imparis* as indicators of hot or cold tolerance respectively (Maysov & Kipyatkov, 2009). Plasticity can be non-reversible (developmental plasticity) or occur over a short time (reversible acclimation) (Piersma & Drent, 2003). Here, we will use a short-term reversible acclimation as a plasticity measurement to test the two non-mutually exclusive hypotheses: (1) the CVH, which predicts that populations which experience more variable temperatures (such as will be experienced by high-elevation populations) will have a greater thermal tolerance and acclimation ability relative to those populations that occur in more stable environments (low-elevation) (2) the trade-off hypothesis, which predicts that increased thermal tolerance will come at the expense of acclimation capacity. An additional hypothesis is that we will see less variation and lower plasticity in upper thermal limits across populations. Besides testing these hypotheses, we will also characterize some environmental thermal characteristics

the populations encounter to ask the question, are there any environmental differences experienced between the high- and low-elevation sites that we can detect? To do this, we will compare the values for the 19 bioclimatic variables available from WorldClim at our sites (Table 2.1) (Fick & Hijmans, 2017; Hijmans, Cameron, Parra, Jones, & Jarvis, 2005). Bioclimatic models typically use macroclimate (M. Austin, 2007) and so might not necessarily reflect the actual temperatures the populations experience. In order to characterize the microclimate, we will employ dataloggers both above and below ground and look for localized differences.

2.2 Methods

We chose populations of *P. imparis* for physiology tests based on their elevation. We wanted populations from both high and low elevation across California, which should reflect high and low temperature variability respectively. Ants were collected from four low elevation sites (71–388m) and from four high elevation sites (973–1442m). Elevation and GPS coordinates were taken at all locations using a Garmin GPS (model, WGS1984; Table 2.2).

Field temperatures

In order to assess the thermal environment at both high- and low-elevation, we collected both macroclimate and microclimate data. For the macroclimate, indices of environmental temperature were calculated from 30 years of average monthly data (1970 – 2000) available from WorldClim. We obtained these 19 bioclimatic variables using the latitude and longitude we collected at the sites with the highest resolution available, approximately 1km (30 arc-seconds) (Fick & Hijmans, 2017; Hijmans et al., 2005). However, remotely sensed environmental data do not necessarily reflect the conditions experienced by ants, so we also collected temperatures locally to better represent those temperatures experienced by the ants. The microclimate was collected at a subset of localities (Table 2.3 & 2.4). At these sites, we measured ambient air temperatures and underground temperature once per hour from January 2015 to August 2017. To do this, we placed iButtons (Maxim Integrated, DS1922L) in the field two meters above the ants' nests and at least 60cm underground at the sites used in this study, as this is the minimum depth we expect to find nesting chambers (Tschinkel, 1987). With these data, we extracted the minimum and maximum temperature at each month for those sites which had available data for every month in a year. We were then able to calculate most of the analogous bioclimatic variables underground and just above the ants' nests. Because we did not have precipitation data, we could not create those variables which included precipitation as a factor (Bio8, Bio9, Bio12 – Bio19). We created these variables using the minimum and maximum temperatures for every month over a year using the *dismo* package (Hijmans, Phillips, Leathwick, & Elith, 2010) in R version 3.3.1 (R Core Team 2016) in RStudio 0.99.473 (RStudio Team 2015) (Table 2.1, Supp.Table B.1). In addition to these data, we also looked at the daily mean temperatures between the low- and high-elevation sites for an entire two years (2015 & 2016).

Physiology trials

Only non-replete foragers were collected for use in physiology experiments. To acclimate these individuals to a constant temperature, they were divided into two separate 20cm diameter plastic tubs containing a dish of 20% sugar water solution and two nesting chambers. Each tub

contained approximately 125 ants when the collection numbers allowed. One plastic tub was placed in an incubator (Fisher Scientific, CAT# 11-690-650D) at 27°C (warm-acclimated) and the other was placed in a Conviron CMP3246 growth chamber at 10°C (cold-acclimated). Both treatments were kept in the dark for the entire acclimation time. To reduce positional effects of acclimation temperature, ant tubs were periodically rearranged within the chamber or incubator. Dead ants were removed and sugar water changed every three days. The ants were kept in these conditions for at least seven days, after which we performed thermal tolerance assays.

We measured chill-coma recovery time (CCRT), which is the time required for ants to resume an upright position after exposure to a chill-coma inducing temperature (Macmillan, Williams, Staples, & Sinclair, 2012). We entombed ants in ice for three hours, which, in preliminary trials is the amount of time it took to ensure all individuals were in chill-coma, but not long enough that they were unable to recover. To do this, ants were placed in a glass petri dish, which was then placed on ice in a Styrofoam cooler. Ice was then placed on top of the glass petri dish, and the cooler lid was closed. After the designated time, they were removed and immediately placed on their backs on a piece of paper in a 140mm Petri dish. CCRT was recorded for each ant. Approximately five replicates of ten ants each were repeated for each population when collection numbers allowed (Table 2.2). Ants that did not recover within 20 minutes of being returned to room temperature were considered to have incurred chill injury (Castañeda, Lardies, & Bozinovic, 2005), these data were recorded as twenty minutes, with a delta of 1 and flagged as being right-censored (see Data analysis, below). Approximately five replicates of ten ants were recorded for each population (Table 2.1).

For heat tolerance assays, we placed replicates of ten ants on a 140mm Petri dish with Insect-A-Slip (BioQuip, CA, USA) coated sides. The Petri dish was floated in a pre-warmed water bath (Fisher Scientific Isotemp digital-control water bath). The surface of the Petri dish was continuously monitored with a self-adhesive thermocouple (SA1-T-SRTC, Omega, CT, USA), and temperature kept at 43° ± 1°C. This temperature was chosen for heat stress because, in preliminary trials, ants at this temperature did not die immediately and experienced knockdown before fifteen minutes (data not shown). The time it took for ants to experience loss of coordination (knockdown time) was recorded for each ant. Approximately five replicates of ten ants each were recorded for each population (Table 2.1).

After thermal testing, all ants used for CCRT and knockdown trials were frozen on dry ice and preserved in 100% ethanol. The dry weight of these samples was taken after evaporating the ethanol in a drying oven for at least one hour.

Data analysis

All data were analyzed in R version 3.3.1 (R Core Team 2016) in RStudio 0.99.473 (RStudio Team 2015). We used accelerated failure time models to analyze both knockdown and chill-coma trials in the *survival* package (Therneau, 2016; Therneau & Grambsch, 2000). For our data, "survival" corresponded to "remaining standing" or "remaining in chill-coma". We included in the model "delta" which corresponds to survival after the temperature trial. This model was chosen over the more commonly used over Cox Proportional Hazards (PH) in order to overcome the violation of proportionality of hazards rates (C. M. Williams et al., 2014). To choose the most parsimonious model, we pooled populations according to elevation, then we compared exponential, Weibull, Gaussian, logistic, lognormal, and loglogistic error distributions. We simplified the model by removing nonsignificant interactions and conditions until no further

simplification was possible. Using a training set, we selected the model where Akaike information criterion (AIC) was smallest (Lebreton, Burnham, Clobert, & Anderson, 1992). To account for the skewed distributions of knockdown and CCRT, we report the predicted means for the survreg object as calculated by the predict function in the *survival* package (Therneau, 2016). These means were then used to calculate the amount of plasticity. Similar to Gunderson and Stillman (2015), we calculated the plasticity (or acclimation response) as the change in knockdown or recovery time with a given change in acclimation temperature. However, these numbers are not comparable to values calculated by Gunderson and Stillman (2015) because they are not change in critical thermal limits with a given change in acclimation temperature (Table 2.5).

2.3 Results

Approximately 250 worker ants were collected from each test population via aspirator primarily during the months of January, February, and March 2015. Samples from one population (Mt. Diablo) were collected March 2017. Average dry weight of the individuals ranged from 0.78 – 1.28mg (Table 2.2). Dry weight of the individuals did not differ between high- and low-elevation ($t = -0.707$, $df = 4.034$, p-value = 0.519).

For each of our temperature datasets (macroclimate, above ground, and below ground) we used a t-test to test for differences experienced between high- and low-elevation populations. Significance was evaluated using Bonferroni-corrected p-values. Our tests indicate there were no differences detected between any of the 19 environmental variables calculated from WorldClim (Table 2.6). For our above ground microclimate data, we were able to calculate 9 bioclimatic variables for the Berkeley, Whittier, Stebbins, Quail Ridge, Castle Rock, Mt. Diablo, and Palomar sites (Table 2.3 & 2.4, Supp. Table B.1). After Bonferroni-correcting for non-independence between our temperatures, we did not detect any differences between the high- and low-elevation populations. For our underground microclimate data, we calculated the same 9 bioclimatic variables for the Berkeley, Whittier, Quail Ridge, Castle Rock, Mt Diablo, and Palomar populations (Table 2.3 & 2.4, Supp. Table B.1). In this case, we detected differences between the annual mean temperature and the mean temperature of the coldest quarter (Bio 1 & Bio 11) between the high- and low- elevation populations (Table 2.6). In both cases, the high-elevation sites experienced cooler temperatures (Supp. Table B.1). During 2015 and 2016, the mean daily above ground field temperatures differed significantly between the low- and high-elevation sites ($t = 12.236$, $df = 1298$, p-value < 0.001). The mean daily temperatures for the low-elevation sites ranged from 5.2°-30.3°C (mean 17.3±4.9°C) and the high-elevation sites experienced average daily above ground temperatures of -3.3°-29.7°C (mean 13.4±7.1°C). In addition, the mean daily below ground field temperatures differed significantly between the low- and high-elevation sites ($t = 20.288$, $df = 1298$, p-value < 0.001). The average daily below ground temperatures for the low-elevation sites ranged from 12.6°-22.6°C (mean 17.3±3.0°C) and the average daily below ground temperatures for the high-elevation sites ranged from of 5.1°-19.1°C (mean 12.5±4.0°C). The high-elevation sites were cooler above ground 809/907 days of the overlapping recorded days and 904/907 days below ground.

Chill-coma recovery

After three hours of ice-entombment, all ants were in chill-coma. Ants that were acclimated to the lower temperature recovered from the chill-coma faster than the ants acclimated to the high temperature ($z = -42.59$, $p < 0.0001$, Table 2.2). The most parsimonious model for CCRT was the Weibull error distribution. The ants from high-elevation sites recovered faster than the ants from low-elevation sites after warm-acclimation (z-score = 5.93, $p<0.0001$). The mean CCRT of the individuals from the low-elevation sites was 173s (cold-acclimated) 739s (warm-acclimated) while the mean CCRT of the individuals from the high-elevation sites was 142s (cold-acclimated and 606s (warm-acclimated) (Fig. 2.1a, Table 2.2).

The acclimation response for CCRT was much larger than knockdown reaction norms (see below), indicating more plasticity in this phenotype. For the low-elevation populations, the individuals from the Berkeley, Stebbins, and Whittier sites took the longest to recover and showed the most plasticity in recovering from the cold. While individuals from the high-elevation sites, Mt Diablo, Palomar Mtn., Yosemite, and Castle Rock as well as individuals from the highest of the low-elevation populations, Quail Ridge, recovered faster and showed less plasticity (Fig. 2.2, Table 2.5).

Knockdown trials

Ants acclimated to a lower temperature succumbed to the heat much faster than they did after they were acclimated to a high temperature (z-score = -9.09, $p<0.0001$). The most parsimonious model for the knockdown trials was the lognormal error distribution. The mean knockdown time for individuals from the four low-elevation populations was 49s (cold-acclimated), whereas they took 105s when warm-acclimated. The mean knockdown time of the individuals from the four high-elevation populations was 57s when cold-acclimated while they took 121s to knockdown when warm-acclimated (Fig. 2.1b, Table 2.5). There was no statistical difference between the time it took for individuals from low- and high-elevation sites to succumb to the heat ($z = -1.42$, $p = 0.16$).

The difference in knockdown times created by acclimating the individuals indicate relatively low levels of plasticity: acclimation increased the ants' ability to withstand the heat by a relatively small amount across all populations. Except for individuals from the Yosemite populations, all other ants lost coordination at roughly similar times. Overall, the Yosemite population seems to be an outlier. The individuals from this population resisted the heat much better than the other populations after both acclimation temperatures (Fig. 2.2, Table 2.5).

2.4 Discussion

The ability of an organism to survive rapid temperature changes will depend on their ability to buffer these changes via adaptive responses such as thermal plasticity (Gunderson & Stillman, 2015; Huey et al., 2012; Somero, 2010). There are two main hypotheses that explain patterns seen in thermal tolerance and acclimation ability. One, the climate variability hypothesis (CVH) posits that organisms from more variable climates will be under greater selection for thermal acclimation ability than those from stable environments (Bozinovic et al. 2011; Sunday et al. 2011). Another one, the "trade-off hypothesis" predicts that organisms that evolve high levels of thermal tolerance do so at the expense of the acclimation ability (Stillman 2003; Hoffmann et al. 2013, Calosi et al 2010). We did not find evidence to support the CVH at either upper or lower limits. Instead we found that the high-elevation sites showed increased tolerance and reduced

capacity in acclimation ability relative to the low-elevation counterparts at their lower limits, suggesting an evolutionary trade-off between tolerance and acclimation ability. We also found that both above and below ground, ants from the high-elevation sites experienced cooler temperatures. This exposure to constantly cooler temperatures allows individuals from high-elevation sites to be better physiologically prepared to survive the cold even after exposure to high-temperatures. This could suggest these individuals have the ability to rapidly acclimate to these temperatures as has been suggested by a study of cane toads in cool-climates (McCann, Kosmala, Greenlees, & Shine, 2018). This also suggests cold tolerance is physiologically costly and could be selected against in warmer conditions (Gibert, Moreteau, Pétavy, Karan, & David, 2007).

Finally, we hypothesized we would find less variation and lower plasticity at the upper thermal limits of the populations. This appears to hold true for our populations. With the exception of individuals from the Yosemite population, all the other individuals succumbed to heat at similar times. In addition to responding to heat in a similar way, all the populations had lower plasticity relative to the amount of plasticity experienced at the lower thermal limits. A pattern of lower acclimation capacity to the heat as we have found here, has also been found in other studies which suggests that acclimation and adaptation to high temperatures is more challenging than low temperatures (Addo-Bediako et al., 2000; García-Robledo, Kuprewicz, Staines, Erwin, & Kress, 2016; Gunderson & Stillman, 2015; Overgaard, Kristensen, Mitchell, & Hoffmann, 2011). This is particularly troubling in the context of climate change as the vulnerability of a taxon to rising temperatures will also depend on their ability to acclimate (Gunderson & Stillman, 2015). The winter ants might have been able to avoid extensive exposure to the heat thus far by remaining underground during the hottest temperatures, but as the climate heats more, they will have to spend more time underground and this could limit their ability to forage successfully.

It is still unclear how thermal tolerance of the workers correlates with overall fitness of the colony or of the queen and how this relationship of tolerance and activity plays out in natural populations. These ants should be able to exploit their small size and use the thermal heterogeneity in the environment. Hemmings and Andrew (2017) found that ants in environments that exceed their thermal tolerances can maintain lower body temperatures than the surrounding temperatures suggesting they are using unknown behavioral or physiological methods to regulate their body temperature.

The localized patterns of plasticity in populations of *P. imparis* could be due to microclimate differences, genetic differences, or maternal affects. Our experimental design does not allow us to distinguish the processes behind the patterns. The importance of these factors could be resolved using a common garden experiment, in which multiple generations are reared under controlled lab conditions (A. Hoffmann & Sgrò, 2017; Kawecki & Ebert, 2004).

Here, we have shown that individuals from our high-elevation sites experience cooler temperatures both above and below ground and show greater thermal tolerance but lower plasticity to the cold, while all populations display less tolerance and reduced plasticity to the heat. This is troubling in the face of climate change, this limited acclimation response at the upper thermal limits suggests evolutionary constraints in heat tolerance, so major changes at the molecular level will be needed for these populations to persist in warmer environments. Low-elevation populations might be particularly vulnerable if they are unable to buffer rapid temperature changes.

2.5 Acknowledgements

We need to thank Philip Lee and Sebastian Lee for being extremely helpful with collecting and hole digging. We would also like to thank Jennifer Robles and Michael Puzzo for help in the field. We also thank Rachel Slatyer for her patience and help with data analysis. We also thank Alex Gunderson and Jonathon Stillman for helpful discussions.

2.6 Figures

Figure 2.1. Survivorship curves for low-and high-elevation populations of *P. imparis*. Each line represents the combined totals of four populations. (a) Chill-coma recovery times of high-elevation (black lines) and low-elevation sites (gray lines) after acclimation to both low (dashed lines) and high (solid lines) temperature. (b) Knockdown times of the high-elevation (black lines) and low-elevation sites (gray lines) after acclimation to both low (dashed lines) and high (solid lines) temperature.

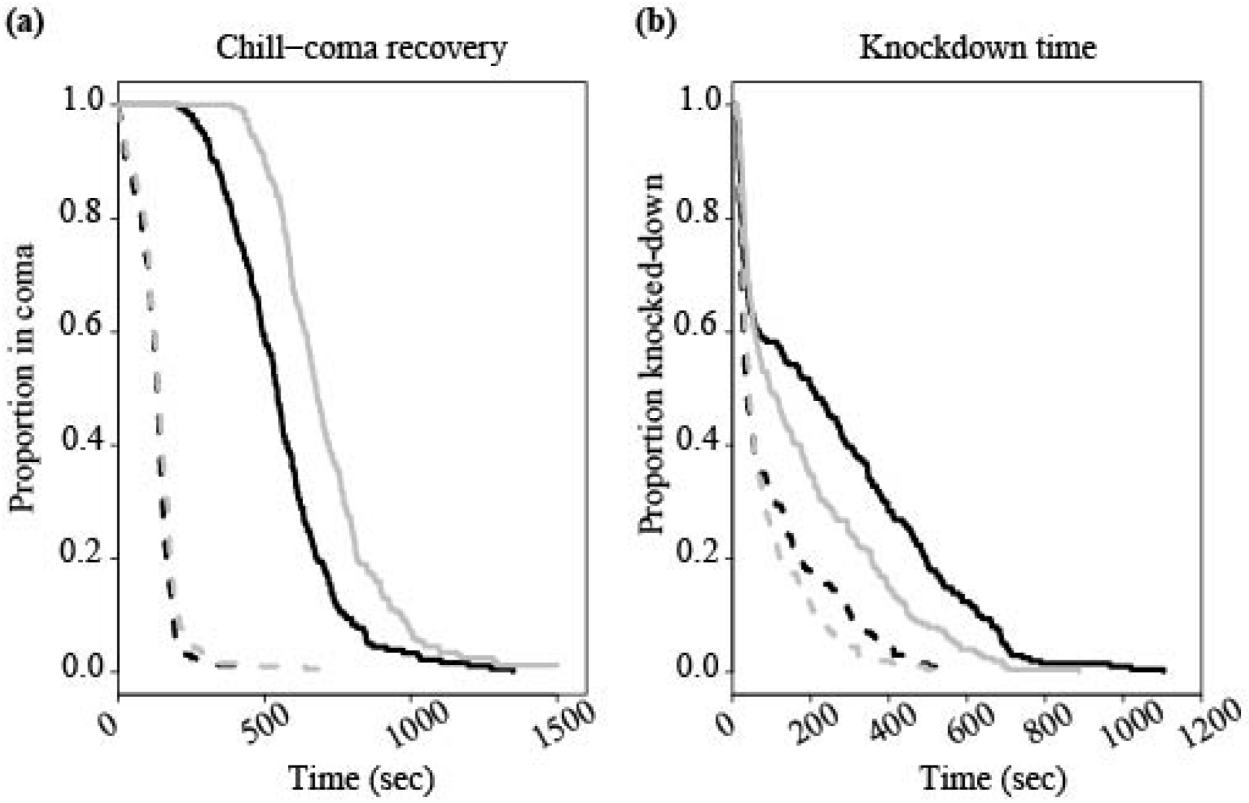

Figure 2.2. Mean chill-coma recovery times (CCRT) and knockdown times for populations of *P. imparis* (± SE). Each line represents the predicted average from all individuals tested. (a) CCRT acclimation response at 10°C and 27°C. (b) Knockdown acclimation response times at 10°C and 27°C.

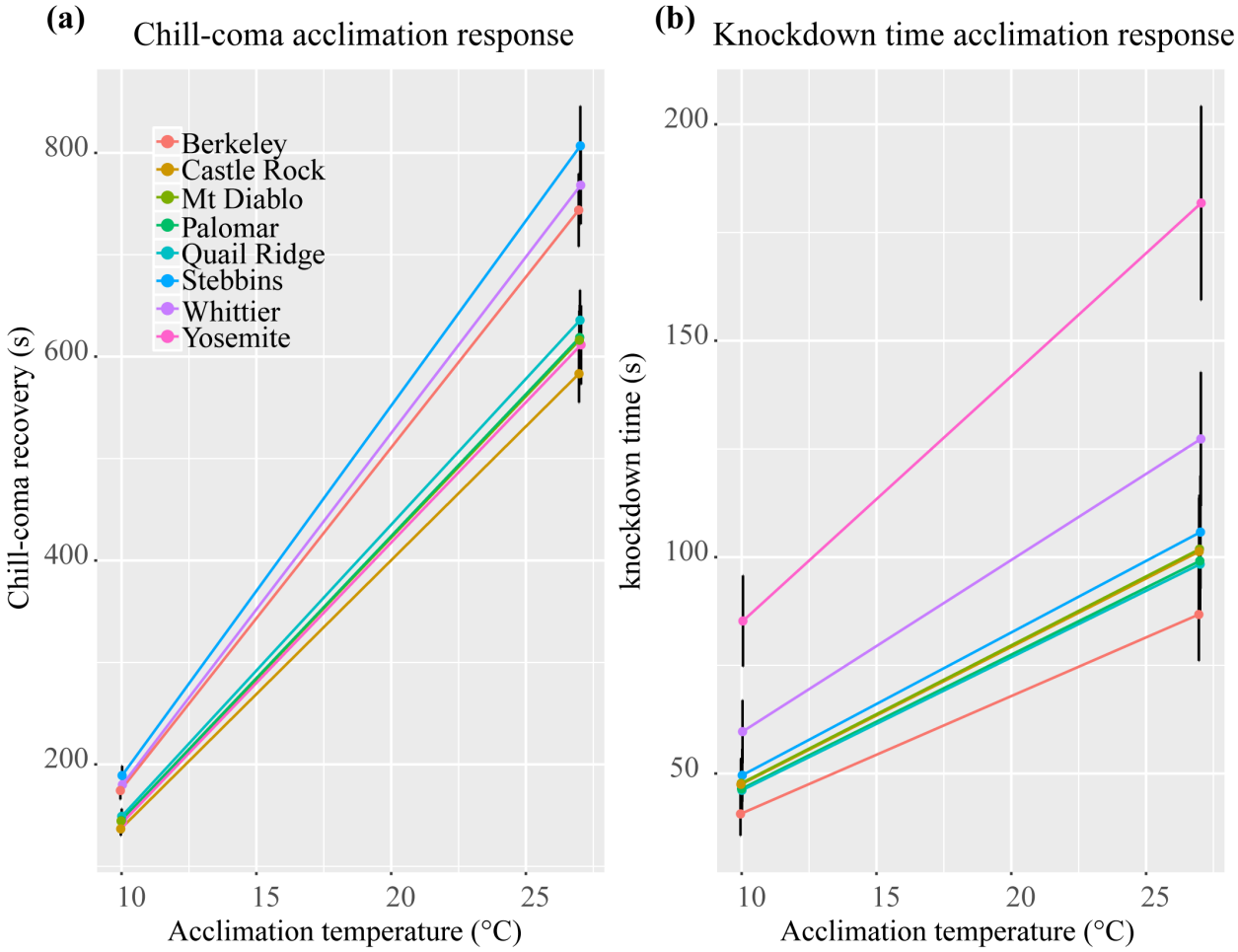

2.7 Tables

Table 2.1. A listing of the 19 climatic variables found in the WorldClim dataset.

abbreviation	environmental variable
Bio1[1]	Annual mean temperature
Bio2[1]	Mean diurnal temperature range (mean of monthly maximum temperature minus minimum temperature)
Bio3[1]	Isothermality (Bio2/Bio7 * 100)
Bio4[1]	Temperature seasonality (standard deviation of monthly temperature)
Bio5[1]	Minimum temperature of the coldest month
Bio6[1]	Maximum temperature of the warmest month
Bio7[1]	Temperature range (maximum temperature of the warmest month minus minimum temperature of the coldest month)
Bio8	Mean temperature of wettest quarter (i.e. mean temperature of four consecutive wettest months)
Bio9	Mean temperature of driest quarter
Bio10[1]	Mean temperature of warmest quarter
Bio11[1]	Mean temperature of coldest quarter
Bio12	Annual precipitation
Bio13	Precipitation of wettest month
Bio14	Precipitation of driest month
Bio15	Precipitation seasonality (standard deviation of monthly precipitation)
Bio16	Precipitation of driest quarter
Bio17	Precipitation of wettest quarter
Bio18	Precipitation of warmest quarter
Bio19	Precipitation of coldest quarter

[1] These environmental variables are calculated irrespective of precipitation

Table 2.2. Locality name, altitude (m), GPS coordinates (longitude and latitude), and mean weight are given. For each trial: chill-coma recovery and knockdown, total number sampled as well as number of biological replicates and the range of individuals per replicate in parentheses for each acclimation temperature is also given.

					CCRT				knockdown			
locality	**alt (m)**	**longitude**	**latitude**	**weight[1] (mg)**	**n 10ºC**	**br**	**n 27ºC**	**br**	**n 10ºC**	**br**	**n 27ºC**	**br**
Berkeley	71	-122.26317	37.87281	1.00	47	5 (8-10)	49	5 (9-10)	50	5 (10)	50	5 (10)
Whittier	100	-118.05395	34.00381	0.78	49	5 (9-11)	51	5 (10-11)	51	5 (10-11)	52	5 (9-13)
Stebbins Cold Canyon Reserve	109	-122.09678	38.50867	0.90	48	5 (9-10)	50	5 (10)	50	5 (10)	50	5 (10)
Quail Ridge Reserve	388	-122.14895	38.48307	0.88	49	5 (9-11)	50	5 (10)	50	5 (10)	50	5 (10)
Castle Rock State Park	973	-122.09495	37.22829	0.82	50	5 (10)	48	5 (8-10)	50	5 (10)	51	5 (10-11)
Mt. Diablo State Park	1130	-121.916667	37.219167	0.83	49	5 (9-10)	49	5 (8-11)	50	5 (10)	50	5 (10)
Yosemite National Park	1233	-119.58584	37.74763	1.28	14	2 (4-10)	36	4 (7-10)	50	5 (10)	50	5 (10)
Palomar Mountain State Park	1442	-116.92146	33.34078	0.95	50	5 (10)	47	5 (8-10)	50	5 (10)	50	5 (10)

[1] Indicates mean dry weight of individuals tested
n = total number of individuals tested
br = total number of biological replicates, with the range of the number of individuals in parentheses

Table 2.3. Populations in which above ground temperature was collected during 2015 and 2016. The number 1 indicates for that site, over the entire month, hourly above ground temperatures were collected.

	2015												2016											2017							
site	**J**	**F**	**M**	**A**	**M**	**J**	**J**	**A**	**S**	**O**	**N**	**D**	**J**	**F**	**M**	**A**	**M**	**J**	**J**	**A**	**S**	**O**	**N**	**D**	**J**	**F**	**M**	**A**	**M**	**J**	**J**
Berkeley	1	1	1	1	1											1	1	1	1	1	1	1	1	1	1	1	1	1			
Whittier	1	1	1	1	1	1	1	1	1	1	1	1	1	1	1	1	1	1	1	1	1	1	1								
Stebbins			1	1	1	1	1	1	1	1	1	1	1	1																	
Quail Ridge	1	1	1	1	1	1	1	1	1	1	1	1	1	1																	
Castle Rock			1	1	1	1	1	1	1	1	1	1	1	1	1	1	1	1	1												
Mt Diablo																1	1	1	1	1	1	1	1	1	1	1	1	1			
Yosemite	1	1	1	1																											
Palomar			1	1	1	1	1	1	1	1	1	1	1	1	1	1	1	1	1	1	1	1	1	1	1	1	1	1	1	1	1

Table 2.4. Populations in which underground temperature was collected during 2015 and 2016. The number 1 indicates for that site, over the entire month, hourly underground temperatures were collected.

	2015												2016												2017							
site	**J**	**F**	**M**	**A**	**M**	**J**	**J**	**A**	**S**	**O**	**N**	**D**	**J**	**F**	**M**	**A**	**M**	**J**	**J**	**A**	**S**	**O**	**N**	**D**	**J**	**F**	**M**	**A**	**M**	**J**	**J**	**A**
Berkeley						1	1	1	1	1	1	1	1	1	1	1	1		1	1	1											
Whittier	1	1	1	1	1	1	1	1	1	1	1	1	1	1	1	1	1	1	1	1	1	1	1									
Quail Ridge	1	1	1	1	1	1	1	1	1	1	1	1	1	1	1	1	1	1	1	1	1	1	1	1	1							
Castle Rock								1	1	1	1	1	1	1	1	1	1	1	1													
Mt Diablo																1	1	1	1	1	1	1	1	1	1	1	1					
Yosemite	1	1	1	1																												
Palomar			1	1	1	1	1	1	1	1	1	1	1	1	1	1	1	1	1	1	1	1	1	1	1	1	1	1	1	1	1	1

Table 2.5. For each locality, chill-coma recovery times (CCRT) and knockdown times after a 10°C and 27°C acclimation are reported. Units for CCRT and knockdown are reported in seconds as calculated from predicted means. The amount of plasticity found in populations of *P. imparis* is also reported. Plasticity was calculated as the change in CCRT or knockdown per degree of temperature change.

	CCRT			knockdown		
locality	**10°C acclimation**	**27°C acclimation**	**plasticity**	**10°C acclimation**	**27°C acclimation**	**plasticity**
Berkeley	174	744	33.50	41	87	2.71
Whittier	180	768	34.60	60	127	3.98
Stebbins	189	807	36.43	50	106	3.30
Quail Ridge	149	636	28.63	46	98	3.07
Castle Rock	137	583	26.27	47	101	3.16
Mt Diablo	144	616	27.75	48	102	3.18
Yosemite	143	612	27.54	85	182	5.68
Palomar	145	619	27.87	46	99	3.10

Table 2.6. Paired samples t-tests comparing high- and low-elevation climatic variables. Significant p-values in bold.

Worldclim				Above ground			Underground		
	t	**df**	***p*-value[a]**	**t**	**df**	***p*-value[b]**	**t**	**df**	***p*-value[b]**
Bio1	2.792	5.644	0.034	4.571	4.873	0.006	-19.793	2.542	**0.001**
Bio2	-0.403	4.335	0.706	-0.728	-0.728	0.501	0.691	3.423	0.533
Bio3	0.608	5.619	0.567	-0.307	4.971	0.771	-1.605	2.597	0.221
Bio4	-0.802	5.797	0.454	-0.077	4.958	0.942	1.655	2.219	0.227
Bio5	0.483	4.201	0.653	1.142	4.461	0.311	-3.860	2.357	0.047
Bio6	2.065	5.925	0.085	4.391	4.873	0.008	-5.775	2.075	0.026
Bio7	-0.543	5.232	0.610	-0.265	4.365	0.803	1.391	2.143	0.291
Bio8	1.871	5.832	0.112	NA	NA	NA	NA	NA	NA
Bio9	1.015	4.218	0.365	NA	NA	NA	NA	NA	NA
Bio10	1.113	4.100	0.327	2.573	4.875	0.051	-4.570	2.162	0.039
Bio11	1.980	5.961	0.095	1.793	4.498	0.139	-7.761	3.416	**0.003**
Bio12	-1.806	5.739	0.123	NA	NA	NA	NA	NA	NA
Bio13	-0.687	4.404	0.527	NA	NA	NA	NA	NA	NA
Bio14	-2.029	3.321	0.127	NA	NA	NA	NA	NA	NA
Bio15	2.494	3.854	0.070	NA	NA	NA	NA	NA	NA
Bio16	-1.419	5.001	0.215	NA	NA	NA	NA	NA	NA
Bio17	-1.889	3.110	0.152	NA	NA	NA	NA	NA	NA
Bio18	1.931	3.271	0.141	NA	NA	NA	NA	NA	NA
Bio19	-1.257	4.811	0.266	NA	NA	NA	NA	NA	NA

[a]significance Bonferroni-corrected p-value < 0.001
[b]significance Bonferroni-corrected p-value < 0.006

Chapter 3 Phylogeography and population genetics of a widespread North American ant, *Prenolepis imparis*

3.1 Introduction

Past climate change has left signatures in population structure and species boundaries. The Quaternary (2.4 mya to the present) glacial cycles are often cited as important in shaping the biodiversity throughout the northern temperate regions. During this time, there were series of major ice ages (Hewitt, 1996). Comparisons of genetic variation spanning historically glaciated and unglaciated regions can reveal phylogeographic barriers and uncover genetic breaks not associated with current geographic boundaries. The Pleistocene epoch (1.8 – 0.01 mya) in particular is known for numerous climatic fluctuations between glacial and interglacial periods (Clark & Mix, 2002). During the last glacial maximum (LGM) in North America (~22-18 kya), ice sheets extended from southern Alaska throughout most of Canada and into the northeastern and northwestern United States (Mann & Hamilton, 1995).

Species-specific traits will allow for individualistic responses to these climate cycles (M. Davis & Shaw, 2001; Soltis, Morris, McLachlan, Manos, & Soltis, 2006; Stewart, Lister, Barnes, & Dalen, 2010). For example, warm-adapted species experienced contractions or retreated to southern refugia as the glacier expanded (Alberdi et al., 2015; M. Davis & Shaw, 2001). In these cases, postglacial expansion into previously uninhabitable regions has likely been important in shaping these populations and species (Guiher & Burbrink, 2008; Hewitt, 1996). These leading populations can show reduced genomic variation as founding events lead to loss of alleles and homozygosity (Lait & Hebert, 2018). In contrast, cold-adapted species retreated to northern refugia during interglacials (Beatty & Provan, 2010; Shapiro et al., 2004; Stewart et al., 2010). In these cases, populations and species there are expected to be characterized by deeper structure and/or distinct genetic lineages (Lee-Yaw, Irwin, & Green, 2008; Loehr et al., 2006).

In addition to species-specific responses, populations south of ice sheets retained higher genetic diversity that was accentuated by topographic features such as mountains and rivers, which created barriers to gene flow or refugia. These low-latitude populations are often characterized by deeper evolutionary histories. For example, populations would have been isolated on the sky-islands of the US Southwest (west Texas, Southern New Mexico, southern Arizona, and southern California) (Galbreath, Hafner, & Zamudio, 2009; Hope et al., 2016; Hope, Panter, Cook, Talbot, & Nagorsen, 2014). Other localities, such as

California, experienced moderate temperature oscillations (Graham, 1999) relative to eastern North America, which allowed populations to expand and contract regionally within and between microrefugia (Gugger, Ikegami, & Sork, 2013; Sork, Gugger, Chen, & Werth, 2016).

The separate biogeographic histories of these regions (northeastern North America, northwestern North America, and sky-islands in the southwest) should be reflected in patterns of faunal diversity, if the fauna evolve *in situ* over evolutionary time in these regions. Widespread taxa can be particularly useful to study the genetic effects of climate cycles on population diversification and fragmentation in these regions (Spellman & Klicka, 2007). In addition to a broad range, those organisms with restricted dispersal capabilities should maintain genetic patterns created while occupying that region (Hewitt, 1996). Ants are excellent models for phylogeographic analyses because they have low vagility (Peeters & Ito, 2001) and can be widespread. The winter ant, *Prenolepis imparis*, is widespread across North America and cold-adapted, making it an ideal organism to infer genetic structure and examine the effects of climatic cycles on demographic history. This species is closely associated with oak trees and, to a lesser extent, pine trees (Cuautle et al., 2016; Frye & Frye, 2012; Wheeler, 1930). It is the only nominal species in North America, and its closest sister taxon (*Prenolepis nitens*) is found throughout southeastern Europe (LaPolla, Brady, & Shattuck, 2010; J. L. Williams & LaPolla, 2016). Molecular evidence suggests *P. imparis* and *P. nitens* diverged in the Miocene approximately 12 – 5 mya (Matos-Maraví et al., 2018). The preference for cold temperatures and oak trees is shared by the common ancestor of both species (*P. heschei*) (Perkovsky, 2011). Morphological data from one or a few specimens suggest there are several subspecies (Fig. 3.1): *P. i. minuta* (United States, District of Columbia), *P. i. pumila* (United States, North Carolina), *P. i. testacea* (United States, District of Columbia), *P. i. californica* (United States, California), *P. i. arizonica* (Arizona), *P. i. colimana* (Mexico, Volcan de Colima), *P. i. coloradensis* (United States, Colorado), *P. i. veracruzensis* (Mexico, Veracruz) (J. L. Williams & LaPolla, 2016).

In this paper, we use genomic data to address the phylogeny of the winter ant in North America and to investigate processes involved in creating contemporary diversity. We sequenced Ultraconserved Elements (UCEs) available for Hymenoptera (Branstetter, Longino, Reyes-López, Schultz, & Brady, 2017) and combined phylogenetic analyses and population level analyses to examine the continental-scale phylogeographic patterns in this species, and given the diversity of historical forces across this spatial scale, we expected to see a variety of different evolutionary patterns. Some patterns between biogeographic regions we might see include 1) populations evolved *in situ* among separate regions, in which case we should see deep divergence between populations that have been isolated relative to shallower divisions between individuals within populations that would represent expansions out of refugia and 2) migration has always been high, in which case, migration between regions has been frequent enough that we won't be able to detect regional divergence, this could result in polytomies and unresolved nodes across the phylogeny.

3.2 Methods

We sequenced 73 individual ants that were collected from sites across the United States and Mexico (Fig. 3.1). We included two outgroup species: *Prenolepis nitens* and *Prenolepis*

naoroji. Samples were either hand collected by the authors or generously donated by collaborators and museums (See Supp. Table C.1).

Samples and DNA extraction

For specimens that were destructively sampled, genomic DNA was extracted from whole ants using a Qiagen DNeasy Blood & Tissue kit (Valencia, CA.). The kit protocol was followed as specified, with the following modifications: Samples were first ground in 1.5mL tubes with a stainless-steel grinding ball, 50µg RNase A and 10µL DTT were added to the lysis step, and finally, samples were eluted in 300µL RNase- and DNase-free water and then put in a vacuum-heater and evaporated down to 100µL. For specimens that were nondestructively sampled, the same modifications were used, except ants were not ground but, instead, placed whole in the lysis buffer and put in a rotating oven for 48 hours, with additional 20µL ProK added after the first 24 hours. These samples were then soaked in 70% ethanol solution before being re-mounted.

Following extraction, DNA was sheared using a Bioruptor sonicator (Diagenode) with 1 or 4 rounds of sonication (1 minute per round on low, 90s on and 90s off). If the sample was collected before the year 2000, or, if the sample was pinned prior to DNA extraction, we assumed the samples were partially degraded and they were only sonicated for a 1 minute shear time total, all others were sheared for 4 minutes. Because of low starting concentrations (often less than 100ng total DNA), the sheared DNA was not visualized on a gel. As the majority of the sequence variation is usually found upstream of the target sites for the UCE probes, we wanted longer size fragments (approximately 400-1000bp). However, without being able to visualize this, we did not know the size fragments of our extractions, so we purified the reaction following shearing using 0.7x low ratio Solid Phase Reversible Immobilization (SPRI) beads in order to remove smaller fragments.

Library preparation and array capture

Following sonication and purification, the DNA library preparation and array capture protocols were used as described in Meyer and Kircher (2010), with minor modifications. Most of those modifications were only introduced during the reaction clean-up. For all the purifications, we used 80% ethanol instead of 70% ethanol as stated in Meyer and Kircher (2010). In addition, 0.7x low ratio SPRI beads were used for purification after blunt-end repair and after indexing reactions in order to remove DNA fragments that are too sheared. Blunt-ends were repaired as in Meyer and Kircher (2010), except our mix had a final concentration of 0.05 U/µL of T4 DNA polymerase and 0.25U/µL of T4 polynucleotide kinase in 20µL of master mix. In addition, we combined three separate indexing PCRs (12 cycles) where every sample had a unique index number and combined identical samples to one final indexed library eluted in 22µL water (instead of EB) before enrichment. We assessed success of library preparation by measuring DNA concentrations with the Qubit flourometer and visualizing the libraries on an agarose gel.

For UCE enrichment, we made pools at equimolar concentrations containing eight uniquely labeled samples that were pooled together to contain 500ng total DNA. We performed enrichments using a custom UCE bait set developed for Hymenoptera (‘hym-v2’). This set has custom-designed probes targeting 2,590 UCE loci in Hymenoptera (Branstetter

et al., 2017). We followed library enrichment procedures for MYcroarray MYBaits kit (Mycroarray, Inc), except we used 0.1X concentration of the standard MYBaits, and added 5μL of the Roche Developer Reagent, and 1.0μL of 10mM custom blocking oligos designed for our custom tags (Meyer & Kircher, 2010). The enrichment was performed at 65°C for 22 hours. We then used 10μL of the library and cycled this 18 times during the amplification. Following post-enrichment PCR, we purified this reaction in 1.2X SPRI beads and eluted in 22 μL EB.

In order to verify enrichment, we performed qPCR on both our post-enrichment and unenriched libraries using a DyNAmo™ Flash SYBR® Green qPCR kit (Thermo Fisher Scientific). We checked that in our post-enrichment libraries, we saw a greater fold enrichment in our positive controls, UCE82, UCE591, and UCE1481, than the unenriched libraries (Faircloth, Branstetter, White, & Brady, 2015). We quantified each enriched pool using a Qubit flourometer, checked peak quality and peak library size using a Bioanalyzer. We then diluted them to less than 100nM and pooled them all at equimolar concentrations into the same sequencing lane. Sequencing was done using an Illumina HiSeq4000.

Bioinformatic processing

We used a custom Perl workflow to process UCE sequence capture data from methods described in Bi *et al.* (2012 and Portik *et al.* (2016). The pipeline for processing *de novo* target capture data are available in github (https://github.com/CGRL-QB3-UCBerkeley/denovoTargetCapturePhylogenomics). Briefly, raw fastq reads were filtered using Cutadapt (Martin, 2011) and Trimmomatic (Bolger et al., 2014) to remove low quality reads and adapter sequences. Exact duplicates were eliminated using Super Deduper (https://github.com/dstreett/Super-Deduper). We used FLASH (Magoč & Salzberg, 2011) to merge overlapping paired-end reads. We then used SPAdes (Bankevich et al., 2012) to assemble cleaned reads via a multi-kmer approach, to generate raw assemblies for each sample. We used BLASTn (S F Altschul, Gish, Miller, Myers, & Lipman, 1990) (evalue cutoff = 1e-10, similarity cutoff = 75) to compare SPAdes raw assemblies of each individual to the UCE baits to identify assembled contigs that stemmed from UCE loci. The resulting non-redundant UCE assemblies from each individual sample were used as a raw reference that includes the targeted UCE and the flanking sequences (+/-500bp to targeted UCE region). Paired-end and merged cleaned reads from each individual were then aligned to the individual-specific assemblies using Novoalign (Li & Durbin, 2009), and we only retained reads that mapped uniquely to the reference. We used Picard (http://broadinstitute.github.io/picard/) to add read groups and GATK (McKenna et al., 2010) to perform re-alignment around insertions/deletions. We finally used SAMtools/BCFtools (Li et al., 2009) to generate individual consensus sequences by calling genotypes and incorporate ambiguous sites in the individual-specific assemblies. Sites were masked as 'N's if the read depth was lower than 5x or if they were within 5bp near an indel. RepeatMasker (Smit et al. n.d., below) was implemented to mask (by using Ns) putatively repetitive elements against and short repeats, using the "ants" database. For each individual we retained a resulting consensus contig if no more than 80% of the nucleotides were Ns after the above masking. Multi-sample alignments of each locus were generated with MAFFT (Katoh & Standley, 2013) and ambiguously aligned regions in alignments were then trimmed using Trimal (Capella-Gutiérrez, Silla-Martínez, & Gabaldón, 2009). We retained alignments where at

least 30% of the samples containing no more than 60% missing data (Ns or gaps). We also calculated average read depth and trimmed off alignment that fell outside of the 2nd and 98th percentile of the distribution. To further control for potential paralogs, we also removed entire alignment in which any site where the maximum proportion of shared heterozygosity is above 0.3. Capture efficiency was evaluated by average per site depth for the target and +/- 500bp flanking regions for each locus, sensitivity, which is the percentage of bases within a target sequence that are recovered in one or more reads, and specificity, which determines the percentage of cleaned reads mapped to target and +/- 500bp flanking sequences.

Several museum samples had extremely low sensitivity, specificity, or coverage and were eliminated from the following analyses.

Phylogenetic analyses

We combined all filtered individual alignments in phylip format and made a partitioned file ready for RAxML analysis. We ran RAxML using several different datasets and analysis methods to account for the effects of missing data and data partitioning (Branstetter et al., 2017). We created one alignment that contained all the UCE loci recovered in our analyses. We also filtered the individual UCE alignments for 100% and 90% taxa present. We then created RAxML formatted alignments of the remaining concatenated loci. For each of the concatenated alignments, we created two files: one partitioned by gene, one unpartitioned. We analyzed each dataset with RAxML v8.1.17 (Stamatakis, 2014) with a rapid bootstrap analysis (100 replicates) plus best tree search (option "-f a") using GTR+Γ as the model of sequence evolution.

Population admixture

To infer the number and composition of our populations, we used both a model-based clustering method and a multivariate method. We used the program STRUCTURE v2.3.4 (Pritchard, Stephens, & Donnelly, 2000) to investigate the number of population clusters and potential admixture between populations in our dataset. This software uses a Bayesian algorithm that creates clusters that maximize Hardy-Weinberg equilibrium and gametic phase equilibrium within clusters and disequilibrium between clusters. We used one random informative SNP per locus from our *P. imparis* individuals only, initial runs of the entire SNP datasets were too computationally demanding. Ten iterations were run for each value of K from 1 (no population structure) to 10 (five more than the number of major clades we detected with RAxML), with a burn-in of 10,000 steps followed by 100,000 MCMC steps, under an admixture model. We summarized the results using CLUMPAK (Kopelman, Mayzel, Jakobsson, Rosenberg, & Mayrose, 2015) and visualized the results using the program DISTRUCT (Rosenberg, 2004). We evaluated populations with using highest ΔK method (Evanno, Regnaut, & Goudet, 2005). After initial runs suggested two main populations (see below), we further split the dataset into those two groups and ran STRUCTURE again on those groups independently using the same inputs as before. We also investigated the genetic split of populations using a discriminant analysis of principal components (DAPC) with ADEGENET 2.0 (Jombart, 2008; Jombart & Ahmed, 2011) in the program R using the function *dapc*. This multivariate analysis combines principal component analysis (PCA) and discriminant analysis to determine the number of genetic clusters. We initially investigated

the number of clusters by using the *k*-means algorithm. The preferred number of clusters was evaluated using the Bayesian information criterion (BIC) scores.

Summary statistics

We calculated the number of polymorphic loci both within and between populations. We used alignments for each UCE locus to calculate diversity within (Watterson's θ, π, Tajima's *D*) and between (corrected Dxy) populations using PopGenome (Pfeifer, Wittelsbuerger, Ramon-Onsins, & Lercher, 2014). Because the levels of diversity within each locus were so variable, we calculated the diversity for each locus individually and then calculated the mean value of all loci. Standard deviation was calculated as the square root of the sample mean/sample size.

3.3 Results

UCE Sequencing

The mean DNA sample concentration for our 75 taxa was 0.87 ng/μL (0.22 – 2.1 ng/μL) post-extraction, and 34.10 ng/μL (22.7 – 44 ng/μL) post-PCR libraries. The number of raw reads averaged at 1322.4 Mb (range: 217.5 – 3610.8 Mb) for individual samples. After cleaning, the average amount of recovered data was 352.7 Mb (range: 19.9 – 1269.6 Mb). The proportion of bases that was covered by least one read in in-target assemblies (sensitivity) was highly conserved across all samples with an average of 98.9% (range: 94.1 – 99.8%). The proportion of cleaned reads that mapped to the targeted UCE bait and +/- 500bp flanking regions (specificity) has an average of 40.6% among samples with a considerably wide range (0.07- 69.1%). Accordingly, coverage for both the target and flanking regions also varied wildly between samples (2.7 - 231X) with the average of 85X. The coverage for +/- 500bp flanking to the UCE regions where more variable sites are expected was also high with an average of 61.9X.

After filtering, our sequence capture recovered a total of 1,402 loci with a concatenated length of 1,029,532 bp. Locus length averaged 734 bp (range: 87 – 1106 bp) and contained an average of 4.6 polymorphisms per locus (range: 0 – 19 polymorphisms). Filtering the dataset to include only those loci that contained data from at least 90% of our samples (67/75 individuals) left us with 1,338 loci with a concatenated length of 1,001,687 bp. Further filtering to include only those loci that contained data from every sample left us with 772 loci with a concatenated length of 605,486 bp.

The UCE phylogeny using RAxML recovered strong geographical structuring of five main clades (Fig. 3.1 & 3.2a). All main clades were recovered with varying support (Supp. Fig. C.1) The strongest support was found when analyzing the 100% filtered dataset partitioned by gene; this tree provided the values we report (Fig. 3.2a). The most basal lineage comes from one individual in Florida (FL). After that, the phylogeny is split into two groups: one group from the east coast of the United States, and another group that spans the Western US and Mexico. These two main groups are further divided. On the east coast, there are two main clades: New England (NE) and southern US (SO; excluding Florida). On the West Coast, there is a group that includes individuals from Oregon and California (CA) and another group with deeply divergent individuals from the southwest and Mexico (AZ).

Within the CA clade, there are three well-supported branches (CAI, CAII, CAIII; Fig. 3.2 & 3.3). The deepest phylogenetic break (CAI) occurs between one individual, a microgynous queen (J. L. Williams & LaPolla, 2016) from the Sierra Nevadas in northern California and all the other individuals from California and Nevada. A second break in the CA clade, splits the Clade into roughly two parts, CAIII found across California and Nevada, and CAII found in southern California. Although all maximum likelihood analyses recovered the same main clades, the node separating the AZ clade and CA clade was only strongly supported with the 90% and 100% filtered dataset, partitioned by gene (Fig 3.2a, Supp. Fig. C.1). The splits between CAII and CAIII were only recovered with the 100% filtered dataset, both partitioned and unpartitioned (Supp. Fig. C.1).

Population admixture

The Bayesian clustering analysis based on 1,378 SNPs resulted in an initial detection of two main groups ($\Delta K = 4336.97$) (Fig. 3.2b). One group contained all the samples from the FL, NE, SO, and AZ clades while the other group consisted of only those samples from Oregon and California (CA clade). After these two groups were further split into two separate runs, the clustering analysis based on 27 individuals from the FL, NE, SO, AZ clades and 1,291 SNPs revealed three groups ($\Delta K = 24528.45$) consistent with main lineages found from the UCE phylogeny. One difference was that the one individual from the Florida clade was lumped either with the NE or SO clade (Fig 3.2c), though at K = 4, the FL clade is separated from the NE and SO clades (Supp. Fig. C.2). Within Oregon and California, the clustering analysis based on 46 individuals and 1,300 SNPs revealed the highest ΔK at three populations ($\Delta K = 67.05$). The most widespread cluster occurs in northern California up to Oregon, (corresponding to CAI and CAII) with admixed individuals in northern California. Another cluster occurs in southern California (corresponding to CAII), with admixed individuals on the central coast of California and on the Tehachapi Mountains (Fig. 3.2c & 3.3).

We used *k*-means clustering to confirm our five clusters of *P. imparis* and substructure within the CA clade. Using the entire dataset of *P. imparis* and SNPs (73 individuals and 36,582 SNPs), increasing the number of clusters from $n = 3$ to $n = 4$ yielded an improvement in BIC. BIC values at $n = 4$ to $n = 5$ were the same, suggesting both clusters are valid. At n = 4, with the exception of the FL and SO ants, each cluster roughly correspond to those clades found with the phylogeography and clusters in STRUCTURE (NE, AZ, CA). The FL and SO clades are grouped together. At $n = 5$, the FL and SO individuals are split into two groups that correspond to the original clade designations (Fig. 3.4a & c) Within the CA clade, the *k*-means clustering did not identify any distinct subpopulations (46 individuals, 19,105 SNPs) (Fig. 3.4b & d).

UCE summary statistics

Using the entire set of 1,402 loci, we estimated population levels of diversity using PopGenome (Table 3.1) (Pfeifer et al., 2014). The percent of polymorphic loci within and among clades varied. Within the major clades, the percent of polymorphic loci ranged from 3.32% – 23.09%, while there was considerably less variation between clades (18.49% – 27.48%). The AZ clade exhibited highest UCE nucleotide diversity (π), followed by the CA

clade, and finally the NE and SO clades exhibited the least amount of diversity. Values of Watterson's theta (θ_W), reflecting contemporary effective population size, followed a similar pattern: the AZ clade was highest, followed by the CA clade, and finally the SO and NE clades (Table 3.1). Tajima's D was lowest in the CA population, however, the standard deviation gives overlapping ranges for all clades.

Mean pairwise sequence divergence between clades ranged from 0.65% – 3.32% (Table 3.2). The CA and NE and SO clades were less than 1% divergent on average from each other. The AZ clade exhibited intermediate levels of divergence (1.18% – 1.52%), while the largest divergence was seen between the FL clade and all other populations (2.53% – 3.32%).

3.4 Discussion

The deep phylogeographic structure detected between five well-supported clades of *P. imparis* is consistent with long-term regional isolation of populations. These phylogenetic relationships among the clades suggest a high degree of geographic structure, as each of the major clades identified correspond to a group of geographically clustered populations. In addition, the populations from each region have separate histories that are reflected in their genome. Previous morphological work suggests there are several morphological types that roughly correspond to our clades, though more work will need to be done to understand the range limits of each morphological type and genomic clade found here.

The clades in the eastern United States (NE, SO) are consistent with what we expected to find in a cold-adapted species. The two lineages with deep division suggest two independently evolving populations that were isolated during the Last Glacial Maximum (LGM) in northern refugia. Species could have survived in close proximity to the Laurentide Ice Sheets (Soltis et al., 2006). The clades currently occupy a broad area, which makes it difficult to determine an exact refugia location, but they roughly overlap other northern refugial locations (e.g. interior plains, southern Highlands, Appalachians) (J. D. Austin, Lougheed, & Boag, 2004; Lee-Yaw et al., 2008). Previous ecological niche modelling done on an eastern North American white oak (*Quercus alba*) found these oaks would have been widespread in eastern North America during the last interglacial period (LIG; ~120 – 140 kya) (Gugger et al., 2013). During the LGM, these oak trees experienced a range contraction to the south. This retreat of their closely associated habitat could have left isolated populations near the edge of the ice sheets in the north that were able to expand into suitable habitat again when the oak trees expanded their range into their current range. The low genetic diversity in both the SO and NE clades seen here suggests recent expansion from these refugia. Interestingly, there are two morphological types that overlap in District of Columbia; we were unable to genotype the morphological specimens, so it is unknown what clade they represent, but both the STRUCTURE and ADEGENET results suggest there are no hybrids between clades.

The high levels of genetic diversity within the AZ clade suggest ancient and probably multiple vicariance events. Our AZ clade represents individuals from mountain ranges of the Madrean Archipelago of southeastern Arizona (Pinal and Chiricahua), the Bradshaw Mountains of central Arizona, the Davis Mountains of west Texas, and the Mexican states of Jalisco and Sonora. These sky-islands may have acted as refugia during unfavorable climatic conditions (Mastretta-Yanes et al., 2018). These mountain ranges are characterized by dry,

inhospitable low elevations and mesic habitats at high elevation (Bezy & Cole, 2014; Gómez-Mendoza & Arriaga, 2007; Jaggar & Palache, 1905). Populations on different mountain ranges that rely on cooler conditions such as those found in the mesic habitats are isolated from each other by the dry, desert conditions experienced at low altitude (Atwood et al., 2011; Carleton, Sáchez, & Vidales, 2002; Kerhoulas & Arbogast, 2010; Tennessen & Zamudio, 2008). These mountain ranges were likely colonized when conditions allowed for migration among contiguous mesic habitat throughout the valleys (McVay, Hauser, Hipp, & Manos, 2017; Tennessen & Zamudio, 2008). Migration between isolated mountain ranges would have depended on mesic corridors (Atwood et al., 2011). The timing of isolation and levels of gene flow among and between these mountain ranges remains unknown for most species. Periodic climate fluctuations during the Pleistocene would have resulted in cyclical contraction-expansion of suitable habitats (Provan & Bennett, 2008). During the LGM, areas such as northern Mexico and southwestern United States would have experienced cooler temperature and increased precipitation (Bradbury, 1997; Metcalfe, O'Hara, Caballero, & Davies, 2000; Pérez-Alquicira et al., 2010). These conditions would have been favorable for cold-adapted species such as *P. imparis*, as well as the oak and pine woodlands they are commonly associated with (Moreno-Letelier & Piñero, 2009). Despite more recent favorable conditions, genetic variation in a broad range of taxa (e.g. jumping spiders (Masta 2000), beetles (Smith and Farrell 2005), birds (McCormack et al. 2008; Puebla-Olivares et al. 2008), lizards (Tennessen and Zamudio 2008), pines (Moreno-Letelier and Piñero 2009), flying squirrels (Kerhoulas and Arbogast 2010), rattlesnakes (Bryson et al. 2011), and *Fouquieria* (Arturo De-Nova et al. 2018)) that occupy sky-islands in North American deserts found that gene flow among mountain ranges and lineages is limited and isolation ancient, while gene flow within ranges and lineages has been influenced by more recent migration during the Pleistocene. The high genetic diversity we see here supports ancient diversification and isolation among ranges. Current conditions in the southwest mountains and Mexico have created isolated populations of flora and fauna restricted to high altitude mountain tops surrounded by uninhabitable dry desert in the low lands (McVay et al., 2017). Given that there are at least four morphological types in this area, it seems likely that there are isolated cryptic lineages awaiting discovery. Further studies should increase sampling in these areas and investigate genetic diversity using a faster evolving marker (i.e. microsatellites) in order to determine the amount of local migration among and within these mountain ranges.

The higher genetic diversity and evidence for multiple populations of *P. imparis* within the CA clade suggest a very different evolutionary history than that of the eastern United States. The deepest phylogenetic break within the CA clade occurs between the microgynous queen (CAI) and the remaining samples (CAII and CAIII). It is unknown if this individual represents a distinct morph or a social parasite (J. L. Williams & LaPolla, 2016). The phylogenetic separation between this individual and all other ants in the CA clade is well-supported, while STRUCTURE attributed most of the genetic makeup to the widespread genotype and not a unique genotype. This is not surprising given STRUCTURE is influenced by sample size (Kalinowski, 2011). Given the distinct phylogenomic makeup of this individual, it would appear to be a social parasite, though more work will need to be done to understand the relationship between this queen and other individuals.

A second phylogenetic break occurs between individuals in northern California/Oregon and southern California (CAIII & CAII). According to populations inferred from the phylogeny, the northern limits of CAII includes individuals from the

Transverse Ranges (Northwest Transverse Range and the Tehachapi Mountains) and continues south to the Palomar Mountains. This implies the Transverse Ranges are important barriers in southern California for this species. Phylogeographic breaks associated with the Transverse Ranges are well documented (Calsbeek, 2003; Gottscho, 2016; Rissler, Hijmans, Graham, Moritz, & Wake, 2006). When it was possible to estimate the timing of separation between lineages, the genetic breaks seems to coincide with orogeny of the ranges and aridification in the region (Calsbeek, 2003). Genetic divergence between CAII and CAIII is relatively low which could reflect a late Pleistocene divergence, which would be coincident with the uplift of the Transverse Ranges. It is unclear if the individuals with mixed ancestry along the Southern Coastal Ranges represent retention of ancestral alleles or recent migration.

The results from STRUCTURE suggested a third genetic type (within CAIII) in the Sierra Nevadas and into the Northern Coastal Ranges. Most individuals with this third type are depicted as individuals with mixed ancestry, only one individual had this ancestry as a majority of its genotype (Fig. 2d & 3). An east/west split between populations in California has been noted many times before; the warm, dry area of the Central Valley poses a strong environmental barrier (Rissler et al., 2006). As suitable habitat retreated and expanded during the Pleistocene climatic fluctuations, populations of *P. imparis* would have been isolated on either side of the Central Valley, creating distinct populations with corridors of suitable habitat allowing migration.

The population differentiation within California suggests incomplete lineage sorting and/or some level of recent dispersal of individuals around California. The spatially concordant distribution of individuals from different populations may reflect range contractions, expansions, and migrations during glacial and interglacial periods, local persistence and maintained gene flow. This pattern is concordant with other studies that have found a relatively stable climate and topographic features relevant in creating differentiation in California (Calsbeek, 2003; Gharehaghaji, Minor, Ashley, Abraham, & Koenig, 2017; Gottscho, 2016; Rissler et al., 2006; Schierenbeck, 2017). Given that ADEGENET did not find evidence for subpopulations, more localized sampling of populations of *P. imparis* will be necessary to evaluate this discrepancy.

The phylogeographic pattern found in *P. imparis* is complex. Although we could not infer the absolute timing of these events, our inference from 1,402 UCE loci and combined analyses suggest that our phylogenetic results are due to *in situ* evolution and is supported by the fact that there are five well-supported clades, each which experienced local effects to the fluctuating climate. Individuals from these clades are genetically isolated and morphologically distinct. This raises the possibility that each clade represents a unique species, though more work will need to be done to determine this. In the east coast of North America, extant clades probably represent the descendants of isolated populations during the LGM that have recently expanded into their current range. In the southwest, we see sky-islands of endemism and high diversity suggesting fragmented populations. Across California and into Oregon, we see a different pattern still. This area was characterized by more moderate disruptions in climate patterns and which allowed persistence and local migration.

3.5 Acknowledgements

We would like to thank the many individuals and museums that provided us with samples: Benjamin Blanchard, Daniella Price, Stephen Yanoviak, James Trager, Jason Williams, Karl Roeder, Andrea Lucky and colleagues at School of Ants, Matthew Prebus, Andy Suarez, Brian Whyte, C Quock, Christian Irian, David Holway, Ida Naughton, Kelsey Schenkle, Matt Bollinger, Phil Ward, Alex Wild, Jack Longino, Robert Johnson, and the Cal Academy of Science. In addition, we would like to thank Michael Branstetter for information about the UCEs and discussions on how to get the best sequences from these ants. We also thank Sean Reilly for help with the California map. This project was funded by the Margaret C. Walker Fund for Systematics, and the Sigma Xi Grant In Aid of Research. This work used the Vincent J. Coates Genomics Sequencing Laboratory at UC Berkeley, supported by NIH S10 OD018174 Instrumentation Grant.

3.6 Figures

Figure 3.1. Map of United States and Mexico with samples used. Triangles denote morphologically designated varieties of *P. imparis*. Circles denote samples used in this study, and colors refer to major lineage as determined by maximum likelihood phylogeny.

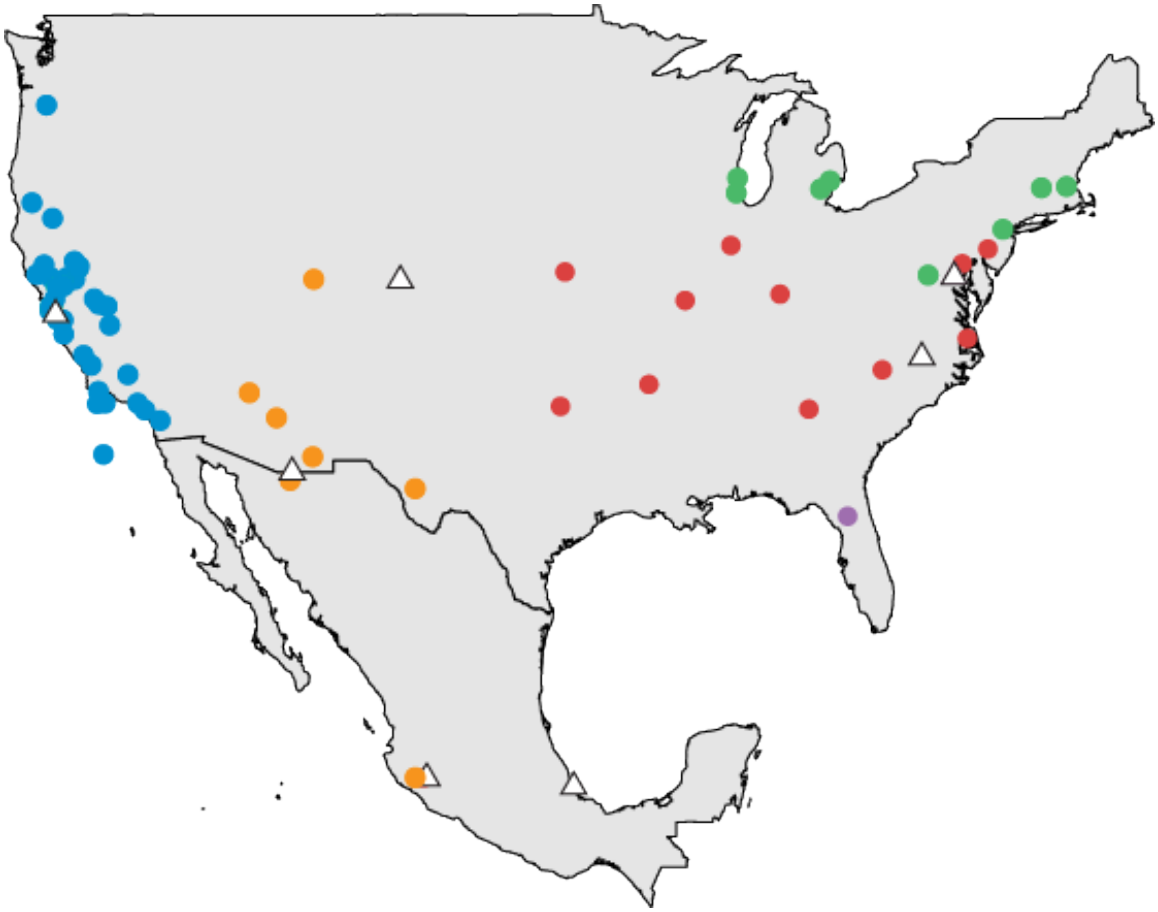

Figure 3.2. Phylogenetic and population clustering of *P. imparis* individuals. a) RAxML maximum likelihood tree created using 772 UCE loci, partitioned by gene, with support values on nodes. b) Population assignment results for 75 individuals and all clades (FL, NE, SO, AZ) based on K = 2 from STRUCTURE. Colors correspond to colored clades on the maximum likelihood tree and horizontal lines represent one individual. For each individual, the color proportion indicates the genetic contributions c) population assignment results for the FL, NE, SO, and AZ groups (K = 3), colors and bars are the same as above. d) Population assignments of the California clade (CA) at K = 3, colors and bars are the same as above.

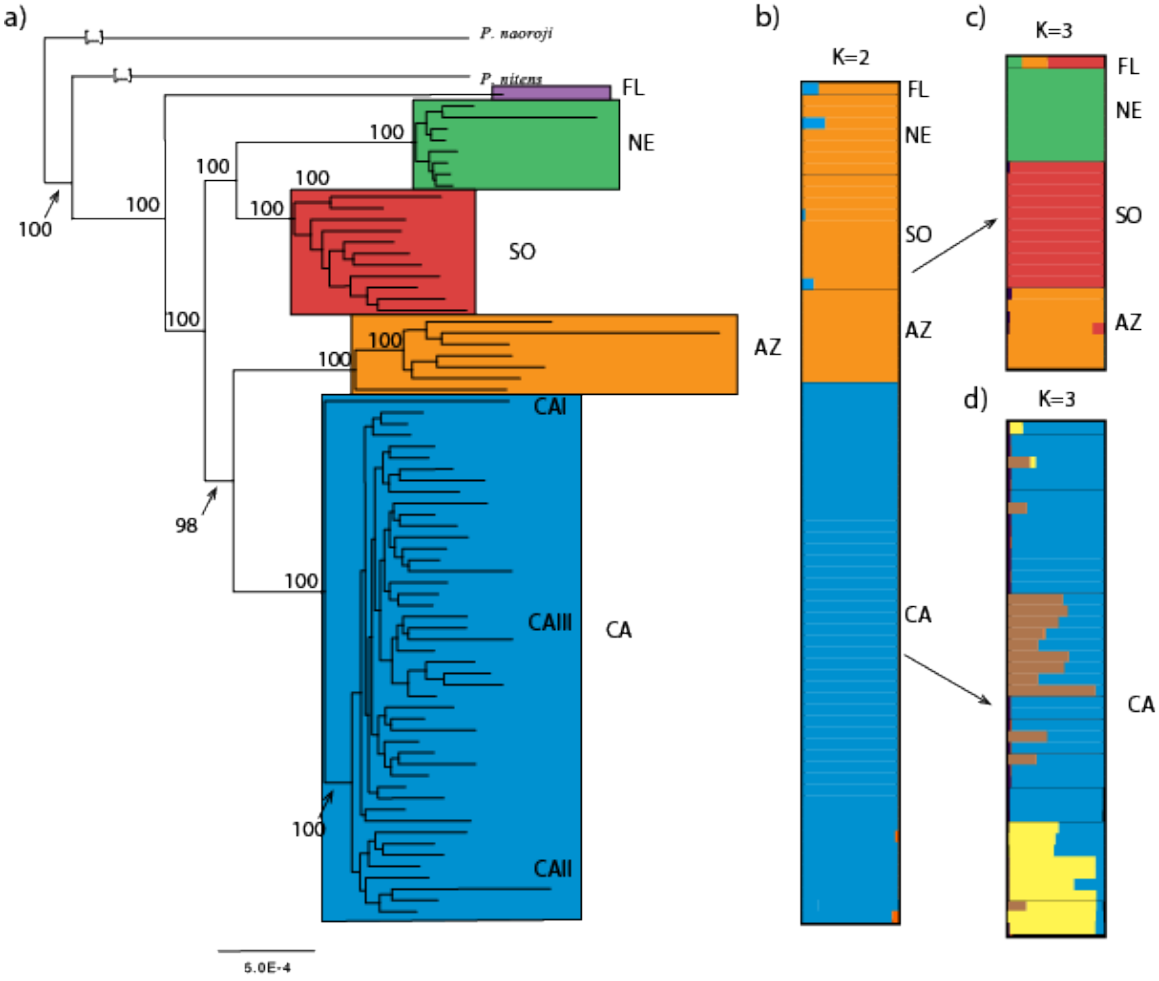

Figure 3.3. Map of California and the localities of genetic samples as circles. The colors of each sample locality correspond to the probabilities that the individual is assigned to one of the three genetic clusters. In addition, they are labeled according to their phylogenetic break. CAI, the microgynous queen, is indicated, CAII is circled, the remaining samples represent individuals from the CAIII cluster.

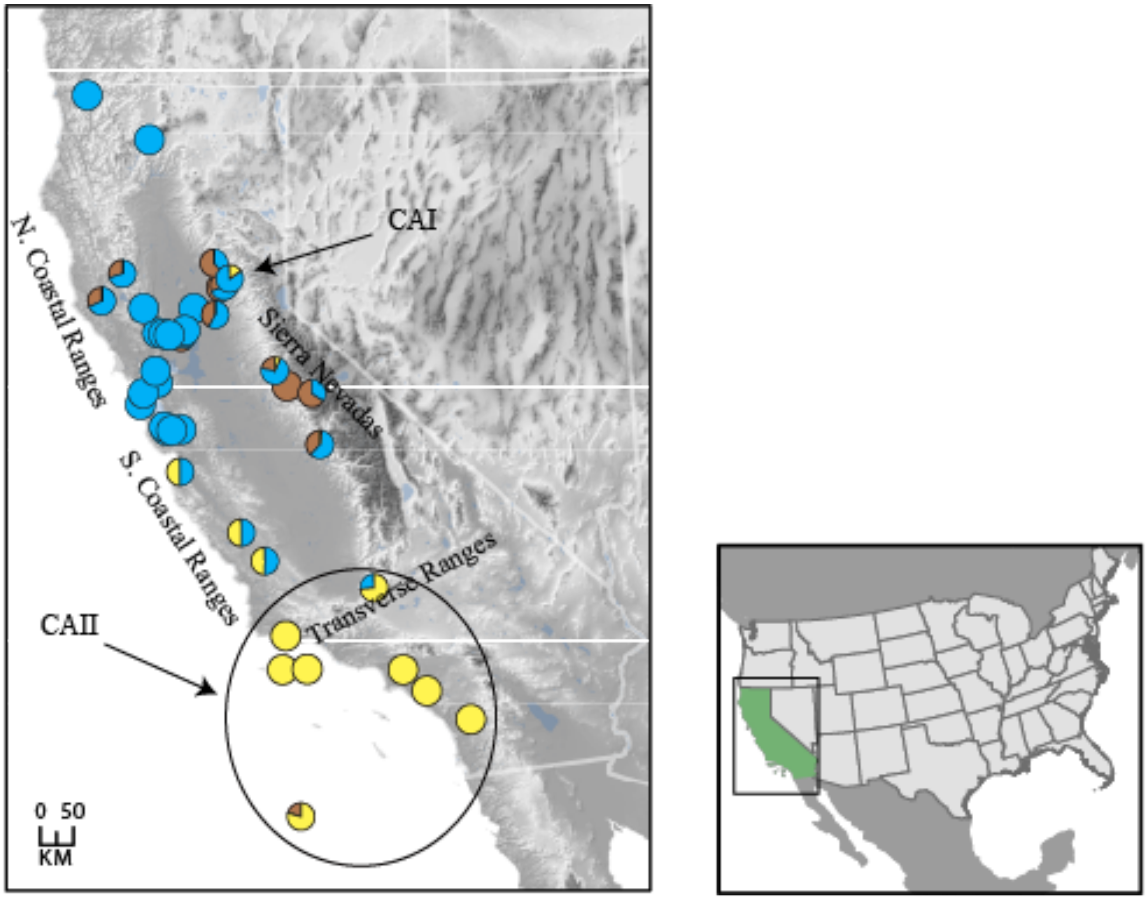

Figure 3.4. Nonparametric *k*-means clustering of total genetic diversity across all samples of *P. imparis*. a) Across all samples, increasing the number of clusters from $n = 3$ to $n = 4$ yielded improvement in Bayesian information criterion (BIC). Increasing the number of clusters from $n = 4$, to $n = 5$ did not reduce or increase our BIC scores. b) Within the CA clade, clustering suggests that all ants are drawn from the same population. c) Principal component analysis (PCA) for all samples. Clades are depicted by different colors and inertia ellipses, while dots represent individuals. d) PCA within the CA clade. Dots represent individuals.

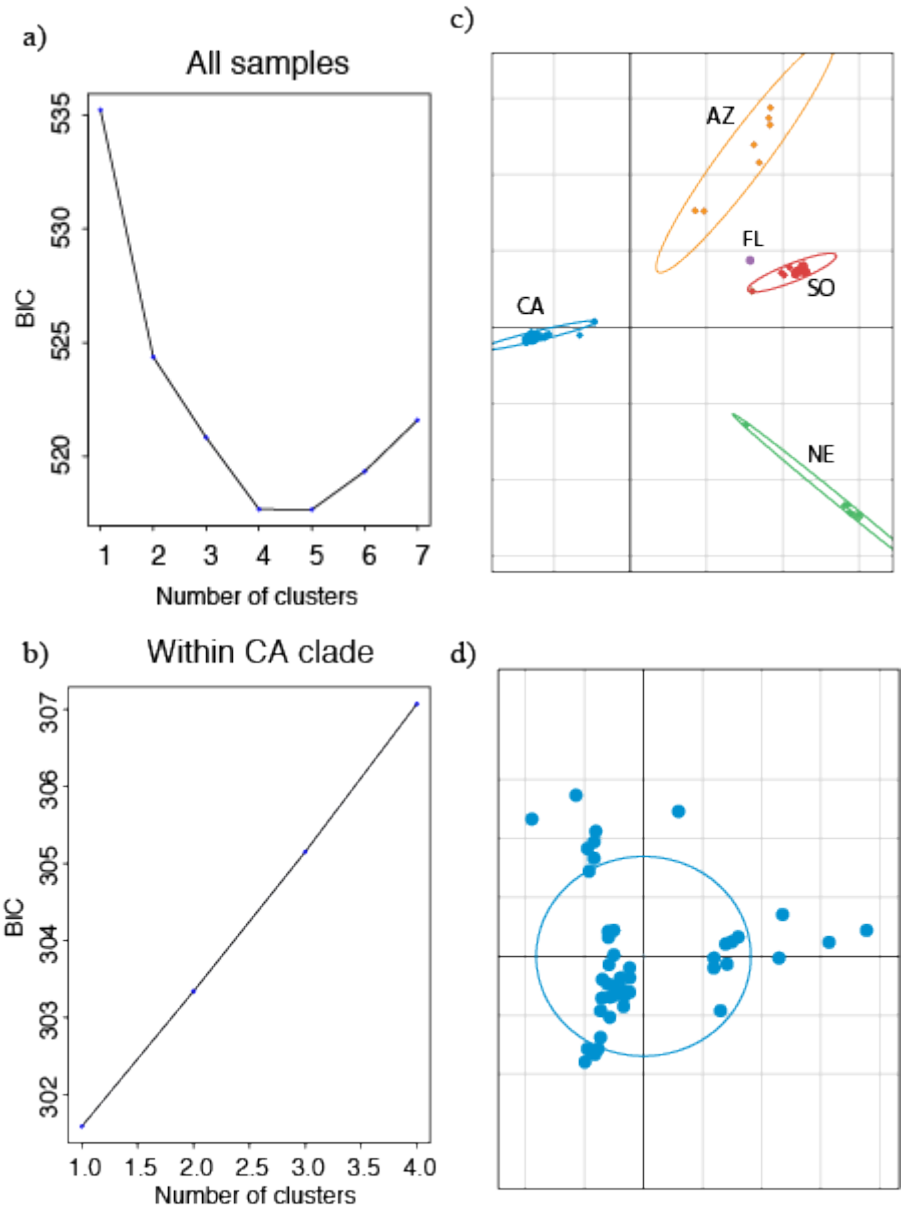

3.7 Tables

Table 3.1. Demographic statistics for UCEs of *P. imparis*. Number of individuals sequenced for each population as well as the number of polymorphic loci within population. Mean values (± SD) of number of polymorphic loci between clades and mean values (± SD) of population genetic summary statistics (Watterson's θ, nucleotide diversity (π; expressed as %), and Tajima's D from the entire UCE dataset.

clade	n	polymorphic loci within clades	polymorphic loci between clades	θ_W	π	Tajima's D
CA	46	20.97	26.36 (4.75)	0.077 (0.200)	0.0025 (0.010)	-1.29 (0.35)
AZ	7	23.09	27.18 (3.95)	0.161 (0.398)	0.0160 (0.047)	-0.88 (0.67)
NE	8	3.32	18.49 (4.92)	0.023 (0.139)	0.0018 (0.012)	-0.84 (1.22)
SO	11	5.57	18.65 (4.96)	0.028 (0.128)	0.0020 (0.011)	-1.08 (0.44)
FL	1	-	23.95 (5.37)	-	-	-

Table 3.2. Mean values (maximum) of corrected sequence divergence between populations.

	CA	AZ	NE	SO
AZ	1.22 (38.88)			
NE	0.66 (69.51)	1.52 (77.74)		
SO	0.35 (23.03)	1.18 (34.58)	0.65 (68.03)	
FL	2.57 (66.23)	3.32 (79.47)	2.91 (68.03)	2.53 (66.23)

Literature Cited

Addo-Bediako, A., Chown, S. L., & Gaston, K. J. (2000). Thermal tolerance, climatic variability and latitude. *Proceedings of the Royal Society B: Biological Sciences*, *267*(1445), 739–745. doi:10.1098/rspb.2000.1065

Alberdi, A., Gilbert, M. T. P., Razgour, O., Aizpurua, O., Aihartza, J., & Garin, I. (2015). Contrasting population-level responses to Pleistocene climatic oscillations in an alpine bat revealed by complete mitochondrial genomes and evolutionary history inference. *Journal of Biogeography*, *42*(9), 1689–1700. doi:10.1111/jbi.12535

Altschul, S. F., Gish, W., Miller, W., Myers, E. W., & Lipman, D. J. (1990). Basic local alignment search tool. *Journal of Molecular Biology*, *215*(3), 403–10. doi:10.1016/S0022-2836(05)80360-2

Altschul, S. F., Madden, T. L., Schäffer, A. A., Zhang, J., Zhang, Z., Miller, W., & Lipman, D. J. (1997). Gapped BLAST and PSI-BLAST: a new generation of protein database search programs. *Nucleic Acids Research*, *25*(17), 3389–3402. doi:10.1093/nar/25.17.3389

Angilletta, M. J., Wilson, R. S., Niehaus, A. C., Sears, M. W., Navas, C. A., & Ribeiro, P. L. (2007). Urban physiology: city ants possess high heat tolerance. *PLoS ONE*, (2), e258. doi:10.1371/journal.pone.0000258

Arndt, V., Dick, N., Tawo, R., Dreiseidler, M., Wenzel, D., Hesse, M., … Höhfeld, J. (2010). Chaperone-Assisted Selective Autophagy Is Essential for Muscle Maintenance. *Current Biology*, *20*(2), 143–148. doi:10.1016/j.cub.2009.11.022

Atwood, T. C., Young, J. K., Beckmann, J. P., Breck, S. W., Fike, J., Rhodes, O. E., & Bristow, K. D. (2011). Modeling connectivity of black bears in a desert sky island archipelago. *Biological Conservation*, *144*(12), 2851–2862. doi:10.1016/j.biocon.2011.08.002

Auld, J. R., Agrawal, A. A., & Relyea, R. A. (2010). Re-evaluating the costs and limits of adaptive phenotypic plasticity. *Proceedings of the Royal Society B: Biological Sciences*, *277*(1681), 503–511. doi:10.1098/rspb.2009.1355

Austin, J. D., Lougheed, S. C., & Boag, P. T. (2004). Discordant temporal and geographic patterns in maternal lineages of eastern north American frogs, *Rana catesbeiana* (Ranidae) and *Pseudacris crucifer* (Hylidae). *Molecular Phylogenetics and Evolution*, *32*(3), 799–816. doi:10.1016/j.ympev.2004.03.006

Austin, M. (2007). Species distribution models and ecological theory: A critical assessment and some possible new approaches. *Ecological Modelling*, *200*(1–2), 1–19. doi:10.1016/j.ecolmodel.2006.07.005

Bankevich, A., Nurk, S., Antipov, D., Gurevich, A. A., Dvorkin, M., Kulikov, A. S., … Pevzner, P. A. (2012). SPAdes: A New Genome Assembly Algorithm and Its Applications to Single-Cell Sequencing. *Journal of Computational Biology*, *19*(5), 455–477.

doi:10.1089/cmb.2012.0021
Barreto, F. S., Schoville, S. D., & Burton, R. S. (2015). Reverse genetics in the tide pool: Knock-down of target gene expression via RNA interference in the copepod *Tigriopus californicus*. *Molecular Ecology Resources*, *15*(4), 868–879. doi:10.1111/1755-0998.12359
Barshis, D. J., Ladner, J. T., Oliver, T. A., Seneca, F. O., Traylor-Knowles, N., & Palumbi, S. R. (2013). Genomic basis for coral resilience to climate change. *Proceedings of the National Academy of Sciences*, *110*(4), 1387–1392. doi:10.1073/pnas.1210224110
Beatty, G. E., & Provan, J. (2010). Refugial persistence and postglacial recolonization of North America by the cold-tolerant herbaceous plant *Orthilia secunda*. *Molecular Ecology*, *19*(22), 5009–5021. doi:10.1111/j.1365-294X.2010.04859.x
Bezy, R. L., & Cole, C. J. (2014). Amphibians and Reptiles of the Madrean Archipelago of Arizona and New Mexico. *American Museum Novitates*, *3810*, 1–24. doi:10.1206/3810.1
Bi, K., Vanderpool, D., Singhal, S., Linderoth, T., Moritz, C., & Good, J. M. (2012). Transcriptome-based exon capture enables highly cost-effective comparative genomic data collection at moderate evolutionary scales. *BMC Genomics*, *13*, 403. doi:10.1186/1471-2164-13-403
Bishop, T. R., Robertson, M. P., Van Rensburg, B. J., & Parr, C. L. (2017). Coping with the cold: minimum temperatures and thermal tolerances dominate the ecology of mountain ants. *Ecological Entomology*, *42*(2), 105–114. doi:10.1111/een.12364
Bolger, A. M., Lohse, M., & Usadel, B. (2014). Trimmomatic: A flexible trimmer for Illumina Sequence Data. Retrieved from http://dx.doi.org/10.1093/bioinformatics/btu170
Bonasio, R., Zhang, G., Ye, C., Mutti, N. S., Fang, X., Qin, N., … Liebig, J. (2010). Genomic Comparison of the Ants *Camponotus floridanus* and *Harpegnathos saltator*. *Science*, *329*, 1068–1071. doi:10.1126/science.1192428
Bozinovic, F., Calosi, P., & Spicer, J. I. (2011). Physiological correlates of geographic range in animals. *Annual Review of Ecology, Evolution, and Systematics*, *42*(1), 155–179. doi:10.1146/annurev-ecolsys-102710-145055
Bradbury, J. P. (1997). Sources of glacial moisture in Mesoamerica. *Quaternary International*, *43–44*(97), 97–110. doi:10.1016/S1040-6182(97)00025-6
Bradshaw, W. E., & Holzapfel, C. M. (2008). Genetic response to rapid climate change: it's seasonal timing that matters. *Molecular Ecology*, *17*, 157–166. doi:10.1111/j.1365-294X.2007.03509.x
Branstetter, M. G., Longino, J. T., Reyes-López, J., Schultz, T. R., & Brady, S. (2017). Into the tropics: phylogenomics and evolutionary dynamics of a contrarian clade of ants. *BioRxiv*, 105–108. doi:10.6056/dkyqt201601023
Bryson, R. W., Murphy, R. W., Lathrop, A., & Lazcano-Villareal, D. (2011). Evolutionary drivers of phylogeographical diversity in the highlands of Mexico: A case study of the *Crotalus triseriatus* species group of montane rattlesnakes. *Journal of Biogeography*, *38*(4), 697–710. doi:10.1111/j.1365-2699.2010.02431.x
Buckley, B. A., Gracey, A. Y., & Somero, G. N. (2006). The cellular response to heat stress in the goby *Gillichthys mirabilis*: a cDNA microarray and protein-level analysis. *Journal of Experimental Biology*, *209*(14), 2660–2677. doi:10.1242/jeb.02292
Buckley, B. A., & Somero, G. N. (2009). cDNA microarray analysis reveals the capacity of the cold-adapted Antarctic fish *Trematomus bernacchii* to alter gene expression in response to heat stress. *Polar Biology*, *32*(3), 403–415. doi:10.1007/s00300-008-0533-x
Bungard, D., Fuerth, B. J., Zeng, P.-Y., Faubert, B., Maas, N. L., Viollet, B., … Berger, S. L.

(2010). Signaling kinase AMPK activates stress-promoted transcription via Histone H2B phosphorylation. *Science*, *329*(September), 1201–1205.

Calosi, P., Bilton, D. T., Spicer, J. I., Votier, S. C., & Atfield, A. (2010). What determines a species' geographical range? Thermal biology and latitudinal range size relationships in European diving beetles (Coleoptera: Dytiscidae). *Journal of Animal Ecology*, *79*(1), 194–204. doi:10.1111/j.1365-2656.2009.01611.x

Calsbeek, R. et al. (2003). Patterns of molecular evolution and diversification in a biodiversity hotspot: the CA Floristic Province. *Molecular Ecology*, *12*, 1021–1029.

Capella-Gutiérrez, S., Silla-Martínez, J. M., & Gabaldón, T. (2009). trimAl: A tool for automated alignment trimming in large-scale phylogenetic analyses. *Bioinformatics*, *25*(15), 1972–1973. doi:10.1093/bioinformatics/btp348

Carleton, M. D., Sáchez, O., & Vidales, G. U. (2002). A new species of *Habromys* (Muroidea: Neotominae) from México, with generic review of species definitions and remarks on diversity patterns among Mesoamerican small mammals restricted to humid montane forests. *Proceedings of the Biological Society of Washington*, *115*(3), 488–533.

Castañeda, L. E., Lardies, M. a, & Bozinovic, F. (2005). Interpopulational variation in recovery time from chill coma along a geographic gradient: a study in the common woodlouse, *Porcellio laevis*. *Journal of Insect Physiology*, *51*(12), 1346–51. doi:10.1016/j.jinsphys.2005.08.005

Chevin, L. M., Lande, R., & Mace, G. M. (2010). Adaptation, plasticity, and extinction in a changing environment: towards a predictive theory. *PLoS Biology*, *8*(4), e1000357. doi:10.1371/journal.pbio.1000357

Chown, S. L., Jumbam, K. R., Sørensen, J. G., & Terblanche, J. S. (2009). Phenotypic variance, plasticity and heritability estimates of critical thermal limits depend on methodological context. *Functional Ecology*, *23*(1), 133–140. doi:10.1111/j.1365-2435.2008.01481.x

Clark, P. U., & Mix, A. C. (2002). Ice sheets and sea level of the Last Glacial Maximum. *Quaternary Science Reviews*, *21*, 1–7. doi:10.1016/S0277-3791(01)00118-4

Clements, J., Schoville, S., Peterson, N., Huseth, A. S., Lan, Q., & Groves, R. L. (2017). RNA interference of three up-regulated transcripts associated with insecticide resistance in an imidacloprid resistant population of *Leptinotarsa decemlineata*. *Pesticide Biochemistry and Physiology*, *135*, 35–40. doi:10.1016/j.pestbp.2016.07.001

Clusella-Trullas, S., Terblanche, J. S., & Chown, S. L. (2010). Phenotypic Plasticity of Locomotion Performance in the Seed Harvester *Messor capensis* (Formicidae). *Physiological and Biochemical Zoology*, *83*(3), 519–530. doi:10.1086/651387

Colinet, H., & Hoffmann, A. (2010). Gene and protein expression of *Drosophila Starvin* during cold stress and recovery from chill coma. *Insect Biochemistry and Molecular Biology*, *40*(5), 425–428. doi:10.1016/j.ibmb.2010.03.002

Colinet, H., Lee, S. F., & Hoffmann, A. (2010a). Functional characterization of the *Frost* gene in *Drosophila melanogaster*: Importance for recovery from chill coma. *PLoS ONE*, *5*(6), e10925. doi:10.1371/journal.pone.0010925

Colinet, H., Lee, S. F., & Hoffmann, A. (2010b). Temporal expression of heat shock genes during cold stress and recovery from chill coma in adult *Drosophila melanogaster*. *Federation of European Biochemical Societies Journal*, *277*, 174–185. doi:10.1111/j.1742-4658.2009.07470.x

Couger, M. B., Pipes, L., Squina, F., Prade, R., Siepel, A., Palermo, R., … Blood, P. D. (2014). Enabling large-scale next-generation sequence assembly with Blacklight. *Concurrency and*

Computation: Practice and Experience, *26*(March), 2157–2166. doi:10.1002/cpe

Coulson, M., Robert, S., & Saint, R. (2005). Drosophila *starvin* encodes a tissue-specific BAG-domain protein required for larval food uptake. *Genetics*, *171*(4), 1799–1812. doi:10.1534/genetics.105.043265

Cuautle, M., Vergara, C. H., & Badano, E. I. (2016). Comparison of Ant Community Diversity and Functional Group Composition Associated to Land Use Change in a Seasonally Dry Oak Forest. *Neotropical Entomology*, *45*(2), 170–179. doi:10.1007/s13744-015-0353-y

Davis, M. B., Shaw, R. G., & Etterson, J. R. (2005). Evolutionary responses to changing climate. *Ecology*, *86*(7), 1704–1714. doi:10.3109/03630269708997523

Davis, M., & Shaw, R. (2001). Range shifts and adaptive responses to Quaternary climate change. *Science*, *292*(April), 673–679. doi:10.1126/science.292.5517.673

De-Nova, J. A., Sánchez-Reyes, L. L., Eguiarte, L. E., & Magallón, S. (2018). Recent radiation and dispersal of an ancient lineage: the case of Fouquieria (Fouquiericeae, Ericales) in North American deserts. *Molecular Phylogenetics and Evolution*, *126*, 92–104. doi:10.1016/j.ympev.2018.03.026

Debec, A., Courgeon, A. M., Maingourd, M., & Masonhaute, C. (1990). The response of the centrosome to heat shock and related stressesin a *Drosophila* cell-line. *Journal of Cell Science*, *96*, 403–412.

DeBiasse, M. B., & Kelly, M. W. (2016). Plastic and evolved responses to global change: What can we learn from comparative transcriptomics? *Journal of Heredity*, *107*(1), 71–81. doi:10.1093/jhered/esv073

Di Ciano, C., Nie, Z., Szászi, K., Lewis, A., Uruno, T., Zhan, X., … Kapus, A. (2002). Osmotic stress-induced remodeling of the cortical cytoskeleton. *American Journal of Physiology. Cell Physiology*, *283*(3), C850-65. doi:10.1152/ajpcell.00018.2002

Diamond, S. E., Chick, L., Perez, A., Strickler, S. A., & Martin, R. A. (2017). Rapid evolution of ant thermal tolerance across an urban-rural temperature cline. *Biological Journal of the Linnean Society*, *121*(2), 248–257. doi:10.1093/biolinnean/blw047

Diamond, S. E., Sorger, D. M., Hulcr, J., Pelini, S. L., Toro, I. Del, Hirsch, C., … Dunn, R. R. (2012). Who likes it hot? A global analysis of the climatic, ecological, and evolutionary determinants of warming tolerance in ants. *Global Change Biology*, *18*(2), 448–456. doi:10.1111/j.1365-2486.2011.02542.x

Doong, H., Vrailas, A., & Kohn, E. C. (2002). What's in the "BAG"? – a functional domain analysis of the BAG-family proteins. *Cancer Letters*, *188*(1–2), 25–32.

Du, X. J., Wang, J. X., Liu, N., Zhao, X. F., Li, F. H., & Xiang, J. H. (2006). Identification and molecular characterization of a peritrophin-like protein from fleshy prawn (*Fenneropenaeus chinensis*). *Molecular Immunology*, *43*(10), 1633–1644. doi:10.1016/j.molimm.2005.09.018

Dunn, R. R., Parker, C. R., & Sanders, N. J. (2007). Temporal patterns of diversity: assessing the biotic and abiotic controls on ant assemblages. *Biological Journal of the Linnean Society*, *91*(2), 191–201. doi:10.1111/j.1095-8312.2007.00783.x

Elsik, C. G., Tayal, A., Diesh, C. M., Unni, D. R., Emery, M. L., Nguyen, H. N., & Hagen, D. E. (2016). Hymenoptera Genome Database: Integrating genome annotations in HymenopteraMine. *Nucleic Acids Research*, *44*(D1), D793–D800. doi:10.1093/nar/gkv1208

Evanno, G., Regnaut, S., & Goudet, J. (2005). Detecting the number of clusters of individuals using the software STRUCTURE: A simulation study. *Molecular Ecology*, *14*(8), 2611–2620. doi:10.1111/j.1365-294X.2005.02553.x

Faircloth, B. C., Branstetter, M. G., White, N. D., & Brady, S. G. (2015). Target enrichment of ultraconserved elements from arthropods provides a genomic perspective on relationships among Hymenoptera. *Molecular Ecology Resources*, *15*(3), 489–501.

Feder, M. E., Cartaño, N. V, Milos, L., Krebs, R. a, & Lindquist, S. L. (1996). Effect of engineering *Hsp70* copy number on Hsp70 expression and tolerance of ecologically relevant heat shock in larvae and pupae of *Drosophila melanogaster*. *The Journal of Experimental Biology*, *199*(Pt 8), 1837–1844.

Feder, M. E., & Hofman, G. E. (1999). Heat-shock proteins, molecular chaperones, and the stress response: evolutionary and ecological physiology. *Annual Review of Physiology*, *61*(1), 243–282. doi:10.1146/annurev.physiol.61.1.243

Fellers, J. H. (1989). Daily and seasonal activity in woodland ants. *Oecologia*, *78*, 69–76.

Fick, S. E., & Hijmans, R. J. (2017). WorldClim2: new 1-km spatial resolution climate surfaces for global land areas. *International Journal of Climatology*, *37*(12), 4302–4315. doi:10.1002/joc.5086

Fink, A. L. (1999). Chaperone-Mediated Protein Folding. *Physiological Reviews*, *79*(2), 425–449. Retrieved from http://physrev.physiology.org/cgi/content/abstract/79/2/425%0Ahttp://www.ncbi.nlm.nih.gov/pubmed/10221986

Finkel, T., & Holbrook, N. J. (2000). Oxidants, oxidative stress and the biology of ageing. *Nature*, *408*(6809), 239–247. doi:10.1038/35041687

Foster, E. R., & Downs, J. A. (2005). Histone H2A phosphorylation in DNA double-strand break repair. *FEBS Journal*, *272*(13), 3231–3240. doi:10.1111/j.1742-4658.2005.04741.x

Franssen, S. U., Gu, J., Winters, G., Huylmans, A. K., Wienpahl, I., Sparwel, M., … Bornberg-Bauer, E. (2014). Genome-wide transcriptomic responses of the seagrasses *Zostera marina* and *Nanozostera noltii* under a simulated heatwave confirm functional types. *Marine Genomics*, *15*, 65–73. doi:10.1016/j.margen.2014.03.004

Fraser, H. B. (2013). Gene expression drives local adaptation in humans. *Genome Research*, *23*(7), 1089–96. doi:10.1101/gr.152710.112

Frye, J. A., & Frye, C. T. (2012). Association of ants (Hymenoptera: Formicidae) on oaks and pines in inland dune and ridge woodlands in Worchester County, Maryland, *5*(4), 41–48.

Fuller, A., Dawson, T., Helmuth, B., Hetem, R. S., Mitchell, D., & Maloney, S. K. (2010). Physiological mechanisms in coping with climate change. *Physiological and Biochemical Zoology*, *83*(5), 713–720. doi:10.1086/652242

Galbreath, K. E., Hafner, D. J., & Zamudio, K. R. (2009). When cold is better: Climate-driven elevation shifts yield complex patterns of diversification and demography in an alpine specialist (american pika, *Ochotona princeps*). *Evolution*, *63*(11), 2848–2863. doi:10.1111/j.1558-5646.2009.00803.x

García-Robledo, C., Kuprewicz, E. K., Staines, C. L., Erwin, T. L., & Kress, W. J. (2016). Limited tolerance by insects to high temperatures across tropical elevational gradients and the implications of global warming for extinction. *Proceedings of the National Academy of Sciences*, *113*(3), 680–685. doi:10.1073/pnas.1507681113

Gehring, W. J., & Wehner, R. (1995). Heat shock protein synthesis and thermotolerance in *Cataglyphis*, an ant from the Sahara desert. *Proceedings of the National Academy of Sciences*, *92*(7), 2994–2998. doi:10.1073/pnas.92.7.2994

Gharehaghaji, M., Minor, E. S., Ashley, M. V., Abraham, S. T., & Koenig, W. D. (2017). Effects of landscape features on gene flow of valley oaks (*Quercus lobata*). *Plant Ecology*, *218*(4),

487–499. doi:10.1007/s11258-017-0705-2

Gibert, P., Moreteau, B., Pétavy, G., Karan, D., & David, J. R. (2007). Chill-coma tolerance, a major climatic adaptation among *Drosophila* species. *Evolution*, *55*(5), 1063–1068. doi:10.1111/j.0014-3820.2001.tb00623.x

Gleason, L. U., & Burton, R. S. (2015). RNA-seq reveals regional differences in transcriptome response to heat stress in the marine snail *Chlorostoma funebralis*. *Molecular Ecology*, *24*(3), 610–627. doi:10.1111/mec.13047

Gómez-Mendoza, L., & Arriaga, L. (2007). Modeling the effect of climate change on the distribution of oak and pine species of Mexico. *Conservation Biology*, *21*(6), 1545–1555. doi:10.1111/j.1523-1739.2007.00814.x

Gong, W. J., & Golic, K. G. (2006). Loss of Hsp70 in drosophila is pleiotropic, with effects on thermotolerance, recovery from heat shock and neurodegeneration. *Genetics*, *172*(1), 275–286. doi:10.1534/genetics.105.048793

Gottscho, A. D. (2016). Zoogeography of the San Andreas Fault system: Great Pacific Fracture Zones correspond with spatially concordant phylogeographic boundaries in western North America. *Biological Reviews*, *91*, 235–254. doi:10.1111/brv.12167

Grabherr, M. G., Haas, B. J., Yassour, M., Levin, J. Z., Thompson, D. a, Amit, I., … Regev, A. (2011). Full-length transcriptome assembly from RNA-Seq data without a reference genome. *Nature Biotechnology*, *29*(7), 644–52. doi:10.1038/nbt.1883

Graham, A. (1999). *Late Cretaceous and Cenozoic History of North American Vegetation*. New York, NY: Oxford University Press.

Gugger, P. F., Ikegami, M., & Sork, V. L. (2013). Influence of late Quaternary climate change on present patterns of genetic variation in valley oak, Quercus lobata Nee. *Molecular Ecology*, *22*(13), 3598–3612. doi:10.1111/mec.12317

Guiher, T. J., & Burbrink, F. T. (2008). Demographic and phylogeographic histories of two venomous North American snakes of the genus *Agkistrodon*. *Molecular Phylogenetics and Evolution*, *48*(2), 543–553. doi:10.1016/j.ympev.2008.04.008

Gunderson, A. R., & Stillman, J. H. (2015). Plasticity in thermal tolerance has limited potential to buffer ectotherms from global warming. *Proceedings of the Royal Society B: Biological Sciences*, *282*(1808), 20150401. doi:http://dx.doi.org/10.1098/rspb.2015.0401

Guo, R., Wang, S., Xue, R., Cao, G., Hu, X., Huang, M., … Gong, C. (2015). The gene expression profile of resistant and susceptible *Bombyx mori* strains reveals cypovirus-associated variations in host gene transcript levels. *Applied Microbiology and Biotechnology*, *99*(12), 5175–5187. doi:10.1007/s00253-015-6634-x

Heinen, C., Acs, K., Hoogstraten, D., & Dantuma, N. P. (2011). C-terminal UBA domains protect ubiquitin receptors by preventing initiation of protein degradation. *Nature Communications*, *2*, 191. doi:10.1038/ncomms1179

Hemmings, Z., & Andrew, N. R. (2017). Effects of microclimate and species identity on body temperature and thermal tolerance of ants (Hymenoptera: Formicidae). *Austral Entomology*, *56*(1), 104–114. doi:10.1111/aen.12215

Hewitt, G. M. (1996). Some genetic consequences of ice ages, and their role in divergence and speciation. *Biological Journal of the Linnean Society*, *58*, 247–276.

Hijmans, R. J., Cameron, S. E., Parra, J. L., Jones, P. G., & Jarvis, A. (2005). Very high resolution interpolated climate surfaces for global land areas. *International Journal of Climatology*, *25*(15), 1965–1978. doi:10.1002/joc.1276

Hijmans, R. J., Phillips, S. A., Leathwick, J., & Elith, J. (2010). dismo: Species distribution

modeling. R package version 0.7-17.
Hoffmann, A. A., Chown, S. L., & Clusella-Trullas, S. (2013). Upper thermal limits in terrestrial ectotherms: How constrained are they? *Functional Ecology*, *27*(4), 934–949. doi:10.1111/j.1365-2435.2012.02036.x
Hoffmann, A., & Sgrò, C. M. (2017). Comparative studies of critical physiological limits and vulnerability to environmental extremes in small ectotherms: how much environmental control is needed? *Integrative Zoology*, 1–30. doi:10.1111/1749-4877.12297.This
Hope, A. G., Malaney, J. L., Bell, K. C., Salazar-Miralles, F., Chavez, A. S., Barber, B. R., & Cook, J. A. (2016). Revision of widespread red squirrels (genus: *Tamiasciurus*) highlights the complexity of speciation within North American forests. *Molecular Phylogenetics and Evolution*, *100*, 170–182. doi:10.1016/j.ympev.2016.04.014
Hope, A. G., Panter, N., Cook, J. A., Talbot, S. L., & Nagorsen, D. W. (2014). Multilocus phylogeography and systematic revision of North American water shrews (genus: *Sorex*). *Journal of Mammalogy*, *95*(4), 722–738. doi:10.1644/13-MAMM-A-196
Huey, R. B., Kearney, M. R., Krockenberger, A., Holtum, J. A. M., Jess, M., & Williams, S. E. (2012). Predicting organismal vulnerability to climate warming: roles of behaviour, physiology and adaptation. *Philosophical Transactions of the Royal Society B: Biological Sciences*, *367*(1596), 1665–1679. doi:10.1098/rstb.2012.0005
Jaggar, T. A., & Palache, C. (1905). Description of bradshaw mountains quadrangle. *U.S. Geological Survey Atlas Folio*, *126*, 1–11.
Jombart, T. (2008). Adegenet: A R package for the multivariate analysis of genetic markers. *Bioinformatics*, *24*(11), 1403–1405. doi:10.1093/bioinformatics/btn129
Jombart, T., & Ahmed, I. (2011). adegenet 1.3-1: New tools for the analysis of genome-wide SNP data. *Bioinformatics*, *27*(21), 3070–3071. doi:10.1093/bioinformatics/btr521
Jumbam, K. R., Jackson, S., Terblanche, J. S., McGeoch, M. A., & Chown, S. L. (2008). Acclimation effects on critical and lethal thermal limits of workers of the Argentine ant, *Linepithema humile*. *Journal of Insect Physiology*, *54*(6), 1008–1014. doi:10.1016/j.jinsphys.2008.03.011
Kabbage, M., & Dickman, M. B. (2008). The BAG proteins: A ubiquitous family of chaperone regulators. *Cellular and Molecular Life Sciences*, *65*(9), 1390–1402. doi:10.1007/s00018-008-7535-2
Kalinowski, S. T. (2011). The computer program STRUCTURE does not reliably identify the main genetic clusters within species: Simulations and implications for human population structure. *Heredity*, *106*(4), 625–632. doi:10.1038/hdy.2010.95
Kalosaka, K., Soumaka, E., Politis, N., & Mintzas, A. C. (2009). Thermotolerance and HSP70 expression in the Mediterranean fruit fly *Ceratitis capitata*. *Journal of Insect Physiology*, *55*(6), 568–573. doi:10.1016/j.jinsphys.2009.02.002
Katoh, K., & Standley, D. M. (2013). MAFFT multiple sequence alignment software version 7: Improvements in performance and usability. *Molecular Biology and Evolution*, *30*(4), 772–780. doi:10.1093/molbev/mst010
Kawecki, T. J., & Ebert, D. (2004). Conceptual issues in local adaptation. *Ecology Letters*, *7*(12), 1225–1241. doi:10.1111/j.1461-0248.2004.00684.x
Kenkel, C. D., & Matz, M. V. (2016). Gene expression plasticity as a mechanism of coral adaptation to a variable environment. *Nature Ecology & Evolution*, *1*(1), 14. doi:10.1038/s41559-016-0014
Kenkel, C. D., Meyer, E., & Matz, M. V. (2013). Gene expression under chronic heat stress in

populations of the mustard hill coral (*Porites astreoides*) from different thermal environments. *Molecular Ecology*, *22*(16), 4322–4334. doi:10.1111/mec.12390

Kerhoulas, N. J., & Arbogast, B. S. (2010). Molecular systematics and Pleistocene biogeography of Mesoamerican flying squirrels. *Journal of Mammalogy*, *91*(3), 654–667. doi:10.1644/09-MAMM-A-260.1.Key

King, A. M., & MacRae, T. H. (2015). Insect heat shock proteins during stress and diapause. *Annual Review of Entomology*, *60*(1), 59–75. doi:10.1146/annurev-ento-011613-162107

Koo, J., Son, T.-G., Kim, S.-Y., & Lee, K.-Y. (2015). Differential responses of *Apis mellifera* heat shock protein genes to heat shock, flower-thinning formulations, and imidacloprid. *Journal of Asia-Pacific Entomology*, *18*(3), 583–589. doi:10.1016/j.aspen.2015.06.011

Kopelman, N. M., Mayzel, J., Jakobsson, M., Rosenberg, N. A., & Mayrose, I. (2015). CLUMPAK: A program for identifying clustering modes and packaging population structure inferences across K. *Molecular Ecology Resources*, *15*(5), 1179–1191. doi:10.1111/1755-0998.12387

Körner, C. (2007). The use of "altitude" in ecological research. *Trends in Ecology and Evolution*, *22*(11), 569–574. doi:10.1016/j.tree.2007.09.006

Kregel, K. C. (2002). Heat Shock proteins: modifying factors in physiological stress responses and acquired thermotolerance. *Journal of Applied Physiology*, *89*(4), 1253–1254. doi:10.1152/japplphysiol.00017.2004

Kurzik-Dumke, U., & Lohmann, E. (1995). Sequence of the new *Drosophila melanogaster* small heat-shock-related gene, *lethal (2) essential for life [l(2)efl]*, at locus 59F4,5. *Gene*, *154*, 171–175.

Lait, L. A., & Hebert, P. D. N. (2018). Phylogeographic structure in three North American tent caterpillar species (Lepidoptera: Lasiocampidae): *Malacosoma americana* , *M. californica* , and *M. disstria*. *PeerJ*, *6*, e4479. doi:10.7717/peerj.4479

Lancaster, L. T., Dudaniec, R. Y., Chauhan, P., Wellenreuther, M., Svensson, E. I., & Hansson, B. (2016). Gene expression under thermal stress varies across a geographic range expansion front. *Molecular Ecology*, *25*, 1141–1156. doi:10.1111/mec.13548

Lang, M., Kanost, M. R., & Gorman, M. J. (2012). Multicopper oxidase-3 is a laccase associated with the peritrophic matrix of *Anopheles gambiae*. *PLoS ONE*, *7*(3), e33985. doi:10.1371/journal.pone.0033985

LaPolla, J. S., Brady, S. G., & Shattuck, S. O. (2010). Phylogeny and taxonomy of the Prenolepis genus-group of ants (Hymenoptera: Formicidae). *Systematic Entomology*, *35*, 118–131.

Lebreton, J.-D., Burnham, K. P., Clobert, J., & Anderson, D. R. (1992). Modeling survival and testing biological hypotheses using marked animals: a unified approach with case studies. *Ecological Monographs*, *62*(1), 67–118. Retrieved from http://www.jstor.org/stable/2937171

Lee-Yaw, J. A., Irwin, J. T., & Green, D. M. (2008). Postglacial range expansion from northern refugia by the wood frog, *Rana sylvatica*. *Molecular Ecology*, *17*(3), 867–884. doi:10.1111/j.1365-294X.2007.03611.x

Lee, H. K., Braynen, W., Keshav, K., & Pavlidis, P. (2005). ErmineJ: Tool for functional analysis of gene expression data sets. *BMC Bioinformatics*, *6*, 1–8. doi:10.1186/1471-2105-6-269

Li, H., & Durbin, R. (2009). Fast and accurate short read alignment with Burrows-Wheeler transform. *Bioinformatics*, *25*(14), 1754–60. doi:10.1093/bioinformatics/btp324

Li, H., Handsaker, B., Wysoker, A., Gennell, T., Ruan, J., Homer, N., … 1000 Genome Project

Data Processing Subgroup, I. (2009). The Sequence Alignment/Map format and SAMtools. *Bioinformatics*, *25*(16), 2078–2079.

Lindquist, S., & Craig, E. A. (1988). The heat -shock proteins. *Annual Review of Genetics*, *22*, 631–677.

Liu, S., Wang, X., Sun, F., Zhang, J., Feng, J., Liu, H., … Liu, Z. (2013). RNA-Seq reveals expression signatures of genes involved in oxygen transport, protein synthesis, folding, and degradation in response to heat stress in catfish. *Physiological Genomics*, *45*(12), 462–476. doi:10.1152/physiolgenomics.00026.2013

Lockwood, B. L., Sanders, J. G., & Somero, G. N. (2010). Transcriptomic responses to heat stress in invasive and native blue mussels (genus *Mytilus*): molecular correlates of invasive success. *Journal of Experimental Biology*, *213*(20), 3548–3558. doi:10.1242/jeb.046094

Loehr, J., Worley, K., Grapputo, A., Carey, J., Veitch, A., & Coltman, D. W. (2006). Evidence for cryptic glacial refugia from North American mountain sheep mitochondrial DNA. *Journal of Evolutionary Biology*, *19*(2), 419–430. doi:10.1111/j.1420-9101.2005.01027.x

Love, M. I., Huber, W., & Anders, S. (2014). Moderated estimation of fold change and dispersion for RNA-seq data with DESeq2. *Genome Biology*, *15*(12), 550. doi:10.1186/s13059-014-0550-8

Lynch, J. F., Balinsky, E. C., & Vail, S. G. (1980). Foraging patterns in three sympatric forest ant species, *Prenolepis imparis*, *Paratrechina melanderi* and *Aphaenogaster rudis* (Hymenoptera: Formicidae). *Ecological Entomology*, *5*, 353–371.

Macmillan, H. A., Williams, C. M., Staples, J. F., & Sinclair, B. J. (2012). Reestablishment of ion homeostasis during chill-coma recovery in the cricket *Gryllus pennsylvanicus*. *Proceedings of the National Academy of Sciences of the United States of America*, *109*(50), 20750–20755. doi:10.1073/pnas.1212788109/-/DCSupplemental.www.pnas.org/cgi/doi/10.1073/pnas.1212788109

Magoč, T., & Salzberg, S. L. (2011). FLASH: Fast length adjustment of short reads to improve genome assemblies. *Bioinformatics*, *27*(21), 2957–2963. doi:10.1093/bioinformatics/btr507

Mann, D. H., & Hamilton, T. D. (1995). Late Pleistocene and Holocene paleoenvironments of the North Pacific coast. *Quaternary Science Reviews*, *14*(5), 449–471. doi:10.1016/0277-3791(95)00016-I

Martin, M. (2011). Cutadapt removes adapter sequences from high-throughput sequencing reads. *EMBnet.journal*, *17*(1), 10. doi:10.14806/ej.17.1.200

Masta, S. E. (2000). Phylogeography of the jumping spider *Habronattus pugillis* (Araneae: Salticidae): Recent vicariance of sky island populations? *Evolution*, *54*(5), 1699–1711.

Mastretta-Yanes, A., Xue, A. T., Moreno-Letelier, A., Jorgensen, T. H., Alvarez, N., Piñero, D., & Emerson, B. C. (2018). Long-term in situ persistence of biodiversity in tropical sky islands revealed by landscape genomics. *Molecular Ecology*, *27*(2), 432–448. doi:10.1111/mec.14461

Matos-Maraví, P., Clouse, R. M., Sarnat, E. M., Economo, E. P., LaPolla, J. S., Borovanska, M., … Janda, M. (2018). An ant genus-group (*Prenolepis*) illuminates the biogeography and drivers of insect diversification in the Indo-Pacific. *Molecular Phylogenetics and Evolution*, *123*(November 2016), 16–25. doi:10.1016/j.ympev.2018.02.007

Maysov, A., & Kipyatkov, V. E. (2009). Critical thermal minima, their spatial and temporal variation and response to hardening in *Myrmica* ants. *Cryo Letters*, *30*(1), 29–40. Retrieved from http://www.ncbi.nlm.nih.gov/pubmed/19274309

McCann, S. M., Kosmala, G. K., Greenlees, M. J., & Shine, R. (2018). Physiological plasticity in

a successful invader: Rapid acclimation to cold occurs only in cool-climate populations of cane toads (*Rhinella marina*). *Conservation Physiology*, *6*(1). doi:10.1093/conphys/cox072

McCormack, J. E., Bowen, B. S., & Smith, T. B. (2008). Integrating paleoecology and genetics of bird populations in two sky island archipelagos. *BMC Biology*, *6*(28), 1–12. doi:10.1186/1741-7007-6-28

McKenna, A., Hanna, M., Banks, E., Sivachenko, A., Cibulskis, K., Kernytsky, A., … DePristo, M. A. (2010). The Genome Analysis Toolkit: A MapReduce framework for analyzing next-generation DNA sequencing data. *Genome Research*, *20*, 1297–1303. doi:10.1101/gr.107524.110.20

McVay, J. D., Hauser, D., Hipp, A. L., & Manos, P. S. (2017). Phylogenomics reveals a complex evolutionary history of lobed-leaf white oaks in western North America. *Genome*, *60*(9), 733–742. doi:10.1139/gen-2016-0206

Metcalfe, S. E., O'Hara, S. L., Caballero, M., & Davies, S. J. (2000). Records of Late Pleistocene-Holocene climatic change in Mexico - A review. *Quaternary Science Reviews*, *19*(7), 699–721. doi:10.1016/S0277-3791(99)00022-0

Meyer, M., & Kircher, M. (2010). Illumina sequencing library preparation for highly multiplexed target capture and sequencing. *Cold Spring Harbor Protocols*, *2010*(6). doi:10.1101/pdb.prot5448

Moreno-Letelier, A., & Piñero, D. (2009). Phylogeographic structure of *Pinus strobiformis* Engelm. across the Chihuahuan Desert filter-barrier. *Journal of Biogeography*, *36*(1), 121–131. doi:10.1111/j.1365-2699.2008.02001.x

Narasimhan, S., Rajeevan, N., Liu, L., Zhao, Y. O., Heisig, J., Pan, J., … Fikrig, E. (2014). Gut microbiota of the tick vector *Ixodes scapularis* modulate colonization of the Lyme disease spirochete. *Cell Host and Microbe*, *15*(1), 58–71. doi:10.1016/j.chom.2013.12.001

Netherer, S., & Schopf, A. (2010). Potential effects of climate change on insect herbivores in European forests—General aspects and the pine processionary moth as specific example. *Forest Ecology and Management*, *259*(4), 831–838. doi:10.1016/j.foreco.2009.07.034

Nguyen, A. D., DeNovellis, K., Resendez, S., Pustilnik, J. D., Gotelli, N. J., Parker, J. D., & Cahan, S. H. (2017). Effects of desiccation and starvation on thermal tolerance and the heat-shock response in forest ants. *Journal of Comparative Physiology B: Biochemical, Systemic, and Environmental Physiology*, *187*(8), 1107–1116. doi:10.1007/s00360-017-1101-x

Nover, L., & Scharf, K. D. (1997). Heat stress proteins and transcription factors. *Cellular and Molecular Life Sciences*, *53*, 80–103. doi:10.1007/PL00000583

Oms, C. S., Cerdá, X., & Boulay, R. (2017). Is phenotypic plasticity a key mechanism for responding to thermal stress in ants? *The Science of Nature*, *104*(5–6), 42. doi:10.1007/s00114-017-1464-6

Overgaard, J., Kristensen, T. N., Mitchell, K. A., & Hoffmann, A. A. (2011). Thermal tolerance in widespread and tropical Drosophila species: Does phenotypic plasticity increase with latitude? *The American Naturalist*, *178*(S1), 80–96. doi:10.1086/661780

Parmesan, C., & Yohe, G. (2003). A globally coherent fingerprint of climate change impacts across natural systems. *Nature*, *421*(6918), 37–42. doi:10.1038/nature01286

Patro, R., Duggal, G., Love, M. I., Irizarry, R. A., & Kingsford, C. (2017). Salmon provides fast and bias-aware quantification of transcript expression. *Nature Methods*, *14*(4), 417–419. doi:10.1038/nmeth.4197

Peeters, C., & Ito, F. (2001). Colony dispersal and the evolution of queen morphology in social Hymenoptera. *Annual Review of Entomology*, *46*, 601–630.

doi:10.1126/science.284.5411.99

Peng, T., Chen, X., Pan, Y., Zheng, Z., Wei, X., Xi, J., … Shang, Q. (2017). Transcription factor *aryl hydrocarbon receptor/aryl hydrocarbon receptor nuclear translocator* is involved in regulation of the xenobiotic tolerance-related cytochrome P450 CYP6DA2 in *Aphis gossypii* Glover. *Insect Molecular Biology*, *26*(5), 485–495. doi:10.1111/imb.12311

Perdew, G. H., & Bradfield, C. A. (1996). Mapping the 90 kDa heat shock protein binding region of the Ah receptor. *Biochemistry and Molecular Biology International*, *39*(3), 589–593.

Pérez-Alquicira, J., Molina-Freaner, F. E., Piñero, D., Weller, S. G., Martínez-Meyer, E., Rozas, J., & Domínguez, C. A. (2010). The role of historical factors and natural selection in the evolution of breeding systems of *Oxalis alpina* in the Sonoran desert "Sky Islands." *Journal of Evolutionary Biology*, *23*(10), 2163–2175. doi:10.1111/j.1420-9101.2010.02075.x

Perkovsky, E. E. (2011). Syninclusions of the Eocene winter ant *Prenolepis henschei* (Hymenoptera: Formicidae) and *Germaraphis aphids* (Hemiptera: Eriosomatidae) in the Late Eocene Baltic and Rovno ambers: some implications. *Russian Entmological Journal*, *20*(3), 303–313.

Pfeifer, B., Wittelsbuerger, U., Ramon-Onsins, S. E., & Lercher, M. J. (2014). PopGenome: An Efficient Swiss Army Knife for Population Genomic Analyses in R. *Molecular Biology and Evolution*, *31*(7), 1929–1936. doi:10.1093/molbev/msu136

Piersma, T., & Drent, J. (2003). Phenotypic flexibility and the evolution of organismal design. *Trends in Ecology and Evolution*, *18*(5), 228–233. doi:10.1016/S0169-5347(03)00036-3

Pither, J. (2003). Climate tolerance and interspecific variation in geographic range size. *Proceedings of the Royal Society B: Biological Sciences*, *270*(1514), 475–481. doi:10.1098/rspb.2002.2275

Portik, D. M., Smith, L. L., & Bi, K. (2016). An evaluation of transcriptome-based exon capture for frog phylogenomics across multiple scales of divergence (Class: Amphibia, Order: Anura). *Molecular Ecology Resources*, *16*(5), 1069–1083. doi:10.1111/1755-0998.12541

Pritchard, J. K., Stephens, M., & Donnelly, P. (2000). Inference of population structure using multilocus genotype data. *Genetics*, *155*(2), 945–959. Retrieved from http://www.pubmedcentral.nih.gov/articlerender.fcgi?artid=1461096&tool=pmcentrez&rendertype=abstract

Provan, J., & Bennett, K. D. (2008). Phylogeographic insights into cryptic glacial refugia. *Trends in Ecology and Evolution*, *23*(10), 564–571. doi:10.1016/j.tree.2008.06.010

Puebla-Olivares, F., Bonaccorso, E., Monteros, A. E. D. L., Omland, K. E., Llorente-Bousquets, J. E., Peterson, A. T., & Navarro-Sigüenza, A. G. (2008). Speciation in the emerald toucanet (Aulacorhynchus Prasinus) complex. *The Auk*, *125*(1), 39–50. doi:10.1525/auk.2008.125.1.39

Ribas, C. R., Campos, R. B. F., Schmidt, F. A., & Solar, R. R. C. (2012). Ants as indicators in Brazil: a review with suggestions to improve the use of ants in environmental monitoring programs. *Psyche*, *2012*(Article ID 636749), 1–23. doi:10.1155/2012/636749

Rinehart, J. P., Li, A., Yocum, G. D., Robich, R. M., Hayward, S. A. L., & Denlinger, D. L. (2007). Up-regulation of heat shock proteins is essential for cold survival during insect diapause. *Proceedings of the National Academy of Sciences*, *104*(27), 11130–11137. doi:10.1073/pnas.0703538104

Rio, D. C., Ares, M., Hannon, G. J., & Nilsen, T. W. (2010). Purification of RNA using TRIzol (TRI reagent). *Cold Spring Harbor Protocols*, *2010*(6). doi:10.1101/pdb.prot5439

Rissler, L. J., Hijmans, R. J., Graham, C. H., Moritz, C., & Wake, D. B. (2006). Phylogeographic

Lineages and Species Comparisons in Conservation Analyses: A Case Study of California Herpetofauna. *The American Naturalist*, *167*(5), 655–666. doi:10.1086/503332

Rosenberg, N. A. (2004). DISTRUCT: A program for the graphical display of population structure. *Molecular Ecology Notes*, *4*(1), 137–138. doi:10.1046/j.1471-8286.2003.00566.x

Sala, O. E., Chapin, S., Armesto, J., Berlow, E., Bloomfield, J., Dirzo, R., … Wall, D. (2000). Global biodiversity scenarios for the year 2100. *Science*, *287*(5459), 1770–1774. doi:10.1126/science.287.5459.1770

Schierenbeck, K. A. (2017). Population-level genetic variation and climate change in a biodiversity hotspot. *Annals of Botany*, *119*(2), 215–228. doi:10.1093/aob/mcw214

Schoville, S. D., Barreto, F. S., Moy, G. W., Wolff, A., & Burton, R. S. (2012). Investigating the molecular basis of local adaptation to thermal stress: population differences in gene expression across the transcriptome of the copepod *Tigriopus californicus*. *BMC Evolutionary Biology*, *12*, 170. doi:10.1186/1471-2148-12-170

Schwartz, D. C., & Hochstrasser, M. (2003). A superfamily of protein tags: ubiquitin, SUMO and related modifiers. *Trends in Biochemical Sciences*, *28*(6), 321–328. doi:10.1016/S0968-0004(03)00113-0

Seebacher, F., White, C. R., & Franklin, C. E. (2015). Physiological plasticity increases resilience of ectothermic animals to climate change. *Nature Climate Change*, *5*(1), 61–66. doi:10.1038/nclimate2457

Shah, A. A., Funk, W. C., & Ghalambor, C. K. (2017). Thermal Acclimation Ability Varies in Temperate and Tropical Aquatic Insects from Different Elevations. *Integrative and Comparative Biology*, *57*(5), 977–987. doi:10.1093/icb/icx101

Shah, A. A., Gill, B. A., Encalada, A. C., Flecker, A. S., Funk, C. W., Guayasamin, J. M., … Ghalambor, C. K. (2017). *Climate variability predicts thermal limits of aquatic insects across elevation and latitude*. *Functional Ecology* (Vol. 31). doi:10.1111/1365-2435.12906

Shapiro, B., Drummond, A. J., Rambaut, A., Wilson, M. C., Matheus, P. E., Sher, A. V, … Cooper, A. (2004). Rise and Fall of the Beringian Steppe Bison. *Science*, *306*(5701), 1561–1565. doi:10.1126/science.1101074

Sima, Y. H., Yao, J. M., Hou, Y. S., Wang, L., & Zhao, L. C. (2011). Variations of hydrogen peroxide and catalase expression in *Bombyx* eggs during diapause initiation and termination. *Archives of Insect Biochemistry and Physiology*, *77*(2), 72–80. doi:10.1002/arch.20422

Simola, D. F., Wissler, L., Donahue, G., Waterhouse, R. M., Helmkampf, M., Roux, J., … Gadau, J. (2013). Social insect genomes exhibit dramatic evolution in gene composition and regulation while preserving regulatory features linked to sociality. *Genome Research*, *23*(8), 1235–1247. doi:10.1101/gr.155408.113

Slater, G. S. C., & Birney, E. (2005). Automated generation of heuristics for biological sequence comparison. *BMC Bioinformatics*, *6*(31). doi:10.1186/1471-2105-6-31

Smit, A., Hubley, R., & Green, P. (n.d.). RepeatMasker Open-4.0.

Smith, C. D., Zimin, A., Holt, C., Abouheif, E., Benton, R., Cash, E., … Tsutsui, N. D. (2011). Draft genome of the globally widespread and invasive Argentine ant (*Linepithema humile*). *Proceedings of the National Academy of Sciences*, *108*(14), 5673–5678. doi:10.1073/pnas.1008617108

Smith, C. I., & Farrell, B. D. (2005). Range expansions in the flightless longhorn cactus beetles, *Moneilema gigas* and *Moneilema armatum*, in response to Pleistocene climate changes. *Molecular Ecology*, *14*(4), 1025–1044. doi:10.1111/j.1365-294X.2005.02472.x

Smith, C. R., Smith, C. D., Robertson, H. M., Helmkampf, M., Zimin, A., Yandell, M., … Gadau, J. (2011). Draft genome of the red harvester ant *Pogonomyrmex barbatus*. *Proceedings of the National Academy of Sciences*, *108*(14), 5667–5672. doi:10.1073/pnas.1007901108

Soltis, D. E., Morris, A. B., McLachlan, J. S., Manos, P. S., & Soltis, P. S. (2006). Comparative phylogeography of unglaciated eastern North America. *Molecular Ecology*, *15*(14), 4261–4293. doi:10.1111/j.1365-294X.2006.03061.x

Somero, G. N. (2010). The physiology of climate change: how potentials for acclimatization and genetic adaptation will determine "winners" and "losers". *The Journal of Experimental Biology*, *213*(6), 912–20. doi:10.1242/jeb.037473

Sørensen, J. G., Dahlgaard, J., & Loeschcke, V. (2001). Genetic variation in thermal tolerance among natural populations of *Drosophila buzzatii*: down regulation of Hsp70 expression and variation in heat stress resistance traits. *Functional Ecology*, *15*, 289–296. doi:10.1046/j.1365-2435.2001.00525.x

Sørensen, J. G., & Loeschcke, V. (2001). Larval crowding in *Drosophila melanogaster* induces Hsp70 expression, and leads to increased adult longevity and adult thermal stress resistance. *Journal of Insect Physiology*, *47*(11), 1301–1307. doi:10.1016/S0022-1910(01)00119-6

Sork, V. L., Gugger, P. F., Chen, J.-M., & Werth, S. (2016). Evolutionary lessons from California plant phylogeography. *Proceedings of the National Academy of Sciences*, *113*(29), 8064–8071. doi:10.1073/pnas.1602675113

Spellman, G. M., & Klicka, J. (2007). Phylogeography of the white-breasted nuthatch (*Sitta carolinensis*): Diversification in North American pine and oak woodlands. *Molecular Ecology*, *16*(8), 1729–1740. doi:10.1111/j.1365-294X.2007.03237.x

Stamatakis, A. (2014). RAxML version 8: A tool for phylogenetic analysis and post-analysis of large phylogenies. *Bioinformatics*, *30*(9), 1312–1313. doi:10.1093/bioinformatics/btu033

Stewart, J. R., Lister, A. M., Barnes, I., & Dalen, L. (2010). Refugia revisited: individualistic responses of species in space and time. *Proceedings of the Royal Society B: Biological Sciences*, *277*(1682), 661–671. doi:10.1098/rspb.2009.1272

Stillman, J. H. (2003). Acclimation capacity underlies susceptibility to climate change. *Science*, *301*, 65.

Stuble, K. L., Pelini, S. L., Diamond, S. E., Fowler, D. a, Dunn, R. R., & Sanders, N. J. (2013). Foraging by forest ants under experimental climatic warming: a test at two sites. *Ecology and Evolution*, *3*(3), 482–491. doi:10.1002/ece3.473

Suen, G., Teiling, C., Li, L., Holt, C., Abouheif, E., Bornberg-Bauer, E., … Currie, C. R. (2011). The genome sequence of the leaf-cutter ant *Atta cephalotes* reveals insights into its obligate symbiotic lifestyle. *PLoS Genetics*, *7*(2), e1002007. doi:10.1371/journal.pgen.1002007

Sunday, J. M., Bates, A. E., & Dulvy, N. K. (2011). Global analysis of thermal tolerance and latitude in ectotherms. *Proceedings of the Royal Society B: Biological Sciences*, *278*(1713), 1823–1830. doi:10.1098/rspb.2010.1295

Supek, F., Bošnjak, M., Škunca, N., & Šmuc, T. (2011). REVIGO summarizes and visualizes long lists of gene ontology terms. *PLoS ONE*, *6*(7), e21800. doi:10.1371/journal.pone.0021800

Talbot, M. (1943). Response of the ant *Prenolepis imparis* Say to temperature and humidity changes. *Ecology*, *24*(3), 345–352.

Teets, N. M., & Denlinger, D. L. (2013). Physiological mechanisms of seasonal and rapid cold-hardening in insects. *Physiological Entomology*, *38*(2), 105–116. doi:10.1111/phen.12019

Telonis-Scott, M., Clemson, A. S., Johnson, T. K., & Sgrò, C. M. (2014). Spatial analysis of gene regulation reveals new insights into the molecular basis of upper thermal limits. *Molecular Ecology*, *23*(24), 6135–6151. doi:10.1111/mec.13000

Tennessen, J. A., & Zamudio, K. R. (2008). Genetic Differentiation among Mountain Island Populations of the Striped Plateau Lizard, Sceloporus virgatus (Squamata: Phrynosomatidae). *Copeia*, (3), 558–564. doi:10.1643/CG-06-038

Therneau, T. M. (2016). A Package for Survival Analysis in S. Retrieved from http://cran.r-project.org/package=survival

Therneau, T. M., & Grambsch, P. M. (2000). *Modeling survival data: extending the Cox Model*. Springer, New York.

Truebano, M., Burns, G., Thorne, M. A. S., Hillyard, G., Peck, L. S., Skibinski, D. O. F., & Clark, M. S. (2010). Transcriptional response to heat stress in the Antarctic bivalve *Laternula elliptica*. *Journal of Experimental Marine Biology and Ecology*, *391*(1–2), 65–72. doi:10.1016/j.jembe.2010.06.011

Tschinkel, W. R. (1987). Seasonal life history and nest architecture of a winter-active ant, *Prenolepis imparis*. *Insectes Sociaux*, *34*(3), 143–164. doi:10.1007/BF02224081

Vázquez, D. P., Gianoli, E., Morris, W. F., & Bozinovic, F. (2017). Ecological and evolutionary impacts of changing climatic variability. *Biological Reviews*, *92*(1), 22–42. doi:10.1111/brv.12216

Wheeler, W. M. (1930). The ant Prenolepis imparis Say. *Annals of the Entomological Society of America*, *13*(1).

Williams, C. M., Watanabe, M., Guarracino, M. R., Ferraro, M. B., Edison, A. S., Morgan, T. J., … Hahn, D. A. (2014). Cold adaptation shapes the robustness of metabolic networks in *Drosophila melanogaster*. *Evolution*, *68*(12), 3505–3523. doi:10.1111/evo.12541

Williams, J. L., & LaPolla, J. S. (2016). Taxonomic revision and phylogeny of the ant genus Prenolepis (Hymenoptera: Formicidae). *Zootaxa*, *4200*(2), 201–258. doi:10.11646/zootaxa.4200.2.1

Wurm, Y., Wang, J., Riba-Grognuz, O., Corona, M., Nygaard, S., Hunt, B. G., … Keller, L. (2011). The genome of the fire ant *Solenopsis invicta*. *Proceedings of the National Academy of Sciences*, *108*(14), 5679–5684. doi:10.1073/pnas.1009690108

Yu, Y., Fuscoe, J. C., Zhao, C., Guo, C., Jia, M., Qing, T., … Wang, C. (2014). A rat RNA-Seq transcriptomic BodyMap across 11 organs and 4 developmental stages. *Nature Communications*, *5*, 3230–3240. doi:10.1038/ncomms4230

Appendix A. Supplementary Information for Chapter 1

A.1 Supplemental Table

Supplemental Table A.1. Differentially expressed genes after a two-hour recovery to heat stress and the fold-change (FC) of their expression relative to the control.

ID	FC	Description
ENSCFLO19236	165.53	gnl|BL_ORD_ID|60852645 KMQ88960.1 protein lethal essential for life-like protein [Lasius niger]
ENSPB20669	67.28	gnl|BL_ORD_ID|56277563 XP_011874149.1 PREDICTED: mantle protein-like [Vollenhovia emeryi]
ENSCFLO23110	22.96	gnl|BL_ORD_ID|56699740 XP_012063429.1 PREDICTED: heat shock 70 kDa protein cognate 4 isoform X1 [Atta cephalotes]
ENSCFLO19899	18.16	gnl|BL_ORD_ID|60851029 KMQ87314.1 bag domain-containing protein samui, partial [Lasius niger]
ENSSI2.2.0_03007	13.99	gnl|BL_ORD_ID|83626749 KYN10430.1 hypothetical protein ALC57_17447 [Trachymyrmex cornetzi]
ENSCFLO19771	13.24	gnl|BL_ORD_ID|74995443 XP_014598923.1 PREDICTED: histone H2B [Polistes canadensis]
ENSACEP19315	12.92	gnl|BL_ORD_ID|59145183 XP_012539422.1 PREDICTED: UBA-like domain-containing protein 2-A isoform X2 [Monomorium pharaonis]
ENSLH26041	12.39	gnl|BL_ORD_ID|5938039 EFZ09173.1 hypothetical protein SINV_03333, partial [Solenopsis invicta]
ENSSI2.2.0_07291	12.29	gnl|BL_ORD_ID|60851538 KMQ87830.1 hypothetical protein RF55_12790, partial [Lasius niger]
ENSPB23714	11.01	gnl|BL_ORD_ID|56280628 XP_011876375.1 PREDICTED: calcium-transporting ATPase type 2C member 1 isoform X2 [Vollenhovia emeryi]
ENSCobs_00196	10.86	gnl|BL_ORD_ID|52335876 XP_011266279.1 PREDICTED: aryl hydrocarbon receptor nuclear translocator homolog isoform X4 [Camponotus floridanus]
ENSCFLO11886	10.60	gnl|BL_ORD_ID|57730226 XP_012219349.1 PREDICTED: uncharacterized protein LOC105670407 isoform X1 [Linepithema humile]
ENSLH21966	10.52	gnl|BL_ORD_ID|74246077 XP_015035128.1 uncharacterized protein Dpse_GA32788 [Drosophila pseudoobscura pseudoobscura]
ENSCFLO11320	10.13	gnl|BL_ORD_ID|60846855 KMQ83055.1 hypothetical protein RF55_21065, partial [Lasius niger]
ENSCFLO17538	9.94	gnl|BL_ORD_ID|57960041 XP_012288860.1 PREDICTED: uncharacterized protein LOC105704330 [Orussus abietinus]
ENSCobs_11803	8.89	gnl|BL_ORD_ID|6880643 EGI68283.1 hypothetical protein G5I_03065 [Acromyrmex echinatior]
ENSSI2.2.0_09805	8.76	gnl|BL_ORD_ID|5942842 EFZ13983.1 hypothetical protein SINV_09805, partial [Solenopsis invicta]

ENSACEP23314	8.69	gnl|BL_ORD_ID|4861177 EFN69086.1 Uncharacterized protein C11orf9-like protein [Camponotus floridanus]
ENSCFLO14657	8.64	gnl|BL_ORD_ID|55956302 XP_011689221.1 PREDICTED: intracellular protein transport protein USO1-like [Wasmannia auropunctata]
ENSCFLO21174	8.64	gnl|BL_ORD_ID|60856667 KMQ93067.1 protein tag-53 [Lasius niger]
ENSCFLO16300	8.60	gnl|BL_ORD_ID|60861512 KMQ98008.1 d-2-hydroxyglutarate mitochondrial [Lasius niger]
ENSPB19494	8.51	gnl|BL_ORD_ID|84334966 KYQ48890.1 hypothetical protein ALC60_11944 [Trachymyrmex zeteki]
ENSCobs_16857	8.31	gnl|BL_ORD_ID|60846475 KMQ82670.1 hypothetical protein RF55_22190 [Lasius niger]
ENSCFLO12788	8.30	gnl|BL_ORD_ID|60861272 KMQ97760.1 bag family molecular chaperone regulator 2-like protein [Lasius niger]
ENSAECH20066	8.28	gnl|BL_ORD_ID|83659834 KYN44957.1 hypothetical protein ALC56_00609 [Trachymyrmex septentrionalis]
ENSCFLO14346	8.27	gnl|BL_ORD_ID|30246182 EZA51046.1 Putative ZDHHC-type palmitoyltransferase [Cerapachys biroi]
ENSCFLO13702	8.17	gnl|BL_ORD_ID|60854605 KMQ90970.1 tata-box-binding protein [Lasius niger]
ENSCFLO15987	8.02	gnl|BL_ORD_ID|83608507 KYM92436.1 hypothetical protein ALC53_00891 [Atta colombica]
ENSCFLO19649	7.95	gnl|BL_ORD_ID|74995087 XP_014598429.1 PREDICTED: DNA repair protein complementing XP-G cells homolog [Polistes canadensis]
ENSCFLO19645	7.71	No_sig_nr_hit
ENSPB24416	7.34	gnl|BL_ORD_ID|60862318 KMR01585.1 hypothetical protein RF55_915 [Lasius niger]
ENSACEP18349	7.29	gnl|BL_ORD_ID|51816736 XP_011168730.1 PREDICTED: GTPase-activating Rap/Ran-GAP domain-like protein 3 isoform X2 [Solenopsis invicta]
ENSCFLO11560	7.23	gnl|BL_ORD_ID|60854219 KMQ90572.1 bel12-ag transposon polyprotein [Lasius niger]
ENSCFLO21243	6.99	gnl|BL_ORD_ID|6871738 EGI59268.1 Armadillo repeat-containing protein 3, partial [Acromyrmex echinatior]
ENSCFLO22876	6.99	gnl|BL_ORD_ID|60860107 KMQ96577.1 cap-specific mrna nucleoside-2-o-methyltransferase 1-like protein [Lasius niger]
ENSCFLO13990	6.94	gnl|BL_ORD_ID|60848687 KMQ84907.1 pumilio domain-containing protein c14orf21 [Lasius niger]
ENSAECH18170	6.89	gnl|BL_ORD_ID|30250910 EZA55826.1 hypothetical protein X777_04001, partial [Cerapachys biroi]
ENSCFLO12539	6.81	gnl|BL_ORD_ID|60853436 KMQ89772.1 eukaryotic translation initiation factor 2-alpha kinase 1-like protein [Lasius niger]
ENSCFLO23122	6.80	gnl|BL_ORD_ID|4865334 EFN73278.1 Islet cell autoantigen 1 [Camponotus floridanus]
ENSPB17219	6.74	gnl|BL_ORD_ID|60857728 KMQ94153.1 protein daughterless [Lasius niger]
ENSCFLO22195	6.72	gnl|BL_ORD_ID|60858537 KMQ94976.1 proline-rich nuclear receptor coactivator 2-like protein [Lasius niger]
ENSLH23664	6.60	No_sig_nr_hit
ENSCFLO17643	6.55	No_sig_nr_hit
ENSCFLO12657	6.53	gnl|BL_ORD_ID|60852102 KMQ88403.1 zinc finger protein 100 [Lasius niger]
ENSCFLO25497	6.37	gnl|BL_ORD_ID|43420414 KFW86551.1 hypothetical protein N305_06502, partial [Manacus vitellinus]
ENSCFLO10256	6.32	gnl|BL_ORD_ID|4853859 EFN61723.1 hypothetical protein EAG_05860 [Camponotus floridanus]

ENSCFLO19024	6.31	gnl|BL_ORD_ID|83646790 KYN31532.1 Nuclear migration protein nudC [Trachymyrmex septentrionalis]
ENSCFLO21799	6.28	gnl|BL_ORD_ID|55955517 XP_011688166.1 PREDICTED: probable ATP-dependent RNA helicase pitchoune [Wasmannia auropunctata]
ENSCFLO17512	6.22	No_sig_nr_hit
ENSCFLO16280	6.19	gnl|BL_ORD_ID|52325280 XP_011255683.1 PREDICTED: uncharacterized protein LOC105250957 isoform X1 [Camponotus floridanus]
ENSCFLO20909	6.14	gnl|BL_ORD_ID|4866826 EFN74785.1 hypothetical protein EAG_10194 [Camponotus floridanus]
ENSCFLO12931	6.09	gnl|BL_ORD_ID|4855881 XP_011262992.1 PREDICTED: cysteine and histidine-rich domain-containing protein [Camponotus floridanus]
ENSCFLO14358	6.09	gnl|BL_ORD_ID|60857014 KMQ93426.1 dnaj protein 1-like protein [Lasius niger]
ENSPB12604	5.88	gnl|BL_ORD_ID|5950348 EFZ21507.1 hypothetical protein SINV_14195, partial [Solenopsis invicta]
ENSCFLO25310	5.84	gnl|BL_ORD_ID|4852936 EFN60798.1 hypothetical protein EAG_05799, partial [Camponotus floridanus]
ENSCFLO13139	5.78	gnl|BL_ORD_ID|60858957 KMQ95404.1 erythroid differentiation-related factor 1 [Lasius niger]
ENSCFLO18391	5.75	gnl|BL_ORD_ID|60859730 KMQ96192.1 ccr4-not transcription complex subunit 6-like isoform x1 protein [Lasius niger]
ENSCFLO15255	5.70	gnl|BL_ORD_ID|60861457 KMQ97952.1 tumor protein p73-like protein [Lasius niger]
ENSCobs_10527	5.61	gnl|BL_ORD_ID|83600570 KYM80219.1 Fasciculation and elongation protein zeta-2 [Atta colombica]
ENSPB13637	5.58	gnl|BL_ORD_ID|68462306 KOX67258.1 hypothetical protein WN51_00037, partial [Melipona quadrifasciata]
ENSCFLO20427	5.52	gnl|BL_ORD_ID|60850064 KMQ86319.1 histone H3 [Lasius niger]
ENSCFLO20971	5.39	gnl|BL_ORD_ID|60858005 KMQ94435.1 prohormone-2 precursor [Lasius niger]
ENSHSAL24707	5.37	gnl|BL_ORD_ID|60847340 KMQ83546.1 transposase-like protein [Lasius niger]
ENSSI2.2.0_16324	5.32	gnl|BL_ORD_ID|83635716 KYN19596.1 Insulin-like growth factor-binding protein complex acid labile subunit [Trachymyrmex cornetzi]
ENSAECH14317	5.31	gnl|BL_ORD_ID|6878479 EGI66088.1 hypothetical protein G5I_05481 [Acromyrmex echinatior]
ENSACEP15159	5.30	gnl|BL_ORD_ID|60852203 KMQ88509.1 antithrombin-iii-like isoform 2 protein [Lasius niger]
ENSPB20728	5.28	No_sig_nr_hit
ENSCFLO17972	5.23	No_sig_nr_hit
ENSCFLO14261	5.21	gnl|BL_ORD_ID|4865786 XP_011265721.1 PREDICTED: caspase-3 [Camponotus floridanus] EFN73736.1 Caspase Nc [Camponotus floridanus]
ENSCFLO22188	5.21	gnl|BL_ORD_ID|83596344 KYM75702.1 hypothetical protein ALC53_13765 [Atta colombica]
ENSCFLO23190	5.19	gnl|BL_ORD_ID|4862543 EFN70459.1 hypothetical protein EAG_09840 [Camponotus floridanus]
ENSCFLO10133	5.17	gnl|BL_ORD_ID|4858630 EFN66524.1 hypothetical protein EAG_11018 [Camponotus floridanus]
ENSPB19329	5.15	gnl|BL_ORD_ID|83621325 KYN04899.1 Acyl-CoA Delta(11) desaturase [Cyphomyrmex costatus]
ENSACEP23583	5.14	gnl|BL_ORD_ID|83616567 KYN00059.1 Protein yorkie [Cyphomyrmex costatus]

ENSCFLO21783	4.90	gnl|BL_ORD_ID|4861023 XP_011255416.1 PREDICTED: chromosome-associated kinesin KIF4-like [Camponotus floridanus]
ENSCFLO25890	4.86	gnl|BL_ORD_ID|4858120 EFN66011.1 Transposable element Tc3 transposase, partial [Camponotus floridanus]
ENSCFLO11282	4.84	gnl|BL_ORD_ID|83619248 KYN02787.1 hypothetical protein ALC62_06365 [Cyphomyrmex costatus]
ENSCFLO11037	4.76	No_sig_nr_hit
ENSCobs_00337	4.76	No_sig_nr_hit
ENSCFLO14811	4.71	gnl|BL_ORD_ID|60860180 KMQ96650.1 hypothetical protein RF55_3047 [Lasius niger]
ENSCFLO15164	4.71	gnl|BL_ORD_ID|60854992 KMQ91363.1 protein charybde-like protein [Lasius niger]
ENSPB23474	4.71	gnl|BL_ORD_ID|83627955 KYN11659.1 hypothetical protein ALC57_16248 [Trachymyrmex cornetzi]
ENSCFLO18261	4.70	gnl|BL_ORD_ID|4855797 EFN63680.1 GATA-binding factor A [Camponotus floridanus]
ENSCFLO17185	4.69	gnl|BL_ORD_ID|60858907 KMQ95354.1 heat shock 70 kda protein 4l-like protein [Lasius niger]
ENSCFLO17791	4.69	gnl|BL_ORD_ID|60859267 KMQ95718.1 hypothetical protein RF55_4050 [Lasius niger]
ENSCFLO22766	4.67	gnl|BL_ORD_ID|4863071 EFN70990.1 hypothetical protein EAG_09879 [Camponotus floridanus]
ENSCFLO10023	4.65	No_sig_nr_hit
ENSCFLO17934	4.65	gnl|BL_ORD_ID|60859322 KMQ95773.1 protein bric-a-brac 1-like protein [Lasius niger]
ENSLH16440	4.59	No_sig_nr_hit
ENSACEP27440	4.57	gnl|BL_ORD_ID|30252628 XP_011333714.1 PREDICTED: sodium- and chloride-dependent GABA transporter ine isoform X1 [Cerapachys biroi]
ENSCFLO17971	4.56	gnl|BL_ORD_ID|55951842 XP_011705615.1 PREDICTED: cytochrome c [Wasmannia auropunctata]
ENSACEP12309	4.49	gnl|BL_ORD_ID|4857472 EFN65360.1 NADP-dependent malic enzyme [Camponotus floridanus]
ENSPB10991	4.47	gnl|BL_ORD_ID|60855606 KMQ91985.1 gag-pol polyprotein [Lasius niger]
ENSACEP27243	4.45	gnl|BL_ORD_ID|83628571 KYN12288.1 hypothetical protein ALC57_15519 [Trachymyrmex cornetzi]
ENSACEP16512	4.43	gnl|BL_ORD_ID|4881577 EFN89678.1 DnaJ-like protein subfamily B member 6 [Harpegnathos saltator]
ENSCFLO10538	4.43	gnl|BL_ORD_ID|84338862 KYQ52888.1 hypothetical protein ALC60_07966, partial [Trachymyrmex zeteki]
ENSCFLO18428	4.43	gnl|BL_ORD_ID|52335504 XP_011265571.1 PREDICTED: cell division cycle protein 20 homolog [Camponotus floridanus]
ENSSI2.2.0_11469	4.42	gnl|BL_ORD_ID|30249977 EZA54878.1 hypothetical protein X777_05381 [Cerapachys biroi]
ENSCFLO18440	4.38	gnl|BL_ORD_ID|4854084 XP_011265538.1 PREDICTED: protein Wnt-5b-like [Camponotus floridanus] EFN61950.1 Protein Wnt-5b [Camponotus floridanus]
ENSCFLO20882	4.35	gnl|BL_ORD_ID|4866355 XP_011257126.1 PREDICTED: popeye domain-containing protein 3-like [Camponotus floridanus]
ENSCFLO17586	4.34	gnl|BL_ORD_ID|50546006 XP_011067981.1 PREDICTED: ELAV-like protein 1 isoform X7 [Acromyrmex echinatior]

ENSCobs_14210	4.33	gnl|BL_ORD_ID|60861768 KMQ98265.1 transcription factor kayak isoform x3 [Lasius niger]
ENSCFLO17664	4.30	gnl|BL_ORD_ID|57729540 XP_012218357.1 PREDICTED: facilitated trehalose transporter Tret1-2 homolog [Linepithema humile]
ENSCFLO12852	4.27	gnl|BL_ORD_ID|4853562 EFN61426.1 hypothetical protein EAG_10802 [Camponotus floridanus]
ENSSI2.2.0_00866	4.27	gnl|BL_ORD_ID|60862821 KMR04828.1 heterogeneous nuclear ribonucleoprotein l-like protein [Lasius niger]
ENSCFLO10399	4.25	gnl|BL_ORD_ID|6881558 EGI69213.1 hypothetical protein G5I_01978 [Acromyrmex echinatior]
ENSLH18550	4.22	No_sig_nr_hit
ENSCFLO16375	4.21	gnl|BL_ORD_ID|60853800 KMQ90144.1 putative e3 ubiquitin-protein ligase herc4 [Lasius niger]
ENSSI2.2.0_07891	4.21	gnl|BL_ORD_ID|52329906 XP_011255429.1 PREDICTED: protein argonaute-2-like [Camponotus floridanus]
ENSHSAL13021	4.20	No_sig_nr_hit
ENSCFLO18654	4.14	gnl|BL_ORD_ID|55960042 XP_011694561.1 PREDICTED: protein FAM46C isoform X1 [Wasmannia auropunctata]
ENSCFLO21860	4.13	No_sig_nr_hit
ENSCFLO23001	4.13	gnl|BL_ORD_ID|4852888 EFN60750.1 hypothetical protein EAG_09389 [Camponotus floridanus]
ENSPB13809	4.13	gnl|BL_ORD_ID|30241892 EZA46710.1 Histone-lysine N-methyltransferase SETMAR [Cerapachys biroi]
ENSCFLO17454	4.12	gnl|BL_ORD_ID|4854233 EFN62101.1 hypothetical protein EAG_04235 [Camponotus floridanus]
ENSCFLO26892	4.04	gnl|BL_ORD_ID|56260116 XP_011876551.1 PREDICTED: uncharacterized protein LOC105566822 [Vollenhovia emeryi]
ENSCFLO13009	3.99	gnl|BL_ORD_ID|60855833 KMQ92215.1 protein ariadne-1-like protein [Lasius niger]
ENSAECH16163	3.98	No_sig_nr_hit
ENSCobs_11606	3.96	gnl|BL_ORD_ID|57725994 XP_012214534.1 PREDICTED: uncharacterized protein LOC105667362 [Linepithema humile]
ENSCFLO24777	3.91	gnl|BL_ORD_ID|83644593 KYN29267.1 hypothetical protein ALC57_01390, partial [Trachymyrmex cornetzi]
ENSCFLO13233	3.90	gnl|BL_ORD_ID|60862559 KMR04463.1 menin-like protein [Lasius niger]
ENSCFLO10054	3.89	gnl|BL_ORD_ID|4858437 EFN66331.1 hypothetical protein EAG_07075 [Camponotus floridanus]
ENSCFLO10548	3.88	gnl|BL_ORD_ID|83634734 KYN18600.1 hypothetical protein ALC57_09079 [Trachymyrmex cornetzi]
ENSCFLO11458	3.88	gnl|BL_ORD_ID|4854335 EFN62203.1 120.7 kDa protein in NOF-FB transposable element, partial [Camponotus floridanus]
ENSACEP20974	3.87	gnl|BL_ORD_ID|83623757 KYN07381.1 TGF-beta receptor type-1, partial [Cyphomyrmex costatus]
ENSCFLO21235	3.87	gnl|BL_ORD_ID|53526687 XP_011351183.1 PREDICTED: B9 domain-containing protein 1 isoform X1 [Cerapachys biroi]
ENSPB11589	3.84	No_sig_nr_hit
ENSSI2.2.0_0399	3.84	No_sig_nr_hit

5		
ENSLH24589	3.81	gnl|BL_ORD_ID|80240647 XP_015377152.1 PREDICTED: cAMP-specific 3',5'-cyclic phosphodiesterase, isoform F-like [Diuraphis noxia]
ENSPB21329	3.81	gnl|BL_ORD_ID|83612660 KYM96201.1 hypothetical protein ALC62_13253, partial [Cyphomyrmex costatus]
ENSCFLO16885	3.80	gnl|BL_ORD_ID|4864151 EFN72079.1 ATPase family AAA domain-containing protein 2 [Camponotus floridanus]
ENSCFLO17576	3.79	gnl|BL_ORD_ID|4853985 EFN61851.1 hypothetical protein EAG_10758 [Camponotus floridanus]
ENSAECH13256	3.78	gnl|BL_ORD_ID|83625291 KYN08942.1 hypothetical protein ALC57_18908 [Trachymyrmex cornetzi]
ENSCFLO26256	3.78	gnl|BL_ORD_ID|84600026 KZC06777.1 hypothetical protein WN55_07550 [Dufourea novaeangliae]
ENSCFLO16318	3.77	gnl|BL_ORD_ID|52325277 XP_011255586.1 PREDICTED: myeloid leukemia factor isoform X3 [Camponotus floridanus]
ENSCFLO10551	3.75	gnl|BL_ORD_ID|4855811 EFN63694.1 hypothetical protein EAG_09620 [Camponotus floridanus]
ENSCFLO18082	3.74	gnl|BL_ORD_ID|60846875 KMQ83075.1 calcyclin-binding protein [Lasius niger]
ENSCFLO22849	3.73	gnl|BL_ORD_ID|60859082 KMQ95531.1 heat shock protein 90 [Lasius niger]
ENSCobs_11970	3.72	No_sig_nr_hit
ENSACEP13261	3.65	No_sig_nr_hit
ENSCFLO25447	3.62	gnl|BL_ORD_ID|35882595 KDR13632.1 Histone-lysine N-methyltransferase SETMAR, partial [Zootermopsis nevadensis]
ENSPB20083	3.61	gnl|BL_ORD_ID|83637203 KYN21122.1 hypothetical protein ALC57_06514 [Trachymyrmex cornetzi]
ENSAECH16300	3.59	gnl|BL_ORD_ID|6874278 EGI61833.1 hypothetical protein G5I_09954 [Acromyrmex echinatior]
ENSCFLO18656	3.59	No_sig_nr_hit
ENSCFLO10627	3.58	gnl|BL_ORD_ID|4866409 EFN74365.1 hypothetical protein EAG_03325 [Camponotus floridanus]
ENSAECH14972	3.56	No_sig_nr_hit
ENSCFLO13969	3.56	gnl|BL_ORD_ID|4859897 EFN67797.1 Protein prenyltransferase alpha subunit repeat-containing protein 1 [Camponotus floridanus]
ENSCFLO17933	3.54	gnl|BL_ORD_ID|60855915 KMQ92297.1 protein bric-a-brac 2 [Lasius niger]
ENSCFLO14492	3.53	gnl|BL_ORD_ID|6878278 EGI65886.1 Prohormone-3 [Acromyrmex echinatior]
ENSLH20558	3.50	gnl|BL_ORD_ID|60862160 KMR00327.1 leucine-rich repeat-containing protein 68 [Lasius niger]
ENSSI2.2.0_06468	3.50	gnl|BL_ORD_ID|30246721 EZA51591.1 hypothetical protein X777_09599 [Cerapachys biroi]
ENSACEP21847	3.48	No_sig_nr_hit
ENSCFLO10838	3.47	gnl|BL_ORD_ID|68464731 KOX69700.1 RIMS-binding protein 2 [Melipona quadrifasciata]
ENSCFLO22746	3.47	gnl|BL_ORD_ID|60862242 KMR01389.1 xenotropic and polytropic retrovirus receptor 1-like protein [Lasius niger]
ENSCFLO24592	3.47	gnl|BL_ORD_ID|83650640 KYN35492.1 Voltage-dependent T-type calcium channel subunit alpha-1G [Trachymyrmex septentrionalis]

ENSCFLO21700	3.45	gnl|BL_ORD_ID|52325732 XP_011263539.1 PREDICTED: oxysterol-binding protein-related protein 9 isoform X1 [Camponotus floridanus]
ENSCFLO24261	3.43	gnl|BL_ORD_ID|4858889 EFN66784.1 Transposable element Tc3 transposase, partial [Camponotus floridanus]
ENSPB15839	3.43	No_sig_nr_hit
ENSCFLO16067	3.41	gnl|BL_ORD_ID|55364665 XP_011632115.1 PREDICTED: endoribonuclease Dicer isoform X2 [Pogonomyrmex barbatus]
ENSCFLO15730	3.39	gnl|BL_ORD_ID|35879414 KDR09774.1 hypothetical protein L798_00266 [Zootermopsis nevadensis]
ENSCFLO19884	3.39	gnl|BL_ORD_ID|60863088 KMR05222.1 sarcoplasmic reticulum histidine-rich calcium-binding [Lasius niger]
ENSCFLO20550	3.37	gnl|BL_ORD_ID|52325519 XP_011259877.1 PREDICTED: T-box protein 2-like [Camponotus floridanus]
ENSCFLO21077	3.37	gnl|BL_ORD_ID|52334506 XP_011263722.1 PREDICTED: insulin-like peptide receptor [Camponotus floridanus]
ENSACEP22868	3.36	gnl|BL_ORD_ID|68467407 KOX72394.1 hypothetical protein WN51_01493 [Melipona quadrifasciata]
ENSCFLO18175	3.34	gnl|BL_ORD_ID|60858663 KMQ95103.1 hypothetical protein RF55_4699 [Lasius niger]
ENSLH19933	3.34	No_sig_nr_hit
ENSCFLO21403	3.33	gnl|BL_ORD_ID|60862238 KMR01381.1 casein kinase i isoform epsilon [Lasius niger]
ENSCFLO16557	3.32	gnl|BL_ORD_ID|60856980 KMQ93392.1 dentin sialophosphoprotein isoform x1 [Lasius niger]
ENSCFLO15410	3.31	gnl|BL_ORD_ID|60861004 KMQ97485.1 structural maintenance of chromosomes protein 3, partial [Lasius niger]
ENSSI2.2.0_00803	3.31	No_sig_nr_hit
ENSCFLO20835	3.30	gnl|BL_ORD_ID|4854326 XP_011265340.1 PREDICTED: L-lactate dehydrogenase-like [Camponotus floridanus]
ENSCFLO19818	3.29	gnl|BL_ORD_ID|60854517 KMQ90881.1 zinc finger protein 26 [Lasius niger]
ENSCobs_11450	3.29	gnl|BL_ORD_ID|59141043 XP_012533760.1 PREDICTED: tolloid-like protein 2 [Monomorium pharaonis]
ENSCFLO22931	3.27	gnl|BL_ORD_ID|4859031 EFN66926.1 hypothetical protein EAG_02431 [Camponotus floridanus]
ENSCFLO10731	3.25	gnl|BL_ORD_ID|4855141 EFN63019.1 hypothetical protein EAG_00723 [Camponotus floridanus]
ENSCFLO13396	3.25	gnl|BL_ORD_ID|52325594 XP_011261303.1 PREDICTED: Krueppel-like factor 3 [Camponotus floridanus]
ENSCFLO13031	3.23	gnl|BL_ORD_ID|60861413 KMQ97907.1 unconventional myosin-xviiia isoform x3 [Lasius niger]
ENSPB10364	3.23	No_sig_nr_hit
ENSSI2.2.0_15338	3.23	gnl|BL_ORD_ID|51819985 XP_011173325.1 PREDICTED: inositol-3-phosphate synthase 1-like [Solenopsis invicta]
ENSCFLO14794	3.22	gnl|BL_ORD_ID|4866156 EFN74108.1 Protein slowmo [Camponotus floridanus]
ENSCFLO13539	3.21	gnl|BL_ORD_ID|83607918 KYM91210.1 hypothetical protein ALC53_01622 [Atta colombica]
ENSCFLO13861	3.20	gnl|BL_ORD_ID|4865856 XP_011264435.1 PREDICTED: homer protein homolog 1 isoform X1 [Camponotus floridanus]

ENSCFLO22133	3.20	gnl|BL_ORD_ID|60851042 KMQ87327.1 wd repeat-containing protein 63 [Lasius niger]
ENSPB16937	3.20	gnl|BL_ORD_ID|83622041 KYN05632.1 hypothetical protein ALC62_03425 [Cyphomyrmex costatus]
ENSCFLO22324	3.19	gnl|BL_ORD_ID|30244818 EZA49670.1 hypothetical protein X777_12215 [Cerapachys biroi]
ENSLH25658	3.18	No_sig_nr_hit
ENSCFLO26382	3.17	gnl|BL_ORD_ID|83630222 KYN13987.1 hypothetical protein ALC57_13817, partial [Trachymyrmex cornetzi]
ENSCFLO11864	3.16	gnl|BL_ORD_ID|74414375 XP_014481789.1 PREDICTED: zinc finger BED domain-containing protein 4 [Dinoponera quadriceps]
ENSCFLO21982	3.16	gnl|BL_ORD_ID|52332194 XP_011259622.1 PREDICTED: retinol dehydrogenase 11-like isoform X3 [Camponotus floridanus]
ENSCobs_04467	3.16	gnl|BL_ORD_ID|59145893 XP_012540376.1 PREDICTED: nephrin-like, partial [Monomorium pharaonis]
ENSPB23117	3.15	gnl|BL_ORD_ID|5945547 EFZ16694.1 hypothetical protein SINV_10670, partial [Solenopsis invicta]
ENSCFLO13180	3.13	gnl|BL_ORD_ID|4856597 EFN64482.1 60 kDa heat shock protein, mitochondrial [Camponotus floridanus]
ENSCFLO13527	3.13	gnl|BL_ORD_ID|4862779 EFN70697.1 SCAN domain-containing protein 3 [Camponotus floridanus]
ENSAECH15642	3.11	gnl|BL_ORD_ID|83609295 KYM93223.1 hypothetical protein ALC53_00159 [Atta colombica]
ENSPB19405	3.11	gnl|BL_ORD_ID|50545111 XP_011053772.1 PREDICTED: ATP-binding cassette sub-family G member 1 isoform X2 [Acromyrmex echinatior]
ENSCFLO15809	3.10	gnl|BL_ORD_ID|4867212 EFN75173.1 Paramyosin, long form [Harpegnathos saltator]
ENSCFLO17608	3.09	gnl|BL_ORD_ID|52335653 XP_011265862.1 PREDICTED: mesoderm induction early response protein 1 isoform X3 [Camponotus floridanus]
ENSCFLO22255	3.08	gnl|BL_ORD_ID|4865204 EFN73144.1 hypothetical protein EAG_15242 [Camponotus floridanus]
ENSAECH11324	3.07	gnl|BL_ORD_ID|83613037 KYM96535.1 hypothetical protein ALC62_12799 [Cyphomyrmex costatus]
ENSPB18739	3.07	gnl|BL_ORD_ID|60862749 KMR04732.1 phosphatase and actin regulator 4 isoform x3 [Lasius niger]
ENSACEP21343	3.06	gnl|BL_ORD_ID|83605863 KYM87049.1 hypothetical protein ALC53_03666 [Atta colombica]
ENSCFLO10834	3.06	gnl|BL_ORD_ID|4881790 EFN89895.1 THAP domain-containing protein 4 [Harpegnathos saltator]
ENSCFLO19113	3.06	gnl|BL_ORD_ID|4866328 XP_011257827.1 PREDICTED: transmembrane protein 135-like [Camponotus floridanus]
ENSCFLO21411	3.06	gnl|BL_ORD_ID|83618092 KYN01616.1 cGMP-dependent protein kinase 1 [Cyphomyrmex costatus]
ENSCFLO10824	3.05	gnl|BL_ORD_ID|52333539 XP_011262115.1 PREDICTED: LOW QUALITY PROTEIN: RNA-binding protein MEX3B [Camponotus floridanus]
ENSCFLO15688	3.05	No_sig_nr_hit
ENSACEP17908	3.03	No_sig_nr_hit
ENSCFLO22426	3.01	gnl|BL_ORD_ID|4854419 EFN62287.1 Myotubularin-related protein 3 [Camponotus floridanus]
ENSPB13104	3.01	gnl|BL_ORD_ID|6878470 EGI66079.1 Protein WWC1 [Acromyrmex echinatior]
ENSPB25688	2.99	gnl|BL_ORD_ID|4881311 EFN89409.1 hypothetical protein EAI_12479 [Harpegnathos saltator]
ENSCFLO16946	2.98	gnl|BL_ORD_ID|60860713 KMQ97191.1 leucine-rich repeat-containing protein [Lasius niger]

ENSCFLO15460	2.95	gnl|BL_ORD_ID|52324917 XP_011268885.1 PREDICTED: uncharacterized protein LOC105258970 isoform X1 [Camponotus floridanus]
ENSCFLO16393	2.94	gnl|BL_ORD_ID|52331101 XP_011257622.1 PREDICTED: uncharacterized protein LOC105252102 isoform X1 [Camponotus floridanus]
ENSCFLO14286	2.93	gnl|BL_ORD_ID|60855729 KMQ92110.1 nanos-like protein 1 protein, partial [Lasius niger]
ENSCobs_10512	2.93	gnl|BL_ORD_ID|74414931 XP_014482457.1 PREDICTED: uncharacterized protein LOC106748452 [Dinoponera quadriceps]
ENSPB26605	2.93	gnl|BL_ORD_ID|84343479 KYQ57639.1 hypothetical protein ALC60_03601, partial [Trachymyrmex zeteki]
ENSCFLO21983	2.92	gnl|BL_ORD_ID|60852941 KMQ89265.1 hypothetical protein RF55_11120 [Lasius niger]
ENSPB10163	2.92	gnl|BL_ORD_ID|4856539 EFN64424.1 Transducin-like enhancer protein 4 [Camponotus floridanus]
ENSSI2.2.0_07592	2.92	gnl|BL_ORD_ID|60852892 KMQ89215.1 ankyrin repeat domain-containing protein 29-like protein, partial [Lasius niger]
ENSCFLO12017	2.91	gnl|BL_ORD_ID|60850310 KMQ86569.1 transposase, partial [Lasius niger]
ENSCFLO18984	2.91	gnl|BL_ORD_ID|60858963 KMQ95410.1 mannosyl-oligosaccharide -alpha-mannosidase ia [Lasius niger]
ENSCFLO20066	2.91	gnl|BL_ORD_ID|4857670 EFN65558.1 Histidine decarboxylase [Camponotus floridanus]
ENSCFLO18468	2.90	gnl|BL_ORD_ID|4854134 EFN62000.1 G2/mitotic-specific cyclin-B [Camponotus floridanus]
ENSCFLO19701	2.90	gnl|BL_ORD_ID|30250404 EZA55309.1 Tensin [Cerapachys biroi]
ENSAECH10828	2.89	No_sig_nr_hit
ENSCFLO16729	2.89	gnl|BL_ORD_ID|60863115 KMR05264.1 ribonucleases p mrp protein subunit pop1 [Lasius niger]
ENSCFLO19527	2.89	gnl|BL_ORD_ID|60862388 KMR02565.1 hypothetical protein RF55_849 [Lasius niger]
ENSCFLO12725	2.88	gnl|BL_ORD_ID|52331327 XP_011257974.1 PREDICTED: uncharacterized protein LOC105252342 [Camponotus floridanus]
ENSCFLO18424	2.87	gnl|BL_ORD_ID|4854115 XP_011265594.1 PREDICTED: nuclear pore membrane glycoprotein 210 [Camponotus floridanus]
ENSCFLO21806	2.87	gnl|BL_ORD_ID|60853057 KMQ89384.1 brisc and brca1-a complex member 1-like protein [Lasius niger]
ENSACEP13424	2.85	gnl|BL_ORD_ID|57734760 XP_012225590.1 PREDICTED: regulating synaptic membrane exocytosis protein 1 isoform X4 [Linepithema humile]
ENSLH24175	2.85	No_sig_nr_hit
ENSPB17283	2.85	No_sig_nr_hit
ENSCFLO19553	2.84	gnl|BL_ORD_ID|4865562 EFN73512.1 hypothetical protein EAG_09530 [Camponotus floridanus]
ENSCFLO15746	2.83	gnl|BL_ORD_ID|60862743 KMR04725.1 sh3 domain-containing ring finger protein 3 [Lasius niger]
ENSCFLO23401	2.83	gnl|BL_ORD_ID|60860184 KMQ96654.1 wd repeat-containing protein 67-like protein [Lasius niger]
ENSCFLO15496	2.82	gnl|BL_ORD_ID|52334037 XP_011262893.1 PREDICTED: S-phase kinase-associated protein 1 isoform X1 [Camponotus floridanus]
ENSCFLO16478	2.82	gnl|BL_ORD_ID|52328943 XP_011253704.1 PREDICTED: sodium/calcium exchanger 2 isoform X2 [Camponotus floridanus]
ENSCFLO21156	2.82	gnl|BL_ORD_ID|60858883 KMQ95325.1 muscle segmentation homeobox, partial [Lasius niger]

ENSACEP16883	2.81	No_sig_nr_hit
ENSAECH15038	2.81	No_sig_nr_hit
ENSCFLO10422	2.81	No_sig_nr_hit
ENSLH25006	2.80	gnl|BL_ORD_ID|83605620 KYM86591.1 hypothetical protein ALC53_04052 [Atta colombica]
ENSSI2.2.0_09773	2.80	No_sig_nr_hit
ENSCFLO18864	2.79	gnl|BL_ORD_ID|60848254 KMQ84471.1 hira-interacting protein 3 [Lasius niger]
ENSPB21748	2.79	gnl|BL_ORD_ID|83658008 KYN43069.1 putative glutathione peroxidase 2 [Trachymyrmex septentrionalis]
ENSCFLO18222	2.78	gnl|BL_ORD_ID|60858804 KMQ95246.1 protein enl [Lasius niger]
ENSPB16258	2.78	gnl|BL_ORD_ID|52330711 XP_011256920.1 PREDICTED: uncharacterized protein LOC105251666 [Camponotus floridanus]
ENSCFLO23425	2.77	gnl|BL_ORD_ID|6871589 EGI59118.1 Orphan sodium- and chloride-dependent neurotransmitter transporter NTT4 [Acromyrmex echinatior]
ENSCFLO25946	2.76	gnl|BL_ORD_ID|6872564 EGI60100.1 hypothetical protein G5I_11734 [Acromyrmex echinatior]
ENSCFLO17393	2.75	No_sig_nr_hit
ENSPB15641	2.75	No_sig_nr_hit
ENSCFLO14241	2.73	gnl|BL_ORD_ID|52331234 XP_011257836.1 PREDICTED: protein Cep78 homolog isoform X1 [Camponotus floridanus]
ENSCFLO12638	2.72	gnl|BL_ORD_ID|4865000 EFN72940.1 Neurogenic protein big brain [Camponotus floridanus]
ENSAECH12092	2.71	gnl|BL_ORD_ID|6879486 EGI67110.1 hypothetical protein G5I_04266 [Acromyrmex echinatior]
ENSCFLO10437	2.71	gnl|BL_ORD_ID|4861789 EFN69704.1 hypothetical protein EAG_07607 [Camponotus floridanus]
ENSCFLO16055	2.70	gnl|BL_ORD_ID|4854578 EFN62446.1 Band 4.1-like protein 4A [Camponotus floridanus]
ENSCFLO21545	2.70	gnl|BL_ORD_ID|4860593 EFN68498.1 Fatty acyl-CoA reductase 1, partial [Camponotus floridanus]
ENSCFLO11057	2.68	gnl|BL_ORD_ID|55373217 XP_011643498.1 PREDICTED: roundabout homolog 2-like [Pogonomyrmex barbatus]
ENSCFLO13033	2.68	gnl|BL_ORD_ID|60855626 KMQ92006.1 sugar transporter erd6 [Lasius niger]
ENSCFLO18978	2.66	gnl|BL_ORD_ID|83649717 KYN34542.1 COP9 signalosome complex subunit 4 [Trachymyrmex septentrionalis]
ENSPB12695	2.66	gnl|BL_ORD_ID|88640094 XP_016907749.1 PREDICTED: small conductance calcium-activated potassium channel protein-like, partial [Apis cerana]
ENSCFLO18002	2.65	gnl|BL_ORD_ID|4859222 EFN67118.1 hypothetical protein EAG_12101 [Camponotus floridanus]
ENSCFLO20926	2.65	gnl|BL_ORD_ID|35884132 KDR15446.1 Syntaxin-1A [Zootermopsis nevadensis]
ENSCFLO12647	2.64	gnl|BL_ORD_ID|60861055 KMQ97539.1 myophilin-like isoform 1 protein [Lasius niger]
ENSCFLO19250	2.64	gnl|BL_ORD_ID|56698934 XP_012062538.1 PREDICTED: inositol-3-phosphate synthase 1-A [Atta cephalotes]
ENSCFLO21576	2.64	gnl|BL_ORD_ID|4868423 EFN76388.1 CUG-BP- and ETR-3-like factor 6 [Harpegnathos saltator]

ENSCFLO10433	2.63	gnl|BL_ORD_ID|83629622 KYN13364.1 Protein couch potato [Trachymyrmex cornetzi]
ENSCFLO14459	2.63	gnl|BL_ORD_ID|4866030 XP_011262418.1 PREDICTED: uncharacterized protein LOC105255056 isoform X1 [Camponotus floridanus]
ENSCFLO19220	2.62	gnl|BL_ORD_ID|4857091 EFN64977.1 hypothetical protein EAG_04703 [Camponotus floridanus]
ENSCFLO20056	2.62	gnl|BL_ORD_ID|74410758 XP_014477333.1 PREDICTED: E3 ubiquitin-protein ligase UHRF1 [Dinoponera quadriceps]
ENSCFLO10380	2.61	gnl|BL_ORD_ID|4865715 EFN73665.1 hypothetical protein EAG_08462 [Camponotus floridanus]
ENSCFLO13738	2.61	gnl|BL_ORD_ID|52330447 XP_011256430.1 PREDICTED: LOW QUALITY PROTEIN: protein sidekick [Camponotus floridanus]
ENSCFLO22551	2.61	No_sig_nr_hit
ENSCFLO10116	2.60	gnl|BL_ORD_ID|5945833 EFZ16980.1 hypothetical protein SINV_12162, partial [Solenopsis invicta]
ENSACEP16203	2.59	gnl|BL_ORD_ID|83633514 KYN17356.1 hypothetical protein ALC57_10332 [Trachymyrmex cornetzi]
ENSACEP17538	2.59	gnl|BL_ORD_ID|83607368 KYM89725.1 hypothetical protein ALC53_02037, partial [Atta colombica]
ENSACEP22929	2.59	gnl|BL_ORD_ID|83629526 KYN13267.1 hypothetical protein ALC57_14564 [Trachymyrmex cornetzi]
ENSCFLO21969	2.59	gnl|BL_ORD_ID|60859613 KMQ96072.1 transmembrane and coiled-coil domains protein 1 [Lasius niger]
ENSCFLO21150	2.58	gnl|BL_ORD_ID|55956170 XP_011689040.1 PREDICTED: maternal protein exuperantia [Wasmannia auropunctata]
ENSCFLO14967	2.57	gnl|BL_ORD_ID|52326800 XP_011269443.1 PREDICTED: uncharacterized protein LOC105259284 [Camponotus floridanus]
ENSPB13867	2.57	gnl|BL_ORD_ID|55363373 XP_011630474.1 PREDICTED: uncharacterized protein LOC105422690 [Pogonomyrmex barbatus]
ENSAECH14757	2.56	gnl|BL_ORD_ID|59133545 XP_012523561.1 PREDICTED: rap guanine nucleotide exchange factor-like [Monomorium pharaonis]
ENSCFLO14055	2.56	gnl|BL_ORD_ID|56282162 XP_011877530.1 PREDICTED: MAP kinase-interacting serine/threonine-protein kinase 1 isoform X1 [Vollenhovia emeryi]
ENSCFLO18219	2.56	gnl|BL_ORD_ID|60859910 KMQ96377.1 neuronal pas domain-containing protein 2 [Lasius niger]
ENSCFLO21387	2.56	gnl|BL_ORD_ID|4865763 EFN73713.1 Elongation of very long chain fatty acids protein 1, partial [Camponotus floridanus]
ENSCFLO23523	2.55	gnl|BL_ORD_ID|60860082 KMQ96552.1 protein tkr [Lasius niger]
ENSCobs_05272	2.55	No_sig_nr_hit
ENSACEP14704	2.54	gnl|BL_ORD_ID|83605727 KYM86748.1 hypothetical protein ALC53_03898 [Atta colombica]
ENSACEP25495	2.54	No_sig_nr_hit
ENSCobs_08932	2.54	No_sig_nr_hit
ENSCFLO19548	2.52	gnl|BL_ORD_ID|52326064 XP_011268162.1 PREDICTED: homeodomain-interacting protein kinase 2 isoform X4 [Camponotus floridanus]
ENSCFLO23534	2.52	gnl|BL_ORD_ID|60860175 KMQ96645.1 protein slit-like protein [Lasius niger]
ENSPB13398	2.52	gnl|BL_ORD_ID|57738622 XP_012231014.1 PREDICTED: oocyte zinc finger protein XlCOF6-like isoform X1 [Linepithema humile]
ENSCFLO14761	2.51	gnl|BL_ORD_ID|59140616 XP_012533186.1 PREDICTED: nephrin isoform X1 [Monomorium pharaonis]
ENSCFLO17264	2.51	gnl|BL_ORD_ID|60860090 KMQ96560.1 putative coiled-coil domain-containing protein 174 [Lasius niger]

ENSSI2.2.0_14088	2.51	gnl|BL_ORD_ID|6870544 EGI58063.1 hypothetical protein G5I_13865 [Acromyrmex echinatior]
ENSCFLO10210	2.49	gnl|BL_ORD_ID|4852567 EFN60426.1 hypothetical protein EAG_02140 [Camponotus floridanus]
ENSCFLO14372	2.49	gnl|BL_ORD_ID|4862805 EFN70723.1 A disintegrin and metalloproteinase with thrombospondin motifs 14 [Camponotus floridanus]
ENSCFLO15411	2.49	gnl|BL_ORD_ID|60854635 KMQ91000.1 thioredoxin domain-containing protein 3-like protein [Lasius niger]
ENSCFLO20630	2.49	gnl|BL_ORD_ID|4856545 EFN64430.1 hypothetical protein EAG_00860 [Camponotus floridanus]
ENSCFLO21412	2.49	gnl|BL_ORD_ID|4855667 XP_011263335.1 PREDICTED: cGMP-dependent protein kinase, isozyme 2 forms cD5/T2-like isoform X2 [Camponotus floridanus]
ENSLH24257	2.49	No_sig_nr_hit
ENSCFLO19038	2.48	gnl|BL_ORD_ID|52336688 XP_011267661.1 PREDICTED: fibrillin-2-like [Camponotus floridanus]
ENSPB19460	2.48	gnl|BL_ORD_ID|30244121 EZA48966.1 SH3 and multiple ankyrin repeat domains protein [Cerapachys biroi]
ENSPB21625	2.48	No_sig_nr_hit
ENSSI2.2.0_12135	2.48	gnl|BL_ORD_ID|60861893 KMQ98394.1 la-related protein [Lasius niger]
ENSCFLO18896	2.47	gnl|BL_ORD_ID|60855429 KMQ91807.1 pre-mrna-splicing factor atp-dependent rna helicase dhx16 [Lasius niger]
ENSCobs_16640	2.47	gnl|BL_ORD_ID|5941562 EFZ12701.1 hypothetical protein SINV_00150, partial [Solenopsis invicta]
ENSCFLO12780	2.46	gnl|BL_ORD_ID|83642700 KYN27309.1 hypothetical protein ALC57_03653 [Trachymyrmex cornetzi]
ENSCFLO12812	2.46	gnl|BL_ORD_ID|52336247 XP_011266941.1 PREDICTED: chromosome-associated kinesin KIF4 [Camponotus floridanus]
ENSCFLO22028	2.46	gnl|BL_ORD_ID|55950762 XP_011690332.1 PREDICTED: roquin-2 isoform X2 [Wasmannia auropunctata]
ENSCobs_06517	2.46	No_sig_nr_hit
ENSACEP26601	2.45	No_sig_nr_hit
ENSCFLO10446	2.45	gnl|BL_ORD_ID|52328175 XP_011252302.1 PREDICTED: puratrophin-1-like isoform X1 [Camponotus floridanus]
ENSCFLO10647	2.44	gnl|BL_ORD_ID|4862348 EFN70264.1 hypothetical protein EAG_11933 [Camponotus floridanus]
ENSCFLO16797	2.44	gnl|BL_ORD_ID|57728518 XP_012217036.1 PREDICTED: WD repeat-containing protein 6 isoform X1 [Linepithema humile]
ENSCFLO20135	2.44	gnl|BL_ORD_ID|4863494 XP_011251790.1 PREDICTED: uncharacterized protein LOC105248608 isoform X1 [Camponotus floridanus]
ENSCFLO24300	2.44	gnl|BL_ORD_ID|57919265 XP_012251050.1 PREDICTED: uncharacterized protein LOC105683193 [Athalia rosae]
ENSACEP20459	2.43	gnl|BL_ORD_ID|56261953 XP_011859192.1 PREDICTED: uncharacterized protein LOC105556711 [Vollenhovia emeryi]
ENSCFLO23437	2.43	gnl|BL_ORD_ID|4874557 EFN82570.1 hypothetical protein EAI_00857 [Harpegnathos saltator]
ENSACEP26606	2.42	gnl|BL_ORD_ID|83612391 KYM95954.1 Histone H2B.3 [Cyphomyrmex costatus]

ENSCFLO15030	2.42	gnl|BL_ORD_ID|60854443 KMQ90807.1 alpha-tocopherol transfer [Lasius niger]
ENSCFLO20241	2.41	gnl|BL_ORD_ID|4863961 EFN71887.1 Low-density lipoprotein receptor-related protein 6 [Camponotus floridanus]
ENSACEP27174	2.40	gnl|BL_ORD_ID|5939297 EFZ10433.1 hypothetical protein SINV_03948, partial [Solenopsis invicta]
ENSCFLO13062	2.40	gnl|BL_ORD_ID|60858995 KMQ95443.1 brain tumor [Lasius niger]
ENSCFLO21833	2.39	gnl|BL_ORD_ID|83616062 KYM99546.1 Pancreatic triacylglycerol lipase [Cyphomyrmex costatus]
ENSCFLO15229	2.38	gnl|BL_ORD_ID|60858762 KMQ95203.1 tudor domain-containing protein 1-like protein [Lasius niger]
ENSCFLO15759	2.38	gnl|BL_ORD_ID|60847150 KMQ83354.1 neural-cadherin-like isoform x6 protein [Lasius niger]
ENSCFLO26139	2.38	gnl|BL_ORD_ID|60852532 KMQ88843.1 hypothetical protein RF55_11602, partial [Lasius niger]
ENSCobs_11829	2.38	gnl|BL_ORD_ID|84344193 KYQ58384.1 hypothetical protein ALC60_02805 [Trachymyrmex zeteki]
ENSAECH26193	2.37	No_sig_nr_hit
ENSCFLO12914	2.37	gnl|BL_ORD_ID|4855904 XP_011263033.1 PREDICTED: 3-oxoacyl-[acyl-carrier-protein] synthase, mitochondrial [Camponotus floridanus]
ENSCFLO20230	2.37	gnl|BL_ORD_ID|52325076 XP_011252092.1 PREDICTED: coronin-2B-like isoform X2 [Camponotus floridanus]
ENSCFLO22745	2.37	gnl|BL_ORD_ID|55364440 XP_011631815.1 PREDICTED: uncharacterized protein LOC105423669 [Pogonomyrmex barbatus]
ENSCFLO26460	2.36	gnl|BL_ORD_ID|52335578 XP_011265705.1 PREDICTED: zinc finger protein 835-like isoform X1 [Camponotus floridanus]
ENSHSAL14829	2.36	No_sig_nr_hit
ENSPB16145	2.36	gnl|BL_ORD_ID|84600381 KZC07271.1 Voltage-dependent T-type calcium channel subunit alpha-1I [Dufourea novaeangliae]
ENSCFLO13148	2.35	gnl|BL_ORD_ID|52326965 XP_011269764.1 PREDICTED: pickpocket protein 28-like isoform X2 [Camponotus floridanus]
ENSCFLO10935	2.33	gnl|BL_ORD_ID|4863602 EFN71526.1 hypothetical protein EAG_08795 [Camponotus floridanus]
ENSPB19245	2.33	gnl|BL_ORD_ID|60857201 KMQ93623.1 dentin sialophospho [Lasius niger]
ENSCFLO12828	2.32	gnl|BL_ORD_ID|60856409 KMQ92803.1 breast cancer type 1 susceptibility protein [Lasius niger]
ENSCFLO18087	2.32	gnl|BL_ORD_ID|4861823 EFN69738.1 hypothetical protein EAG_10059 [Camponotus floridanus]
ENSPB19443	2.32	gnl|BL_ORD_ID|27575862 XP_006618300.1 PREDICTED: voltage-dependent calcium channel type D subunit alpha-1-like [Apis dorsata]
ENSSI2.2.0_13975	2.32	No_sig_nr_hit
ENSCFLO12680	2.31	gnl|BL_ORD_ID|4865089 EFN73029.1 hypothetical protein EAG_11321 [Camponotus floridanus]
ENSCFLO15432	2.31	gnl|BL_ORD_ID|52328581 XP_011253039.1 PREDICTED: uncharacterized protein LOC105249346 [Camponotus floridanus]
ENSCFLO22772	2.31	gnl|BL_ORD_ID|60861803 KMQ98300.1 puratrophin-1-like protein [Lasius niger]
ENSAECH14983	2.30	gnl|BL_ORD_ID|6873735 EGI61285.1 hypothetical protein G5I_10533 [Acromyrmex echinatior]
ENSCFLO12912	2.30	gnl|BL_ORD_ID|60858265 KMQ94701.1 leucine-rich repeat-containing protein, partial [Lasius niger]

ENSCFLO16122	2.30	gnl|BL_ORD_ID|64876670 KOB69819.1 Uncharacterized protein OBRU01_08180 [Operophtera brumata]
ENSCFLO17201	2.29	gnl|BL_ORD_ID|52330334 XP_011256185.1 PREDICTED: uncharacterized protein LOC105251246 [Camponotus floridanus]
ENSCFLO18179	2.29	gnl|BL_ORD_ID|55949291 XP_011704383.1 PREDICTED: LIM/homeobox protein Awh-like [Wasmannia auropunctata]
ENSCFLO20496	2.29	gnl|BL_ORD_ID|60857313 KMQ93735.1 raf-like serine threonine-protein kinase phl-like protein [Lasius niger]
ENSCFLO26101	2.29	gnl|BL_ORD_ID|52330745 XP_011256975.1 PREDICTED: histone-lysine N-methyltransferase pr-set7 [Camponotus floridanus]
ENSCFLO23167	2.28	gnl|BL_ORD_ID|74502217 KRT82617.1 RNA binding protein [Oryctes borbonicus]
ENSCFLO17456	2.27	gnl|BL_ORD_ID|60858593 KMQ95032.1 ubiquitin carboxyl-terminal hydrolase 36, partial [Lasius niger]
ENSCFLO26085	2.27	gnl|BL_ORD_ID|52330333 XP_011256184.1 PREDICTED: zinc finger protein 148-like isoform X2 [Camponotus floridanus]
ENSCFLO15567	2.26	gnl|BL_ORD_ID|5940255 EFZ11392.1 hypothetical protein SINV_15130, partial [Solenopsis invicta]
ENSCFLO11231	2.25	gnl|BL_ORD_ID|4860178 EFN68083.1 Homeobox protein B-H1, partial [Camponotus floridanus]
ENSCFLO17452	2.25	gnl|BL_ORD_ID|52335461 XP_011265475.1 PREDICTED: protein PFC0760c-like [Camponotus floridanus]
ENSCFLO21970	2.25	gnl|BL_ORD_ID|60859616 KMQ96075.1 intron-binding protein aquarius [Lasius niger]
ENSCFLO21975	2.25	gnl|BL_ORD_ID|55956534 XP_011689548.1 PREDICTED: ran-binding protein 9 isoform X1 [Wasmannia auropunctata]
ENSCFLO22011	2.25	gnl|BL_ORD_ID|60852045 KMQ88346.1 pin2-interacting protein x1 [Lasius niger]
ENSCobs_01222	2.25	gnl|BL_ORD_ID|88645079 XP_016915769.1 PREDICTED: transcription factor 7-like, partial [Apis cerana]
ENSPB25048	2.25	gnl|BL_ORD_ID|60859111 KMQ95560.1 zinc finger protein 1-like isoform x2 protein, partial [Lasius niger]
ENSCFLO13984	2.24	gnl|BL_ORD_ID|52333731 XP_011262414.1 PREDICTED: protein CBFA2T1 [Camponotus floridanus]
ENSCFLO26754	2.24	gnl|BL_ORD_ID|53530696 XP_011333143.1 PREDICTED: uncharacterized protein LOC105276867 [Cerapachys biroi]
ENSCFLO16553	2.23	gnl|BL_ORD_ID|4865132 XP_011268760.1 PREDICTED: coiled-coil domain-containing protein 51-like [Camponotus floridanus]
ENSCFLO20546	2.23	gnl|BL_ORD_ID|60859288 KMQ95739.1 hypothetical protein RF55_4027 [Lasius niger]
ENSAECH14154	2.22	gnl|BL_ORD_ID|83647730 KYN32496.1 hypothetical protein ALC56_13354, partial [Trachymyrmex septentrionalis]
ENSCFLO14371	2.22	gnl|BL_ORD_ID|4862804 XP_011252754.1 PREDICTED: histone-lysine N-methyltransferase, H3 lysine-79 specific [Camponotus floridanus]
ENSCFLO18160	2.22	gnl|BL_ORD_ID|52334295 XP_011263322.1 PREDICTED: uncharacterized protein LOC105255619 isoform X1 [Camponotus floridanus]
ENSCFLO20870	2.22	gnl|BL_ORD_ID|51806500 XP_011172926.1 PREDICTED: uncharacterized protein LOC105205270 isoform X2 [Solenopsis invicta]
ENSAECH16863	2.21	No_sig_nr_hit
ENSCFLO14899	2.21	gnl|BL_ORD_ID|4864788 XP_011269502.1 PREDICTED: vang-like protein 1 [Camponotus floridanus] EFN72721.1 Vang-like protein 1 [Camponotus floridanus]
ENSAECH10808	2.20	gnl|BL_ORD_ID|83600244 KYM79861.1 hypothetical protein ALC53_09783 [Atta colombica]
ENSPB24971	2.20	gnl|BL_ORD_ID|84344851 KYQ59061.1 hypothetical protein ALC60_01896 [Trachymyrmex zeteki]

ENSAECH15397	2.19	gnl|BL_ORD_ID|83608398 KYM92321.1 hypothetical protein ALC53_00776 [Atta colombica]
ENSAECH23701	2.19	No_sig_nr_hit
ENSCFLO21222	2.19	gnl|BL_ORD_ID|57725965 XP_012214514.1 PREDICTED: uncharacterized protein LOC105667345 isoform X1 [Linepithema humile]
ENSCFLO22381	2.19	gnl|BL_ORD_ID|55367616 XP_011635989.1 PREDICTED: S-adenosylmethionine decarboxylase proenzyme isoform X2 [Pogonomyrmex barbatus]
ENSCFLO26820	2.19	gnl|BL_ORD_ID|83615166 KYM98635.1 hypothetical protein ALC62_10603 [Cyphomyrmex costatus]
ENSCobs_14640	2.19	gnl|BL_ORD_ID|60850816 KMQ87090.1 rna-directed dna polymerase from mobile element jockey-like protein [Lasius niger]
ENSCFLO13120	2.18	gnl|BL_ORD_ID|52327565 XP_011251248.1 PREDICTED: msx2-interacting protein isoform X2 [Camponotus floridanus]
ENSCFLO15010	2.18	gnl|BL_ORD_ID|52328902 XP_011253619.1 PREDICTED: phospholipase DDHD1-like [Camponotus floridanus]
ENSCFLO21560	2.18	gnl|BL_ORD_ID|52327083 XP_011250444.1 PREDICTED: origin recognition complex subunit 2 [Camponotus floridanus]
ENSCFLO21834	2.18	gnl|BL_ORD_ID|60860856 KMQ97335.1 serine arginine repetitive matrix protein 2-like isoform x2 protein [Lasius niger]
ENSCFLO26807	2.18	gnl|BL_ORD_ID|60850082 KMQ86337.1 reverse transcriptase, partial [Lasius niger]
ENSPB11531	2.17	gnl|BL_ORD_ID|60856970 KMQ93382.1 excitatory amino acid transporter 2 [Lasius niger]
ENSAECH22831	2.16	gnl|BL_ORD_ID|68464132 KOX69099.1 Histone-lysine N-methyltransferase SETMAR [Melipona quadrifasciata]
ENSCFLO25824	2.16	gnl|BL_ORD_ID|52329432 XP_011254546.1 PREDICTED: transcriptional repressor scratch 2-like [Camponotus floridanus]
ENSCFLO14347	2.15	gnl|BL_ORD_ID|60855756 KMQ92137.1 oxidative stress-induced growth inhibitor 1 [Lasius niger]
ENSCFLO16561	2.15	gnl|BL_ORD_ID|60862600 KMR04521.1 protein casc3 [Lasius niger]
ENSCFLO17327	2.15	gnl|BL_ORD_ID|60861501 KMQ97997.1 niemann-pick c1 protein [Lasius niger]
ENSCFLO19606	2.15	gnl|BL_ORD_ID|60855432 KMQ91810.1 rapamycin-insensitive companion of mtor [Lasius niger]
ENSCFLO22910	2.15	gnl|BL_ORD_ID|52331572 XP_011258441.1 PREDICTED: spastin isoform X3 [Camponotus floridanus]
ENSCFLO14222	2.14	gnl|BL_ORD_ID|74396511 XP_014467438.1 PREDICTED: protein lethal(2)essential for life [Dinoponera quadriceps]
ENSCFLO22895	2.14	gnl|BL_ORD_ID|83617410 KYN00922.1 Poly(A) RNA polymerase protein cid1 [Cyphomyrmex costatus]
ENSCFLO23322	2.13	gnl|BL_ORD_ID|51806162 XP_011168313.1 PREDICTED: afadin-like [Solenopsis invicta]
ENSACEP22682	2.12	gnl|BL_ORD_ID|83654689 KYN39657.1 hypothetical protein ALC56_06152, partial [Trachymyrmex septentrionalis]
ENSCFLO10584	2.12	gnl|BL_ORD_ID|4853101 EFN60963.1 hypothetical protein EAG_06416 [Camponotus floridanus]
ENSCFLO12247	2.12	gnl|BL_ORD_ID|53537398 XP_011346049.1 PREDICTED: uncharacterized protein LOC105284344 [Cerapachys biroi]
ENSCFLO16853	2.12	No_sig_nr_hit
ENSCFLO17965	2.12	gnl|BL_ORD_ID|52332940 XP_011261023.1 PREDICTED: protein smoothened isoform X3 [Camponotus floridanus]
ENSCFLO17975	2.12	gnl|BL_ORD_ID|60855816 KMQ92198.1 disks large-like protein 5 protein, partial [Lasius niger]
ENSCFLO10444	2.11	gnl|BL_ORD_ID|4863093 EFN71012.1 hypothetical protein EAG_09902 [Camponotus floridanus]

ENSCFLO12774	2.11	No_sig_nr_hit
ENSCFLO14620	2.11	gnl|BL_ORD_ID|52336646 XP_011267594.1 PREDICTED: BTB/POZ domain-containing protein 17 [Camponotus floridanus]
ENSCFLO18340	2.11	gnl|BL_ORD_ID|52325943 XP_011267171.1 PREDICTED: phospholipid-transporting ATPase ID isoform X5 [Camponotus floridanus]
ENSCFLO21529	2.11	gnl|BL_ORD_ID|74417295 XP_014485118.1 PREDICTED: exportin-7 isoform X1 [Dinoponera quadriceps]
ENSCFLO16589	2.10	gnl|BL_ORD_ID|4877580 EFN85627.1 hypothetical protein EAI_11082 [Harpegnathos saltator]
ENSCFLO16899	2.10	gnl|BL_ORD_ID|60857063 KMQ93479.1 beta- -n-acetylgalactosaminyltransferase bre-4 [Lasius niger]
ENSCFLO17006	2.10	gnl|BL_ORD_ID|60860742 KMQ97220.1 hypothetical protein RF55_2454 [Lasius niger]
ENSAECH10763	2.09	gnl|BL_ORD_ID|30247888 EZA52770.1 hypothetical protein X777_08485 [Cerapachys biroi]
ENSCFLO10650	2.09	gnl|BL_ORD_ID|4863686 EFN71610.1 hypothetical protein EAG_11599 [Camponotus floridanus]
ENSCFLO11290	2.09	gnl|BL_ORD_ID|84335725 KYQ49663.1 hypothetical protein ALC60_11258 [Trachymyrmex zeteki]
ENSCFLO18608	2.09	gnl|BL_ORD_ID|52332792 XP_011260797.1 PREDICTED: micronuclear linker histone polyprotein isoform X1 [Camponotus floridanus]
ENSCFLO18951	2.09	gnl|BL_ORD_ID|60861338 KMQ97828.1 ubiquitin carboxyl-terminal hydrolase 20-like protein [Lasius niger]
ENSCFLO19023	2.09	gnl|BL_ORD_ID|55957974 XP_011691562.1 PREDICTED: nuclear migration protein nudC [Wasmannia auropunctata]
ENSCFLO20122	2.09	gnl|BL_ORD_ID|52331287 XP_011257901.1 PREDICTED: uncharacterized protein LOC105252294 isoform X1 [Camponotus floridanus]
ENSPB10996	2.09	gnl|BL_ORD_ID|5949971 EFZ21128.1 hypothetical protein SINV_06368, partial [Solenopsis invicta]
ENSPB18881	2.09	gnl|BL_ORD_ID|4867221 EFN75182.1 hypothetical protein EAI_08843 [Harpegnathos saltator]
ENSCFLO17271	2.08	gnl|BL_ORD_ID|4860559 XP_011256262.1 PREDICTED: caseinolytic peptidase B protein homolog [Camponotus floridanus]
ENSCFLO21167	2.08	gnl|BL_ORD_ID|60860102 KMQ96572.1 tribbles-like protein [Lasius niger]
ENSCFLO22406	2.07	gnl|BL_ORD_ID|52330667 XP_011256857.1 PREDICTED: fat-like cadherin-related tumor suppressor homolog isoform X5 [Camponotus floridanus]
ENSLH11848	2.07	gnl|BL_ORD_ID|83613015 KYM96522.1 hypothetical protein ALC62_12823 [Cyphomyrmex costatus]
ENSPB13215	2.07	gnl|BL_ORD_ID|83651510 KYN36392.1 hypothetical protein ALC56_09352 [Trachymyrmex septentrionalis]
ENSPB18031	2.07	gnl|BL_ORD_ID|4854603 EFN62471.1 Bullous pemphigoid antigen 1, isoforms 6/9/10 [Camponotus floridanus]
ENSCFLO13963	2.06	gnl|BL_ORD_ID|4859887 EFN67787.1 hypothetical protein EAG_02734 [Camponotus floridanus]
ENSCFLO21589	2.06	gnl|BL_ORD_ID|4857748 XP_011260385.1 PREDICTED: peroxiredoxin 1 [Camponotus floridanus] EFN65636.1 Peroxiredoxin 1 [Camponotus floridanus]
ENSCFLO21807	2.06	gnl|BL_ORD_ID|52329872 XP_011255363.1 PREDICTED: E3 ubiquitin-protein ligase MSL2 isoform X1 [Camponotus floridanus]
ENSCFLO15353	2.05	gnl|BL_ORD_ID|52329765 XP_011255141.1 PREDICTED: muskelin [Camponotus floridanus]
ENSCFLO17218	2.05	gnl|BL_ORD_ID|60860753 KMQ97231.1 citron rho-interacting kinase-like protein [Lasius niger]
ENSCFLO17670	2.05	gnl|BL_ORD_ID|50546682 XP_011069112.1 PREDICTED: potassium voltage-gated channel subfamily H member 6 isoform X10 [Acromyrmex echinatior]
ENSCFLO20078	2.05	gnl|BL_ORD_ID|4856421 XP_011262274.1 PREDICTED: serine/threonine-protein kinase Warts [Camponotus floridanus]

ENSCFLO20416	2.05	gnl|BL_ORD_ID|83624553 KYN08194.1 Serine/threonine-protein kinase NLK [Cyphomyrmex costatus]
ENSHSAL11766	2.05	gnl|BL_ORD_ID|83623526 KYN07143.1 hypothetical protein ALC62_01891 [Cyphomyrmex costatus]
ENSSI2.2.0_07584	2.05	gnl|BL_ORD_ID|82111866 XP_015591473.1 PREDICTED: uncharacterized protein LOC107265982 [Cephus cinctus]
ENSCFLO20272	2.04	gnl|BL_ORD_ID|60862191 KMR00778.1 transferase caf17 mitochondrial-like protein [Lasius niger]
ENSPB10517	2.04	gnl|BL_ORD_ID|60854820 KMQ91186.1 hypothetical protein RF55_8981 [Lasius niger]
ENSSI2.2.0_12995	2.04	No_sig_nr_hit
ENSCFLO10566	2.03	No_sig_nr_hit
ENSCFLO13257	2.03	No_sig_nr_hit
ENSCFLO13698	2.03	gnl|BL_ORD_ID|60858137 KMQ94571.1 brain tumor protein, partial [Lasius niger]
ENSCFLO15414	2.03	gnl|BL_ORD_ID|60861006 KMQ97487.1 nf-kappa-b inhibitor cactus [Lasius niger]
ENSCFLO20061	2.03	gnl|BL_ORD_ID|60856177 KMQ92567.1 protein dok-7 [Lasius niger]
ENSCFLO22773	2.03	gnl|BL_ORD_ID|56264085 XP_011861911.1 PREDICTED: puratrophin-1-like isoform X1 [Vollenhovia emeryi]
ENSPB26711	2.03	gnl|BL_ORD_ID|60860195 KMQ96665.1 putative zinc finger protein 211 isoform 2 [Lasius niger]
ENSCFLO15948	2.02	gnl|BL_ORD_ID|4865345 XP_011268494.1 PREDICTED: protein unc-45 homolog B [Camponotus floridanus]
ENSCFLO22229	2.02	gnl|BL_ORD_ID|60860417 KMQ96890.1 brefeldin a-inhibited guanine nucleotide-exchange protein 2 [Lasius niger]
ENSCFLO10002	2.01	gnl|BL_ORD_ID|30250479 EZA55384.1 Dystrophin, isoform B [Cerapachys biroi]
ENSCFLO14690	2.01	gnl|BL_ORD_ID|51808616 XP_011156841.1 PREDICTED: autophagy-related protein 16-1 isoform X3 [Solenopsis invicta]
ENSCFLO15415	2.01	gnl|BL_ORD_ID|60861005 KMQ97486.1 stress-induced-phosphoprotein 1 [Lasius niger]
ENSCFLO19140	2.01	gnl|BL_ORD_ID|52333106 XP_011261318.1 PREDICTED: laccase-4-like isoform X1 [Camponotus floridanus]
ENSCFLO21264	2.01	gnl|BL_ORD_ID|60855202 KMQ91577.1 olfactomedin-like protein 2b protein [Lasius niger]
ENSCFLO21520	2.01	gnl|BL_ORD_ID|59136513 XP_012527605.1 PREDICTED: host cell factor isoform X2 [Monomorium pharaonis]
ENSCFLO12651	-2.00	gnl|BL_ORD_ID|52326516 XP_011268967.1 PREDICTED: uncharacterized protein LOC105259011 isoform X1 [Camponotus floridanus]
ENSCFLO13269	-2.00	gnl|BL_ORD_ID|4863539 XP_011251748.1 PREDICTED: involucrin-like [Camponotus floridanus]
ENSCFLO14338	-2.00	gnl|BL_ORD_ID|60860839 KMQ97318.1 potassium channel subfamily k member 13 [Lasius niger]
ENSCFLO15186	-2.00	gnl|BL_ORD_ID|60861109 KMQ97593.1 protein extra-macrochaetae [Lasius niger]
ENSCFLO19268	-2.00	gnl|BL_ORD_ID|4860851 EFN68757.1 hypothetical protein EAG_04127 [Camponotus floridanus]
ENSPB10073	-2.01	gnl|BL_ORD_ID|60852490 KMQ88801.1 enzymatic polyprotein endonuclease reverse [Lasius niger]

ENSCFLO13689	-2.02	gnl|BL_ORD_ID|57042059 XP_012147484.1 PREDICTED: cyclic nucleotide-gated channel cone photoreceptor subunit alpha-like isoform X3 [Megachile rotundata]
ENSCFLO16596	-2.02	gnl|BL_ORD_ID|60860559 KMQ97035.1 proton-coupled amino acid transporter 4-like protein [Lasius niger]
ENSCFLO25463	-2.02	gnl|BL_ORD_ID|52330694 XP_011256898.1 PREDICTED: zinc finger protein 648-like [Camponotus floridanus]
ENSPB26286	-2.02	gnl|BL_ORD_ID|52335585 XP_011265717.1 PREDICTED: zinc finger protein OZF-like [Camponotus floridanus]
ENSCFLO18783	-2.03	gnl|BL_ORD_ID|60862577 KMR04487.1 hypothetical protein RF55_688 [Lasius niger]
ENSCFLO22032	-2.03	gnl|BL_ORD_ID|50555736 XP_011064603.1 PREDICTED: uncharacterized protein LOC105152180 isoform X1 [Acromyrmex echinatior]
ENSCFLO22245	-2.03	gnl|BL_ORD_ID|4854850 XP_011264441.1 PREDICTED: ankyrin repeat and death domain-containing protein 1A-like isoform X2 [Camponotus floridanus]
ENSCFLO12746	-2.04	gnl|BL_ORD_ID|60858759 KMQ95200.1 j domain-containing protein [Lasius niger]
ENSCFLO19261	-2.04	gnl|BL_ORD_ID|4861182 EFN69091.1 Lachesin [Camponotus floridanus]
ENSCFLO18017	-2.05	gnl|BL_ORD_ID|55957211 XP_011690485.1 PREDICTED: elongation of very long chain fatty acids protein AAEL008004-like [Wasmannia auropunctata]
ENSCFLO13802	-2.06	gnl|BL_ORD_ID|60862706 KMR04662.1 fam179b protein [Lasius niger]
ENSCFLO14174	-2.06	gnl|BL_ORD_ID|55968776 XP_011706776.1 PREDICTED: uncharacterized protein LOC105461951 [Wasmannia auropunctata]
ENSCFLO20531	-2.06	gnl|BL_ORD_ID|60862771 KMR04763.1 peptidyl-prolyl cis-trans isomerase sdccag10 [Lasius niger]
ENSCFLO22237	-2.06	gnl|BL_ORD_ID|60855304 KMQ91680.1 forkhead box protein p4 [Lasius niger]
ENSCFLO22907	-2.06	gnl|BL_ORD_ID|4859044 EFN66939.1 hypothetical protein EAG_02444 [Camponotus floridanus]
ENSCFLO13757	-2.08	gnl|BL_ORD_ID|4860323 XP_011256346.1 PREDICTED: calexcitin-2 [Camponotus floridanus]
ENSCFLO14503	-2.08	gnl|BL_ORD_ID|52327846 XP_011251716.1 PREDICTED: alpha-2A adrenergic receptor [Camponotus floridanus]
ENSCFLO13198	-2.09	gnl|BL_ORD_ID|60857303 KMQ93725.1 protein sprouty [Lasius niger]
ENSCFLO13058	-2.10	gnl|BL_ORD_ID|4855267 EFN63148.1 hypothetical protein EAG_12887 [Camponotus floridanus]
ENSCFLO13504	-2.10	gnl|BL_ORD_ID|52333963 XP_011262753.1 PREDICTED: patched domain-containing protein 3-like isoform X1 [Camponotus floridanus]
ENSCFLO21236	-2.10	gnl|BL_ORD_ID|52327830 XP_011251683.1 PREDICTED: uncharacterized protein LOC105248541 isoform X1 [Camponotus floridanus]
ENSCFLO13330	-2.11	gnl|BL_ORD_ID|57248382 XP_012166898.1 PREDICTED: longitudinals lacking protein, isoforms H/M/V-like isoform X45 [Bombus terrestris]
ENSCFLO19915	-2.11	gnl|BL_ORD_ID|52324799 XP_011255721.1 PREDICTED: potassium/sodium hyperpolarization-activated cyclic nucleotide-gated channel 2-like [Camponotus floridanus]
ENSCFLO20038	-2.11	gnl|BL_ORD_ID|51810928 XP_011160238.1 PREDICTED: uncharacterized protein LOC105196162 [Solenopsis invicta]
ENSCFLO20511	-2.11	gnl|BL_ORD_ID|4866239 EFN74191.1 Sodium-dependent dopamine transporter [Camponotus floridanus]
ENSCFLO22805	-2.11	gnl|BL_ORD_ID|56273750 XP_011871057.1 PREDICTED: uncharacterized protein LOC105563770 [Vollenhovia emeryi]
ENSPB25094	-2.11	gnl|BL_ORD_ID|4864307 EFN72236.1 Cytochrome P450 4C1 [Camponotus floridanus]

ENSCFLO13137	-2.12	gnl|BL_ORD_ID|6879919 EGI67549.1 Kinesin-like protein KIF9 [Acromyrmex echinatior]
ENSCFLO17470	-2.12	gnl|BL_ORD_ID|56280785 XP_011876480.1 PREDICTED: sodium-dependent nutrient amino acid transporter 1-like [Vollenhovia emeryi]
ENSCFLO14149	-2.13	gnl|BL_ORD_ID|52328726 XP_011253287.1 PREDICTED: LOW QUALITY PROTEIN: histidine decarboxylase [Camponotus floridanus]
ENSCFLO15511	-2.13	gnl|BL_ORD_ID|4854371 EFN62239.1 Fatty acyl-CoA reductase 1 [Camponotus floridanus]
ENSCFLO23151	-2.13	gnl|BL_ORD_ID|52332873 XP_011260919.1 PREDICTED: scavenger receptor class B member 1 isoform X2 [Camponotus floridanus]
ENSCFLO23145	-2.14	gnl|BL_ORD_ID|86731092 OAD60995.1 Upstream-binding protein 1 [Eufriesea mexicana]
ENSCobs_05845	-2.14	No_sig_nr_hit
ENSCFLO22639	-2.15	gnl|BL_ORD_ID|4859912 EFN67812.1 Broad-complex core protein isoforms 1/2/3/4/5 [Camponotus floridanus]
ENSCFLO12519	-2.16	gnl|BL_ORD_ID|51817586 XP_011169986.1 PREDICTED: zinc finger BED domain-containing protein 4-like [Solenopsis invicta]
ENSCFLO15883	-2.16	gnl|BL_ORD_ID|60846909 KMQ83109.1 hypothetical protein RF55_20902 [Lasius niger]
ENSCFLO10405	-2.17	gnl|BL_ORD_ID|4865205 EFN73145.1 hypothetical protein EAG_15243 [Camponotus floridanus]
ENSCFLO14748	-2.18	gnl|BL_ORD_ID|56291219 XP_011882741.1 PREDICTED: lysophospholipid acyltransferase 5 [Vollenhovia emeryi]
ENSCFLO17068	-2.19	gnl|BL_ORD_ID|52325216 XP_011254515.1 PREDICTED: endothelin-converting enzyme 1 isoform X1 [Camponotus floridanus]
ENSCFLO21019	-2.19	gnl|BL_ORD_ID|4862338 EFN70254.1 Endocuticle structural glycoprotein SgAbd-1 [Camponotus floridanus]
ENSCFLO12455	-2.20	gnl|BL_ORD_ID|52333715 XP_011262395.1 PREDICTED: uncharacterized protein LOC105255042 [Camponotus floridanus]
ENSCFLO16045	-2.20	gnl|BL_ORD_ID|55950893 XP_011692048.1 PREDICTED: uncharacterized protein LOC105452539 isoform X2 [Wasmannia auropunctata]
ENSCFLO23003	-2.20	gnl|BL_ORD_ID|60859995 KMQ96462.1 pituitary homeobox-like protein ptx1 protein [Lasius niger]
ENSPB26908	-2.21	gnl|BL_ORD_ID|84336691 KYQ50645.1 Longitudinals lacking protein, isoforms N/O/W/X/Y, partial [Trachymyrmex zeteki]
ENSCFLO16472	-2.21	gnl|BL_ORD_ID|52326368 XP_011268679.1 PREDICTED: uncharacterized protein LOC105258840 [Camponotus floridanus]
ENSCFLO17352	-2.21	gnl|BL_ORD_ID|60860016 KMQ96483.1 dynein light chain axonemal [Lasius niger]
ENSCobs_13302	-2.21	gnl|BL_ORD_ID|83612101 KYM95699.1 Putative nuclease HARBI1, partial [Cyphomyrmex costatus]
ENSCFLO16502	-2.22	gnl|BL_ORD_ID|60854427 KMQ90791.1 ankyrin repeat domain-containing protein 6 [Lasius niger]
ENSCFLO18176	-2.22	gnl|BL_ORD_ID|52334425 XP_011263566.1 PREDICTED: uncharacterized protein LOC105255775 isoform X2 [Camponotus floridanus]
ENSCFLO19974	-2.22	gnl|BL_ORD_ID|60856299 KMQ92691.1 histone-lysine n-methyltransferase 2d-like isoform x1 protein, partial [Lasius niger]
ENSCFLO13759	-2.23	gnl|BL_ORD_ID|56274881 XP_011872584.1 PREDICTED: synaptic vesicle glycoprotein 2B-like isoform X1 [Vollenhovia emeryi]
ENSCFLO14026	-2.23	gnl|BL_ORD_ID|52336717 XP_011267696.1 PREDICTED: esterase FE4 [Camponotus floridanus] XP_011267697.1
ENSACEP22773	-2.24	gnl|BL_ORD_ID|60862888 KMR04926.1 udp-glucuronosyltransferase 2c1, partial [Lasius niger]
ENSCFLO19763	-2.24	gnl|BL_ORD_ID|57736477 XP_012228000.1 PREDICTED: UNC93-like protein [Linepithema humile]
ENSCFLO25467	-2.24	gnl|BL_ORD_ID|27523472 XP_006567607.1 PREDICTED: longitudinals lacking protein, isoforms A/B/D/L-like isoform X25 [Apis mellifera]

ENSCFLO15603	-2.25	gnl|BL_ORD_ID|60850748 KMQ87022.1 fatty acid synthase [Lasius niger]
ENSCFLO13327	-2.26	gnl|BL_ORD_ID|4860129 EFN68034.1 Zinc finger protein 569 [Camponotus floridanus]
ENSCFLO15636	-2.26	gnl|BL_ORD_ID|4855059 XP_011264175.1 PREDICTED: alpha-(1,3)-fucosyltransferase C-like [Camponotus floridanus]
ENSCFLO17533	-2.26	gnl|BL_ORD_ID|4862762 EFN70680.1 Sugar transporter ERD6-like 6, partial [Camponotus floridanus]
ENSCFLO18497	-2.26	gnl|BL_ORD_ID|52336735 XP_011267737.1 PREDICTED: farnesyl pyrophosphate synthase isoform X2 [Camponotus floridanus]
ENSCFLO19469	-2.26	gnl|BL_ORD_ID|52329524 XP_011254722.1 PREDICTED: ABC transporter G family member 23 isoform X1 [Camponotus floridanus]
ENSAECH16960	-2.27	No_sig_nr_hit
ENSCFLO14665	-2.27	gnl|BL_ORD_ID|52331759 XP_011258790.1 PREDICTED: tachykinins isoform X1 [Camponotus floridanus]
ENSCFLO17921	-2.27	gnl|BL_ORD_ID|60858640 KMQ95080.1 pollen-specific leucine-rich repeat extensin-like protein 3 isoform x1 protein [Lasius niger]
ENSCFLO12700	-2.28	gnl|BL_ORD_ID|60854384 KMQ90745.1 tektin-4-like protein [Lasius niger]
ENSCFLO16387	-2.29	gnl|BL_ORD_ID|51218625 XP_011152005.1 PREDICTED: putative carbonic anhydrase 3 [Harpegnathos saltator]
ENSHSAL12161	-2.29	gnl|BL_ORD_ID|84339549 KYQ53592.1 hypothetical protein ALC60_00119, partial [Trachymyrmex zeteki]
ENSCFLO18612	-2.31	gnl|BL_ORD_ID|52332804 XP_011260813.1 PREDICTED: solute carrier organic anion transporter family member 4A1 isoform X1 [Camponotus floridanus]
ENSCFLO20954	-2.32	gnl|BL_ORD_ID|84338824 KYQ52848.1 Fibrillin-2 [Trachymyrmex zeteki]
ENSCFLO12542	-2.33	gnl|BL_ORD_ID|51218454 XP_011151709.1 PREDICTED: chaoptin isoform X2 [Harpegnathos saltator]
ENSCFLO13502	-2.33	gnl|BL_ORD_ID|52333965 XP_011262761.1 PREDICTED: protein notum homolog [Camponotus floridanus]
ENSCFLO17931	-2.33	gnl|BL_ORD_ID|60855649 KMQ92030.1 alpha-tocopherol transfer [Lasius niger]
ENSCFLO14647	-2.34	gnl|BL_ORD_ID|4853437 XP_011266602.1 PREDICTED: organic cation transporter protein-like [Camponotus floridanus]
ENSCFLO15591	-2.34	gnl|BL_ORD_ID|52332472 XP_011260147.1 PREDICTED: centrosomal protein of 164 kDa isoform X2 [Camponotus floridanus]
ENSCFLO17873	-2.34	gnl|BL_ORD_ID|60857223 KMQ93645.1 acyl- delta desaturase [Lasius niger]
ENSCFLO17313	-2.35	gnl|BL_ORD_ID|4858598 EFN66492.1 Serologically defined colon cancer antigen 8-like protein [Camponotus floridanus]
ENSCFLO19433	-2.35	gnl|BL_ORD_ID|84334360 KYQ48273.1 Transcription factor collier [Trachymyrmex zeteki]
ENSCFLO11574	-2.36	gnl|BL_ORD_ID|4866543 EFN74500.1 Cytochrome P450 4C1, partial [Camponotus floridanus]
ENSCFLO19842	-2.36	gnl|BL_ORD_ID|52327771 XP_011251588.1 PREDICTED: uncharacterized protein LOC105248477, partial [Camponotus floridanus]
ENSCFLO21237	-2.37	gnl|BL_ORD_ID|52327830 XP_011251683.1 PREDICTED: uncharacterized protein LOC105248541 isoform X1 [Camponotus floridanus]
ENSSI2.2.0_09746	-2.37	gnl|BL_ORD_ID|60847405 KMQ83611.1 protein of unknown function DUF1592 [Lasius niger]
ENSCFLO17550	-2.38	gnl|BL_ORD_ID|60857390 KMQ93814.1 elongation of very long chain fatty acids protein 4-like protein [Lasius niger]
ENSCFLO18554	-2.38	gnl|BL_ORD_ID|83622903 KYN06508.1 ATP-binding cassette sub-family G member 1 [Cyphomyrmex costatus]

ENSPB18191	-2.38	gnl|BL_ORD_ID|52332042 XP_011259350.1 PREDICTED: multidrug resistance-associated protein 4-like [Camponotus floridanus]
ENSCFLO13333	-2.39	gnl|BL_ORD_ID|60858623 KMQ95062.1 longitudinals lacking isoform g [Lasius niger]
ENSCFLO15926	-2.40	gnl|BL_ORD_ID|52334815 XP_011264313.1 PREDICTED: mitochondrial thiamine pyrophosphate carrier-like [Camponotus floridanus]
ENSCFLO17926	-2.42	gnl|BL_ORD_ID|52334288 XP_011263311.1 PREDICTED: uncharacterized protein LOC105255614 isoform X3 [Camponotus floridanus]
ENSCFLO23250	-2.42	gnl|BL_ORD_ID|60853441 KMQ89777.1 neutral and basic amino acid transport protein rbat-like isoform x2 protein [Lasius niger]
ENSSI2.2.0_07739	-2.42	gnl|BL_ORD_ID|4863213 XP_011252140.1 PREDICTED: cytochrome P450 6k1-like [Camponotus floridanus]
ENSCFLO23511	-2.44	gnl|BL_ORD_ID|50555016 XP_011063397.1 PREDICTED: probable multidrug resistance-associated protein lethal(2)03659 isoform X1
ENSSI2.2.0_15518	-2.44	No_sig_nr_hit
ENSCFLO19498	-2.45	gnl|BL_ORD_ID|52329615 XP_011254860.1 PREDICTED: uncharacterized protein LOC105250458, partial [Camponotus floridanus]
ENSCFLO19832	-2.45	gnl|BL_ORD_ID|74393210 XP_014478768.1 PREDICTED: uncharacterized protein LOC106746561 isoform X1 [Dinoponera quadriceps]
ENSCFLO13174	-2.46	gnl|BL_ORD_ID|60859625 KMQ96084.1 set and mynd domain-containing protein 4-like protein [Lasius niger]
ENSCFLO14142	-2.46	gnl|BL_ORD_ID|4858571 EFN66465.1 hypothetical protein EAG_12614 [Camponotus floridanus]
ENSCFLO20786	-2.46	gnl|BL_ORD_ID|53529930 XP_011331596.1 PREDICTED: dehydrogenase/reductase SDR family member 11 isoform X1 [Cerapachys biroi]
ENSPB25106	-2.46	No_sig_nr_hit
ENSCFLO14322	-2.47	gnl|BL_ORD_ID|51811224 XP_011160661.1 PREDICTED: pancreas transcription factor 1 subunit alpha-like, partial [Solenopsis invicta]
ENSCFLO14812	-2.47	gnl|BL_ORD_ID|52334923 XP_011264509.1 PREDICTED: leucine-rich repeats and immunoglobulin-like domains protein 1 [Camponotus floridanus]
ENSCFLO18189	-2.47	gnl|BL_ORD_ID|52329514 XP_011254700.1 PREDICTED: ataxin-7-like isoform X1 [Camponotus floridanus]
ENSCFLO27013	-2.47	gnl|BL_ORD_ID|60857817 KMQ94244.1 protein yellow [Lasius niger]
ENSPB10137	-2.47	gnl|BL_ORD_ID|56279643 XP_011875633.1 PREDICTED: general odorant-binding protein 19a [Vollenhovia emeryi]
ENSCFLO21028	-2.49	gnl|BL_ORD_ID|4862326 XP_011253415.1 PREDICTED: 1-phosphatidylinositol 4,5-bisphosphate phosphodiesterase-like [Camponotus floridanus]
ENSCFLO21289	-2.49	gnl|BL_ORD_ID|60853524 KMQ89861.1 luciferin 4-monooxygenase [Lasius niger]
ENSPB14974	-2.50	gnl|BL_ORD_ID|60857729 KMQ94154.1 glutamate receptor 1, partial [Lasius niger]
ENSCFLO23491	-2.51	gnl|BL_ORD_ID|42296003 AII96915.1 vitellogenin-like protein C, partial [Formica exsecta]
ENSCFLO20964	-2.53	gnl|BL_ORD_ID|4865310 EFN73254.1 Organic cation transporter protein [Camponotus floridanus]
ENSCobs_11704	-2.53	gnl|BL_ORD_ID|56264431 XP_011862380.1 PREDICTED: uncharacterized protein LOC105559004 [Vollenhovia emeryi]
ENSPB27035	-2.53	gnl|BL_ORD_ID|52332562 XP_011260361.1 PREDICTED: alaserpin-like [Camponotus floridanus]
ENSCFLO15057	-2.54	gnl|BL_ORD_ID|4862239 EFN70155.1 Maltase 1 [Camponotus floridanus]

ENSCFLO15970	-2.54	gnl|BL_ORD_ID|52328774 XP_011253360.1 PREDICTED: relaxin receptor 1 [Camponotus floridanus]
ENSCFLO19511	-2.54	gnl|BL_ORD_ID|52326086 XP_011268217.1 PREDICTED: glutamate [NMDA] receptor subunit 1 isoform X2 [Camponotus floridanus]
ENSCFLO14652	-2.57	gnl|BL_ORD_ID|60862763 KMR04754.1 solute carrier family 22 member 3 [Lasius niger]
ENSCFLO19903	-2.57	gnl|BL_ORD_ID|51817035 XP_011169182.1 PREDICTED: synaptic vesicle glycoprotein 2C-like [Solenopsis invicta]
ENSCFLO25250	-2.57	gnl|BL_ORD_ID|52335258 XP_011265100.1 PREDICTED: probable G-protein coupled receptor Mth-like 10 [Camponotus floridanus]
ENSCFLO14544	-2.60	gnl|BL_ORD_ID|57729824 XP_012218777.1 PREDICTED: LIRP isoform X3 [Linepithema humile]
ENSCFLO20394	-2.60	gnl|BL_ORD_ID|52336717 XP_011267696.1 PREDICTED: esterase FE4 [Camponotus floridanus]
ENSCFLO22477	-2.61	gnl|BL_ORD_ID|60858082 KMQ94516.1 alanine--glyoxylate aminotransferase 2-like protein, partial [Lasius niger]
ENSPB26907	-2.61	gnl|BL_ORD_ID|60860799 KMQ97277.1 longitudinals lacking isoforms a b d l [Lasius niger]
ENSCFLO23343	-2.62	gnl|BL_ORD_ID|52333080 XP_011261275.1 PREDICTED: E3 ubiquitin-protein ligase TRIM71-like, partial [Camponotus floridanus]
ENSACEP25329	-2.62	gnl|BL_ORD_ID|53530617 XP_011332964.1 PREDICTED: uncharacterized protein LOC105276773, partial [Cerapachys biroi]
ENSPB10122	-2.63	gnl|BL_ORD_ID|56279644 XP_011875634.1 PREDICTED: general odorant-binding protein 69a-like [Vollenhovia emeryi]
ENSCFLO10689	-2.64	gnl|BL_ORD_ID|52327221 XP_011250657.1 PREDICTED: uncharacterized protein LOC105247896 [Camponotus floridanus]
ENSCFLO24507	-2.64	gnl|BL_ORD_ID|60854661 KMQ91026.1 krueppel-like proteinous protein 1 protein [Lasius niger]
ENSCFLO14208	-2.65	gnl|BL_ORD_ID|30256407 EZA61402.1 Ornithine decarboxylase [Cerapachys biroi]
ENSAECH13827	-2.67	gnl|BL_ORD_ID|57738863 XP_012231347.1 PREDICTED: putative uncharacterized protein FLJ37770 [Linepithema humile]
ENSCFLO10866	-2.67	gnl|BL_ORD_ID|84338530 KYQ52551.1 TIP41-like protein [Trachymyrmex zeteki]
ENSCFLO18045	-2.67	gnl|BL_ORD_ID|4866533 XP_011254683.1 PREDICTED: cadherin-23 [Camponotus floridanus] EFN74490.1 Cadherin-23 [Camponotus floridanus]
ENSCFLO15480	-2.70	gnl|BL_ORD_ID|4866936 EFN74895.1 hypothetical protein EAG_04117 [Camponotus floridanus]
ENSCFLO10066	-2.71	gnl|BL_ORD_ID|55954394 XP_011686577.1 PREDICTED: longitudinals lacking protein, isoforms A/B/D/L isoform X14 [Wasmannia auropunctata]
ENSACEP27021	-2.72	No_sig_nr_hit
ENSCFLO13326	-2.72	gnl|BL_ORD_ID|60860802 KMQ97280.1 longitudinals lacking isoforms a b d l [Lasius niger]
ENSPB26793	-2.72	No_sig_nr_hit
ENSCFLO12123	-2.73	gnl|BL_ORD_ID|60863181 KMR05366.1 la-related protein [Lasius niger]
ENSCFLO13399	-2.73	gnl|BL_ORD_ID|57728152 XP_012216530.1 PREDICTED: laccase-5 [Linepithema humile]
ENSCFLO24454	-2.74	gnl|BL_ORD_ID|60857350 KMQ93772.1 putative zinc finger protein 729 [Lasius niger]
ENSCFLO21247	-2.75	gnl|BL_ORD_ID|60855634 KMQ92015.1 trehalase-like isoform x2 protein, partial [Lasius niger]
ENSCFLO18013	-2.76	gnl|BL_ORD_ID|52326133 XP_011268291.1 PREDICTED: elongation of very long chain fatty acids protein AAEL008004-like [Camponotus floridanus]
ENSCFLO21072	-2.76	gnl|BL_ORD_ID|4855333 XP_011263731.1 PREDICTED: uncharacterized protein LOC105255894 [Camponotus floridanus]

ENSSI2.2.0_16373	-2.78	gnl|BL_ORD_ID|5946248 EFZ17397.1 hypothetical protein SINV_16373, partial [Solenopsis invicta]
ENSCFLO19811	-2.79	gnl|BL_ORD_ID|56266876 XP_011865678.1 PREDICTED: transmembrane channel-like protein 3 [Vollenhovia emeryi]
ENSCFLO14831	-2.81	gnl|BL_ORD_ID|56267388 XP_011866377.1 PREDICTED: cytochrome P450 6k1-like [Vollenhovia emeryi]
ENSCFLO20295	-2.81	gnl|BL_ORD_ID|59134039 XP_012524225.1 PREDICTED: uncharacterized protein LOC105829723 [Monomorium pharaonis]
ENSSI2.2.0_13474	-2.83	No_sig_nr_hit
ENSCFLO11404	-2.84	gnl|BL_ORD_ID|83646034 KYN30739.1 hypothetical protein ALC56_14983 [Trachymyrmex septentrionalis]
ENSCFLO13222	-2.84	gnl|BL_ORD_ID|60858017 KMQ94447.1 facilitated trehalose transporter tret1-like protein [Lasius niger]
ENSCFLO15914	-2.85	gnl|BL_ORD_ID|60848956 KMQ85185.1 proto-oncogene tyrosine-protein kinase ros [Lasius niger]
ENSACEP20736	-2.88	gnl|BL_ORD_ID|59145281 XP_012539556.1 PREDICTED: putative glutamate synthase [NADPH] isoform X2 [Monomorium pharaonis]
ENSCFLO13323	-2.88	gnl|BL_ORD_ID|56290373 XP_011882297.1 PREDICTED: longitudinals lacking protein, isoform G-like [Vollenhovia emeryi]
ENSAECH26247	-2.91	gnl|BL_ORD_ID|83647144 KYN31894.1 hypothetical protein ALC56_14033 [Trachymyrmex septentrionalis]
ENSCFLO13324	-2.91	gnl|BL_ORD_ID|52330692 XP_011256896.1 PREDICTED: zinc finger protein 333-like [Camponotus floridanus]
ENSCFLO17139	-2.91	gnl|BL_ORD_ID|60857388 KMQ93812.1 hypothetical protein RF55_6064 [Lasius niger]
ENSCFLO13365	-2.92	gnl|BL_ORD_ID|60855154 KMQ91529.1 putative kinase-like protein [Lasius niger]
ENSLH11570	-2.92	gnl|BL_ORD_ID|55953387 XP_011685133.1 PREDICTED: uncharacterized protein LOC105448326 isoform X1 [Wasmannia auropunctata]
ENSCFLO19000	-2.93	gnl|BL_ORD_ID|60853578 KMQ89916.1 tubulin beta-4b chain isoform x1 [Lasius niger]
ENSPB10861	-2.93	gnl|BL_ORD_ID|60859686 KMQ96147.1 zinc finger protein xfin [Lasius niger]
ENSCFLO23120	-2.96	gnl|BL_ORD_ID|52326285 XP_011268533.1 PREDICTED: multiple epidermal growth factor-like domains protein 10 [Camponotus floridanus]
ENSCFLO21551	-2.98	gnl|BL_ORD_ID|4861039 EFN68947.1 Probable G-protein coupled receptor Mth-like 10 [Camponotus floridanus]
ENSSI2.2.0_08017	-2.99	gnl|BL_ORD_ID|83613892 KYM97339.1 hypothetical protein ALC62_11983 [Cyphomyrmex costatus]
ENSCFLO12038	-3.00	gnl|BL_ORD_ID|84338657 KYQ52679.1 hypothetical protein ALC60_08211 [Trachymyrmex zeteki]
ENSCFLO12261	-3.00	gnl|BL_ORD_ID|55964755 XP_011701332.1 PREDICTED: uncharacterized protein K02A2.6-like [Wasmannia auropunctata]
ENSCFLO23127	-3.02	gnl|BL_ORD_ID|60857692 KMQ94116.1 peptidoglycan-recognition protein lb-like protein [Lasius niger]
ENSCFLO15338	-3.03	gnl|BL_ORD_ID|52329795 XP_011255204.1 PREDICTED: uncharacterized protein LOC105250686 [Camponotus floridanus]
ENSPB26902	-3.03	gnl|BL_ORD_ID|5946602 EFZ17752.1 hypothetical protein SINV_08391, partial [Solenopsis invicta]
ENSCFLO16001	-3.04	gnl|BL_ORD_ID|60850702 KMQ86974.1 hypothetical protein RF55_13891 [Lasius niger]

ENSCFLO23546	-3.04	gnl|BL_ORD_ID|4863743 XP_011251442.1 PREDICTED: sodium- and chloride-dependent GABA transporter 1-like [Camponotus floridanus]
ENSCFLO15479	-3.07	gnl|BL_ORD_ID|60854612 KMQ90977.1 sodium-coupled monocarboxylate transporter 1, partial [Lasius niger]
ENSCFLO22752	-3.10	gnl|BL_ORD_ID|5948208 XP_011157644.1 PREDICTED: facilitated trehalose transporter Tret1-like isoform X2 [Solenopsis invicta]
ENSCFLO19295	-3.11	gnl|BL_ORD_ID|60847159 KMQ83363.1 hypothetical protein RF55_20240, partial [Lasius niger]
ENSPB26269	-3.11	gnl|BL_ORD_ID|56261511 XP_011858681.1 PREDICTED: cytochrome P450 4C1-like [Vollenhovia emeryi]
ENSCFLO20888	-3.12	gnl|BL_ORD_ID|52325354 XP_011256991.1 PREDICTED: X-linked retinitis pigmentosa GTPase regulator [Camponotus floridanus]
ENSCFLO21687	-3.12	gnl|BL_ORD_ID|60848490 KMQ84708.1 p protein [Lasius niger]
ENSCFLO14713	-3.15	gnl|BL_ORD_ID|55966505 XP_011703883.1 PREDICTED: LOW QUALITY PROTEIN: protein lava lamp [Wasmannia auropunctata]
ENSCFLO11269	-3.20	gnl|BL_ORD_ID|51818123 XP_011170740.1 PREDICTED: uncharacterized protein LOC105203604 isoform X1 [Solenopsis invicta]
ENSCFLO14680	-3.23	gnl|BL_ORD_ID|60862465 KMR03324.1 lysyl oxidase-like protein 3 protein [Lasius niger]
ENSCFLO17914	-3.25	gnl|BL_ORD_ID|60862411 KMR02902.1 activating signal cointegrator 1 complex subunit 2-like protein [Lasius niger]
ENSCFLO13908	-3.34	gnl|BL_ORD_ID|4865903 EFN73854.1 hypothetical protein EAG_06496 [Camponotus floridanus]
ENSSI2.2.0_16235	-3.34	No_sig_nr_hit
ENSCFLO20435	-3.35	gnl|BL_ORD_ID|4860583 EFN68488.1 hypothetical protein EAG_06056 [Camponotus floridanus]
ENSPB26900	-3.35	gnl|BL_ORD_ID|52330686 XP_011256889.1 PREDICTED: GDNF-inducible zinc finger protein 1-like [Camponotus floridanus]
ENSCFLO19184	-3.36	gnl|BL_ORD_ID|52332234 XP_011259695.1 PREDICTED: putative fatty acyl-CoA reductase CG5065 [Camponotus floridanus]
ENSCobs_13404	-3.37	gnl|BL_ORD_ID|51217147 XP_011149430.1 PREDICTED: putative nuclease HARBI1 [Harpegnathos saltator]
ENSCFLO19925	-3.40	gnl|BL_ORD_ID|4867044 XP_011260206.1 PREDICTED: cysteine sulfinic acid decarboxylase [Camponotus floridanus] XP_011260294.1
ENSCFLO24343	-3.40	gnl|BL_ORD_ID|53534733 XP_011340991.1 PREDICTED: LOW QUALITY PROTEIN: uncharacterized protein LOC105281438 [Cerapachys biroi]
ENSCFLO22495	-3.43	gnl|BL_ORD_ID|52336809 XP_011267858.1 PREDICTED: uncharacterized protein LOC105258342 [Camponotus floridanus]
ENSCFLO12471	-3.46	gnl|BL_ORD_ID|83623936 KYN07563.1 hypothetical protein ALC62_01469 [Cyphomyrmex costatus]
ENSCFLO12251	-3.47	gnl|BL_ORD_ID|33774484 ADF18552.1 endonuclease-reverse transcriptase [Bombyx mori]
ENSCFLO10095	-3.49	gnl|BL_ORD_ID|6875735 EGI63306.1 hypothetical protein G5I_08335 [Acromyrmex echinatior]
ENSCFLO14082	-3.51	gnl|BL_ORD_ID|56264483 XP_011862439.1 PREDICTED: neprilysin-11 [Vollenhovia emeryi] XP_011862440.1
ENSCFLO13495	-3.52	gnl|BL_ORD_ID|6877641 EGI65237.1 Elongation of very long chain fatty acids protein [Acromyrmex echinatior]
ENSCFLO23301	-3.52	gnl|BL_ORD_ID|52336100 XP_011266654.1 PREDICTED: uncharacterized protein LOC105257618 [Camponotus floridanus]
ENSCFLO13985	-3.53	gnl|BL_ORD_ID|52333726 XP_011262408.1 PREDICTED: neuromedin-B receptor isoform X2 [Camponotus floridanus]
ENSPB20096	-3.54	gnl|BL_ORD_ID|55968975 XP_011707021.1 PREDICTED: uncharacterized protein LOC105462192 [Wasmannia auropunctata]

ENSCFLO13329	-3.58	gnl|BL_ORD_ID|60858624 KMQ95064.1 zinc finger protein 28 [Lasius niger]
ENSCFLO12190	-3.60	gnl|BL_ORD_ID|60848582 KMQ84801.1 hypothetical protein RF55_17103 [Lasius niger]
ENSAECH16406	-3.60	gnl|BL_ORD_ID|56259215 XP_011860316.1 PREDICTED: uncharacterized protein LOC105557630 [Vollenhovia emeryi]
ENSCFLO13325	-3.65	gnl|BL_ORD_ID|60860795 KMQ97273.1 putative zinc finger protein 771 [Lasius niger]
ENSCFLO22253	-3.66	gnl|BL_ORD_ID|60862610 KMR04537.1 ester hydrolase c11orf54-like protein [Lasius niger]
ENSCFLO15758	-3.67	gnl|BL_ORD_ID|30243887 EZA48726.1 Tyrosine aminotransferase [Cerapachys biroi]
ENSCobs_03644	-3.67	gnl|BL_ORD_ID|51818974 XP_011171915.1 PREDICTED: zinc finger protein 354A-like [Solenopsis invicta]
ENSCFLO11199	-3.72	gnl|BL_ORD_ID|55373739 XP_011644207.1 PREDICTED: suppressor of lurcher protein 1 isoform X1 [Pogonomyrmex barbatus]
ENSCFLO12751	-3.75	gnl|BL_ORD_ID|4859315 XP_011258038.1 PREDICTED: monocarboxylate transporter 9-like [Camponotus floridanus]
ENSCFLO23116	-3.97	gnl|BL_ORD_ID|52326270 XP_011268507.1 PREDICTED: angiotensin-converting enzyme [Camponotus floridanus]
ENSCFLO18240	-4.11	gnl|BL_ORD_ID|4853411 XP_011266636.1 PREDICTED: anoctamin-4 [Camponotus floridanus]
ENSCFLO18734	-4.15	gnl|BL_ORD_ID|52333941 XP_011262725.1 PREDICTED: uncharacterized protein LOC105255251 [Camponotus floridanus]
ENSCFLO19195	-4.21	gnl|BL_ORD_ID|60863109 KMR05258.1 hexamerin 2 [Lasius niger]
ENSCFLO24753	-4.21	gnl|BL_ORD_ID|56262337 XP_011859689.1 PREDICTED: uncharacterized protein LOC105557131 [Vollenhovia emeryi]
ENSPB20411	-4.31	gnl|BL_ORD_ID|56701894 XP_012055065.1 PREDICTED: skin secretory protein xP2-like [Atta cephalotes]
ENSCFLO23129	-4.32	gnl|BL_ORD_ID|4866017 EFN73968.1 26S proteasome non-ATPase regulatory subunit 10 [Camponotus floridanus]
ENSCFLO11763	-4.33	gnl|BL_ORD_ID|60850415 KMQ86680.1 proto-oncogene tyrosine-protein kinase ros, partial [Lasius niger]
ENSPB14648	-4.45	No_sig_nr_hit
ENSCFLO18449	-4.46	gnl|BL_ORD_ID|52335498 XP_011265551.1 PREDICTED: probable chitinase 3 [Camponotus floridanus] XP_011265553.1
ENSCobs_14257	-4.47	gnl|BL_ORD_ID|55120757 XP_011554514.1 PREDICTED: uncharacterized protein LOC105385780, partial [Plutella xylostella]
ENSCFLO21552	-4.49	gnl|BL_ORD_ID|56289047 XP_011881614.1 PREDICTED: gustatory receptor for sugar taste 64f-like isoform X2 [Vollenhovia emeryi]
ENSPB20000	-4.68	No_sig_nr_hit
ENSCFLO20469	-4.70	gnl|BL_ORD_ID|60849497 KMQ85740.1 proto-oncogene tyrosine-protein kinase ros [Lasius niger]
ENSSI2.2.0_15831	-4.70	gnl|BL_ORD_ID|5944357 EFZ15501.1 hypothetical protein SINV_15831, partial [Solenopsis invicta]
ENSCobs_07205	-4.72	gnl|BL_ORD_ID|60851242 KMQ87528.1 rna-directed dna polymerase from mobile element jockey-like protein [Lasius niger]
ENSACEP15358	-4.75	gnl|BL_ORD_ID|60859188 KMQ95639.1 arginine kinase [Lasius niger]
ENSCFLO11678	-4.77	gnl|BL_ORD_ID|60847563 KMQ83770.1 proto-oncogene tyrosine-protein kinase ros [Lasius niger]
ENSCFLO26680	-4.77	gnl|BL_ORD_ID|94239493 JAS79726.1 hypothetical protein g.45181 [Homalodisca liturata]

ENSCFLO23058	-4.79	gnl|BL_ORD_ID|52324783 XP_011252521.1 PREDICTED: fatty acid synthase-like [Camponotus floridanus]
ENSCFLO18694	-4.88	gnl|BL_ORD_ID|52330283 XP_011256073.1 PREDICTED: LOW QUALITY PROTEIN: probable cytochrome P450 6a14 [Camponotus floridanus]
ENSCFLO15332	-4.94	gnl|BL_ORD_ID|4858755 XP_011258869.1 PREDICTED: putative defense protein 3 [Camponotus floridanus]
ENSCFLO19382	-5.01	gnl|BL_ORD_ID|60852688 KMQ89004.1 proto-oncogene tyrosine-protein kinase ros [Lasius niger]
ENSCFLO11878	-5.14	gnl|BL_ORD_ID|83638286 KYN22222.1 THAP domain-containing protein 9, partial [Trachymyrmex cornetzi]
ENSCFLO18279	-5.38	gnl|BL_ORD_ID|60848803 KMQ85028.1 proto-oncogene tyrosine-protein kinase ros [Lasius niger]
ENSCFLO19048	-5.41	gnl|BL_ORD_ID|74412094 XP_014478854.1 PREDICTED: caveolin-3-like [Dinoponera quadriceps]
ENSCFLO16597	-5.69	gnl|BL_ORD_ID|81823522 XP_015509379.1 PREDICTED: proton-coupled amino acid transporter 1-like [Neodiprion lecontei]
ENSCFLO13671	-5.71	gnl|BL_ORD_ID|4853448 EFN61311.1 Protein sevenless [Camponotus floridanus]
ENSCFLO13334	-5.75	gnl|BL_ORD_ID|4860119 XP_011256874.1 PREDICTED: transcriptional repressor scratch 1-like [Camponotus floridanus]
ENSCFLO11108	-5.85	gnl|BL_ORD_ID|60849649 KMQ85894.1 hypothetical protein RF55_15295, partial [Lasius niger]
ENSCFLO23255	-5.85	gnl|BL_ORD_ID|4878069 XP_011136930.1 PREDICTED: uncharacterized protein LOC105181683 [Harpegnathos saltator]
ENSCFLO15913	-5.92	gnl|BL_ORD_ID|4864403 EFN72335.1 Proto-oncogene tyrosine-protein kinase ROS, partial [Camponotus floridanus]
ENSCFLO13598	-6.14	gnl|BL_ORD_ID|60851641 KMQ87935.1 proto-oncogene tyrosine-protein kinase ros [Lasius niger]
ENSCFLO23591	-6.85	gnl|BL_ORD_ID|60846483 KMQ82678.1 proto-oncogene tyrosine-protein kinase ros [Lasius niger]
ENSCFLO23431	-6.87	gnl|BL_ORD_ID|57764271 XP_012249128.1 PREDICTED: proto-oncogene tyrosine-protein kinase ROS [Bombus impatiens]
ENSCFLO20020	-7.07	gnl|BL_ORD_ID|60860389 KMQ96862.1 hypothetical protein RF55_2829 [Lasius niger]
ENSCFLO22778	-7.40	gnl|BL_ORD_ID|60852676 KMQ88992.1 protein g12 [Lasius niger]
ENSCFLO13660	-7.71	gnl|BL_ORD_ID|60854789 KMQ91155.1 proto-oncogene tyrosine-protein kinase ros [Lasius niger]
ENSCFLO11774	-7.73	gnl|BL_ORD_ID|60847231 KMQ83437.1 proto-oncogene tyrosine-protein kinase ros, partial [Lasius niger]
ENSCFLO20488	-9.47	gnl|BL_ORD_ID|52327078 XP_011250438.1 PREDICTED: ephrin type-B receptor 1-like [Camponotus floridanus]

Appendix B. Supplementary Information for Chapter 2

B.1 Supplemental Table

Supplemental Table B.1. Bioclimatic variables for populations of *P. imparis* that were used for tolerance assays. Data from WorldClim was calculated using 30 year averages from 1970-2000. Above ground and below ground data was calculated using temperature recorded by iButtons during 2015-2017. Units for Bio1, Bio2, Bio5, Bio6, Bio7, Bio9, Bio10, Bio11 are ºC, for Bio4 and Bio15 units are %, units for Bio12, Bio13, Bio14, Bio16, Bio17, Bio18, and Bio19 are mm.

	Bio1	Bio2	Bio3	Bio4	Bio5	Bio6	Bio7	Bio8	Bio9	Bio10	Bio11	Bio12	Bio13	Bio14	Bio15	Bio16	Bio17	Bio18	Bio19
WorldClim																			
Berkeley	14.2	9.1	52.0	2888	23.3	5.8	17.5	10.3	17.0	17.5	10.3	614	134	1	88	334	7	10	334
Whittier	18.1	13.1	54.0	3751	30.6	6.5	24.1	14.1	22.6	23.3	13.6	389	84	0	94	235	5	13	217
Stebbins	15.9	15.7	48.0	5796	34.3	2.2	32.1	8.5	23.1	23.1	8.5	616	139	1	92	346	7	7	346
Quail Ridge	14.9	14.7	48.0	5598	32.9	2.4	30.5	8.1	22.0	22.1	8.1	765	167	1	91	421	9	15	421
Castle Rock	12.1	11.9	50.0	4320	26.0	2.3	23.7	7.7	17.7	18.1	7.5	870	164	2	84	444	12	18	435
Mt Diablo	14.7	14.0	54.0	4259	29.0	3.1	25.9	9.4	19.9	20.2	9.4	632	136	1	91	346	5	11	346
Yosemite	11.8	15.3	45.0	6689	31.4	-2.5	33.9	3.9	20.6	20.7	3.9	890	152	6	76	431	26	33	431
Palomar	12.5	14.0	47.0	5721	29.5	1.0	29.4	6.6	20.2	20.4	6.2	711	125	3	79	370	31	48	351
Above ground																			
Berkeley	20.4	21.2	66.0	2916	35.2	3.0	32.1	-	-	22.4	16.7	-	-	-	-	-	-	-	-
Whittier	22.0	26.7	68.2	5559	44.1	0.6	43.5	-	-	27.4	14.4	-	-	-	-	-	-	-	-
Stebbins	18.6	16.2	39.5	7874	44.1	3.1	41.0	-	-	27.9	9.5	-	-	-	-	-	-	-	-
Quail Ridge	18.8	24.5	59.0	6719	41.1	-0.5	41.6	-	-	26.1	10.0	-	-	-	-	-	-	-	-
Castle Rock	14.2	21.1	60.2	5783	33.1	-2.0	35.1	-	-	20.4	6.6	-	-	-	-	-	-	-	-
Mt Diablo	14.0	23.3	51.2	7274	41.6	-4.0	45.6	-	-	23.4	5.4	-	-	-	-	-	-	-	-

	Diablo																			
	Palomar	16.4	29.2	71.2	4550	37.6	-3.5	41.1	-	-	22.4	11.8	-	-	-	-	-	-	-	-
Underground																				
	Berkeley	17.7	1.4	24.0	163	20.7	14.7	6.0	-	-	19.7	15.8	-	-	-	-	-	-	-	-
	Whittier	18.0	2.7	24.3	340	23.6	12.6	11.0	-	-	22.3	14.0	-	-	-	-	-	-	-	-
	Quail Ridge	18.0	3.1	22.2	369	24.2	10.1	14.1	-	-	22.6	13.4	-	-	-	-	-	-	-	-
	Castle Rock	12.6	2.5	18.2	370	18.1	4.6	13.5	-	-	17.1	8.4	-	-	-	-	-	-	-	-
	Mt Diablo	11.8	2.5	19.6	416	18.1	5.1	13.0	-	-	17.0	6.8	-	-	-	-	-	-	-	-
	Palomar	12.5	3.5	23.9	415	19.1	4.5	14.5	-	-	17.6	7.6	-	-	-	-	-	-	-	-

Appendix C. Supplementary Information for Chapter 3

C.1 Supplemental Figures

Supplemental Figure C.1. Phylogenetic clusters of *P. imparis*. RAxML maximum likelihood tree with support values on nodes for all runs. Above the nodes are the support values obtained when partitioned by gene with all loci/90% filtered dataset/100% filtered dataset. Below the nodes are the support values obtained when not partitioned with all loci/90% filtered dataset/100%filtered dataset. Stars indicate support ≥ 99 for each dataset. Dashes indicate that particular topology was not recovered.

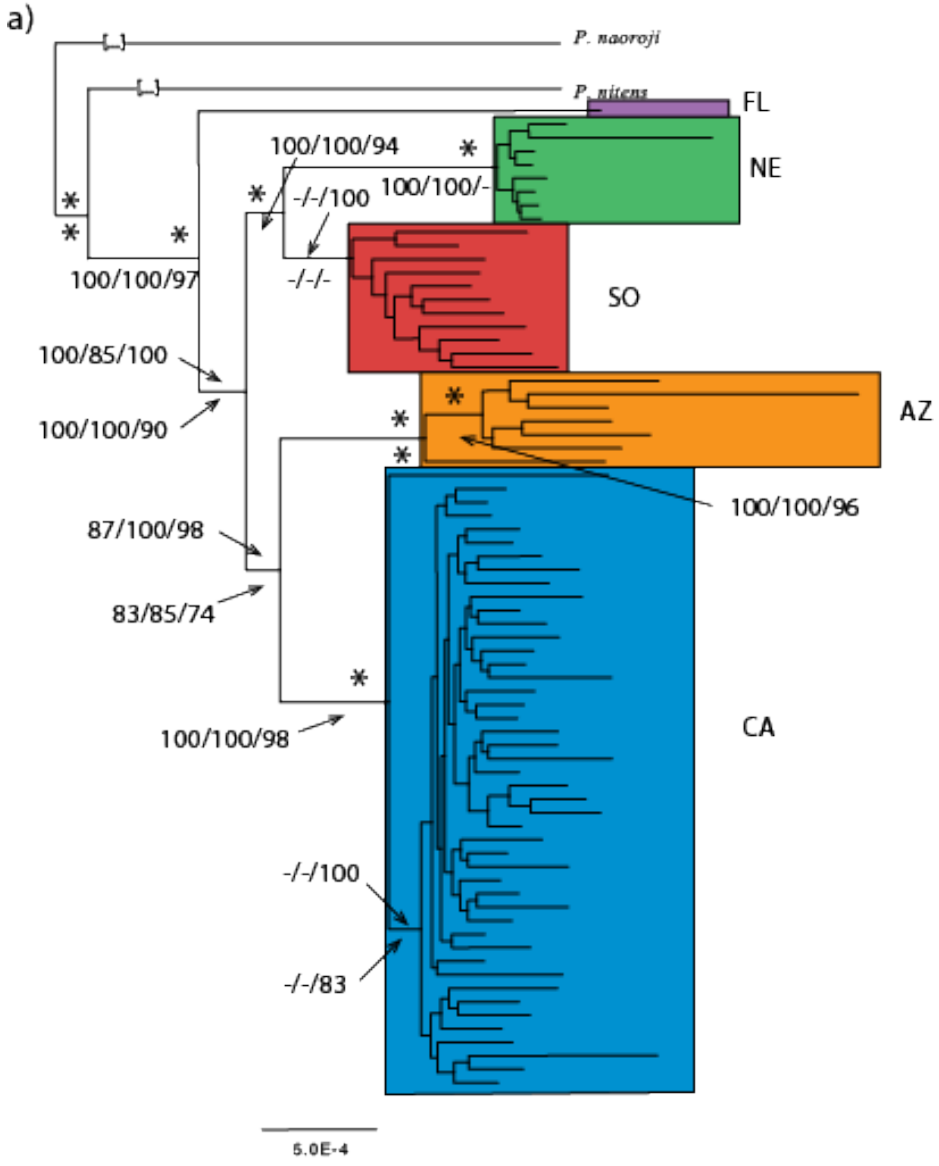

Supplemental Figure C.2. STRUCTURE results for K = 3 and K = 4 for individuals within the CA clade of *P. imparis*. Colors correspond to clades in main figures, vertical lines represent one individual, the color proportion indicates the genetic contribution.

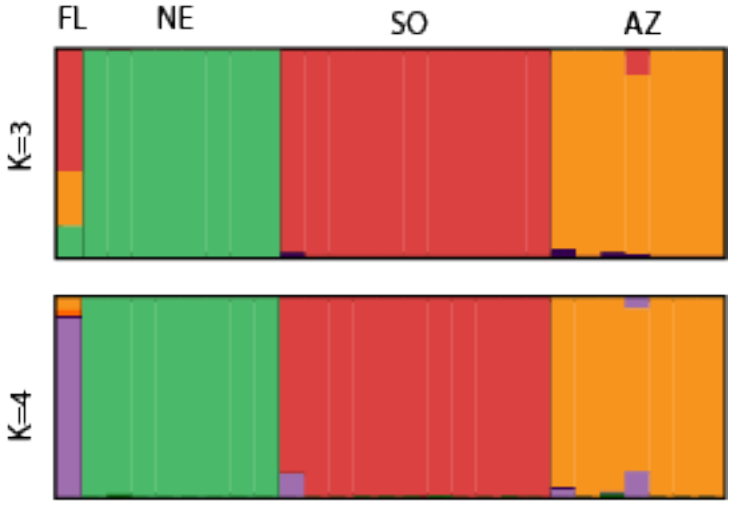

C.2 Supplemental Table

Supplemental Table C.1. Samples of *P. imparis* included in this study.

Sample Number	Latitude	Longitude	Cluster	Country	State	Collector
BDB662	39.07513	-96.57065	SO	USA	Kansas	Benjamin D. Blanchard
PM009	34.729	-92.355	SO	USA	Arkansas	Daniella Prince, Stephen Yanoviak
Bel0306	38.216	-85.761	SO	USA	Louisville	Daniella Prince, Stephen Yanoviak
JT01	37.97215	-90.53236	SO	USA	Missouri	James Trager
JWill01	39.3928	-76.6047	SO	USA	Maryland	Jason Williams
KR01	33.881536	-96.800234	SO	USA	Oklahoma	Karl Roeder
SOA953	33.773118	-84.317659	SO	USA	Georgia	School of Ants
SOA1062	35.292581	-80.624117	SO	USA	North Carolina	School of Ants
SOA675	36.507486	-76.353738	SO	USA	North Carolina	School of Ants
SOA305	39.961672	-75.315589	SO	USA	Pennsylvania	School of Ants
Champ1	40.0975	-88.23355	SO	USA	Illinois	unknown
BDB654	42.2806	-83.7269	NE	USA	Michigan	Benjamin D. Blanchard
SOA1189	42.12218	-87.960137	NE	USA	Illinois	School of Ants
SOA3636	42.323794	-72.626542	NE	USA	Massachusetts	School of Ants
SOA439	42.375748	-71.366259	NE	USA	Massachusetts	School of Ants
SOA3311	42.593247	-83.252536	NE	USA	Michigan	School of Ants
SOA3844	40.720603	-74.564692	NE	USA	New Jersey	School of Ants
SOA2592	42.698523	-87.894501	NE	USA	Wisonsan	School of Ants
MMP01918	38.95174298	-78.32301202	NE	USA	Virginia	M.M. Prebus
AVS56	33.73	-117.6833	CA	USA	California	Andy Suarez
BW01	35.10626944	-118.5404	CA	USA	California	Brian Whyte
CQS071	37.5789	-122.4657	CA	USA	California	CD Quock
CQS076	37.7283	-122.489	CA	USA	California	CD Quock
CQS083	37.7404	-122.4406	CA	USA	California	CD Quock
Toni073	38.0301361	-122.2143277	CA	USA	California	Christian Irian
DH01	32.023205	-119.76576	CA	USA	California	David Holway, I Naughton
EMS3069	41.74818	-123.3592	CA	USA	California	E.M. Sarnat
ES01	38.544905	-121.740516	CA	USA	California	Eli Sarnet
IN01	34.00166667	-119.6772222	CA	USA	California	Ida Naughton

NRG1012	38.9729527	-123.1163916	CA	USA	California	Kelsey Schenkle
SOA1123	38.789282	-121.208789	CA	USA	California	School of Ants
Acad02	33.97958	-120.07861	CA	USA	California	M.L. Borowiec
MLB1241	38.03541	-120.22726	CA	USA	California	M.L. Borowiec
MLB177	38.87306	-121.56889	CA	USA	California	M.L. Borowiec
MLB0039	37.33059	-122.09131	CA	USA	California	M.L.Bollinger
MMP01779	34.46023	-120.02376	CA	USA	California	M.M. Prebus
MMP01085	38.50551	-122.10197	CA	USA	California	M.M. Prebus
MMP01092	38.86064	-122.41792	CA	USA	California	M.M. Prebus
MMP01113	39.21485	-121.04213	CA	USA	California	M.M. Prebus
MMP01174	41.14958	-122.32423	CA	USA	California	M.M. Prebus
MMP01734	39.34424	-122.75392	CA	USA	California	M.M. Prebus
MMP00222	45.51983	-122.62574	CA	USA	Oregon	M.M. Prebus
Bead2	37.74763	-119.58584	CA	USA	California	Maria Tonione
Bead4	37.219167	-121.916667	CA	USA	California	Maria Tonione
Bead5	33.334444	-116.9175	CA	USA	California	Maria Tonione
Bead6	38.48307	-122.14895	CA	USA	California	Maria Tonione
Bead8	37.23647	-122.11702	CA	USA	California	Maria Tonione
Bead9	37.872916	-122.2631	CA	USA	California	Maria Tonione
Toni002	37.21223	-121.79686	CA	USA	California	Maria Tonione
Toni065	37.74467	-119.58472	CA	USA	California	Maria Tonione
Toni086	38.511697	-122.100433	CA	USA	California	Maria Tonione
Toni088	38.496	-122.123419	CA	USA	California	Maria Tonione
Toni090	38.515508	-122.080406	CA	USA	California	Maria Tonione
Bead3	38.50867	-122.09678	CA	USA	California	Maria Tonione
Bead7	34.00381	-118.05395	CA	USA	California	Maria Tonione
Toni066	37.82903	-120.00413	CA	USA	California	Maria Tonione
Toni071	37.2297027	-122.0780638	CA	USA	California	Maria Tonione
NDT01	39.4856138	-121.2311583	CA	USA	California	Neil Tsutsui
NDT673	35.467778	-120.376944	CA	USA	California	Neil Tsutsui
NDT670	36.67	-121.768611	CA	USA	California	Neil Tsutsui
NDT671	35.850556	-120.770556	CA	USA	California	Neil Tsutsui
PSW14050	37.016667	-119.45	CA	USA	California	Phil Ward
PSW16240	39.216667	-121.035	CA	USA	California	Phil Ward

PSW16713	38.52922	-121.76615	CA	USA	California	Phil Ward
AW1195	39.283333	-120.983333	CA	USA	California	Alex Wild
SOA3830	29.634173	-82.367064	FL	USA	Florida	School of Ants
JTL8031	38.79069	-109.19692	AZ	USA	Utah	Jack Longino
MMP02470	30.70167	-104.10069	AZ	USA	Texas	M.M. Prebus
PSW14708	31.933333	-109.252222	AZ	USA	Arizona	Phil Ward
PSW9284	19.516667	-103.683333	AZ	Mexico	Jalisco	Phil Ward
RAJ5745	34.40666667	-112.435	AZ	USA	Arizona	Robert A Johnson
RAJ5767	33.43666667	-111.0683333	AZ	USA	Arizona	Robert A Johnson
RAJ5593	31.01666667	-110.3841667	AZ	Mexico	Sonora	Robert A Johnson